Dual pathogenicity island transfer by piggybacking lateral transduction

Cell

Dual pathogenicity island transfer by piggybacking lateral transduction

--Manuscript Draft--

Manuscript Number:	CELL-D-22-02349R4
Full Title:	Dual pathogenicity island transfer by piggybacking lateral transduction
Article Type:	Research Article
Keywords:	Phages; pathogenicity islands; lateral transduction; concatamers; SaPIs; PICIs; Staphylococcus aureus; cotransduction
Corresponding Author:	John Chen, Ph.D. Singapore, SINGAPORE
First Author:	Melissa Su Juan Chee
Order of Authors:	Melissa Su Juan Chee
	Ester Serrano
	Yin Ning Chiang
	Joshua Harling-Lee
	Rebecca Man
	Rodrigo Bacigalupe
	J. Ross Fitzgerald
	José R. Penadés
	John Chen, Ph.D.
Abstract:	Lateral transduction (LT) is the process by which temperate phages mobilize large sections of bacterial genomes. Despite its importance, LT has only been observed during prophage induction. Here we report that superantigen-carrying staphylococcal pathogenicity islands (SaPIs) employ a related but more versatile and complex mechanism of gene transfer to drive chromosomal hypermobility while self-transferring with additional virulence genes co-opted from the chromosome. We found that after phage infection or prophage induction, activated SaPIs form concatamers in the host chromosome by switching between parallel genomic tracks in replication bubbles. This dynamic lifecycle enables SaPIbov1 to piggyback its LT of staphylococcal pathogenicity island vSaα, which encodes an array of genes involved in host-pathogen interactions, allowing both islands to be mobilized intact and transferred in a single infective particle. Our findings highlight previously unknown roles of pathogenicity islands in bacterial virulence and show that their evolutionary impact extends beyond the genes they carry.

Dual pathogenicity island transfer by piggybacking lateral transduction

Melissa Su Juan Chee[1,†], Ester Serrano[2,†], Yin Ning Chiang[1], Joshua Harling-Lee[3], Rebecca Man[3], Rodrigo Bacigalupe[3], J. Ross Fitzgerald[3], José R. Penadés[4,5,*], John Chen[1,6,*]

Affiliations:

[1]Infectious Diseases Translational Research Programme and Department of Microbiology and Immunology, Yong Loo Lin School of Medicine, National University of Singapore, Singapore 117545, Singapore.

[2]School of Infection and Immunity, College of Medical, Veterinary and Life Sciences, University of Glasgow, Glasgow, G12 8TA, UK.

[3]The Roslin Institute, University of Edinburgh, Easter Bush Campus, Edinburgh EH259RG, UK

[4]Dep. Ciencias Biomédicas, Universidad CEU Cardenal Herrera, 46113 Moncada, Spain.

[5]Centre for Bacterial Resistance Biology, Imperial College London, SW7 2AZ, UK.

[6]Lead contact author.

[†]Equal contribution.

[*]Corresponding authors:
John Chen
Infectious Diseases Translational Research Programme
Department of Microbiology and Immunology
Yong Loo Lin School of Medicine
National University of Singapore
e-mail: miccjy@nus.edu.sg

José R. Penadés
Centre for Bacterial Resistance Biology
Imperial College London
e-mail: j.penades@imperial.ac.uk

Summary

Lateral transduction (LT) is the process by which temperate phages mobilize large sections of bacterial genomes. Despite its importance, LT has only been observed during prophage induction. Here we report that superantigen-carrying staphylococcal pathogenicity islands (SaPIs) employ a related but more versatile and complex mechanism of gene transfer to drive chromosomal hypermobility while self-transferring with additional virulence genes from the host. We found that after phage infection or prophage induction, activated SaPIs form concatamers in the bacterial chromosome by switching between parallel genomic tracks in replication bubbles. This dynamic life cycle enables SaPIbov1 to piggyback its LT of staphylococcal pathogenicity island vSaα, which encodes an array of genes involved in host-pathogen interactions, allowing both islands to be mobilized intact and transferred in a single infective particle. Our findings highlight previously unknown roles of pathogenicity islands in bacterial virulence and show that their evolutionary impact extends beyond the genes they carry.

Keywords

Phages, pathogenicity islands, lateral transduction, concatamers, SaPIs, PICIs, *Staphylococcus aureus*, cotransduction

Introduction

Pathogenicity islands are a class of genetic elements in pathogenic bacteria that encode virulence factors and accessory proteins. They are large gene clusters that are regarded as mobile and their acquisition via horizontal gene transfer can transform a benign bacterium into a dangerous pathogen, though mobility has only been demonstrated for a small subset of these elements. The *Staphylococcus aureus* pathogenicity islands (SaPIs) are a family of small (generally 15-18 kilobases) and highly mobile genetic elements that carry genes for superantigens and toxins.[1,2] They are prototypical members of the phage-inducible chromosomal islands (PICIs) found in gram-positive and gram-negative bacteria,[3-5] and they are regarded as molecular parasites because they exploit bacteriophages (phages), the viruses of bacteria, for their reproduction and dissemination. Normally, SaPIs reside in the chromosomes of their *S. aureus* hosts under the maintenance of their master repressor StI.[6] Their life cycles are activated by the phages that they parasitize (depicted in Figure S1B), following the formation of a complex between StI and "helper" phage-encoded antirepressor proteins that lift StI repression and initiate the SaPI excision-replication-packaging (ERP) program.[7]

In the lysogenic cycle, temperate phages reproduce as DNA (or prophages) in the genomes of their lysogenic bacterial hosts during bacterial cell division. Phage maturation occurs in the lytic cycle, following host cell infection or induction from the lysogenic cycle (depicted in Figure S1A). In both cases, the viral genome often circularizes episomally and undergoes DNA replication to form long head-to-tail concatemers.[8,9] DNA packaging begins when a phage packaging site (*pac*) is recognized by the phage small terminase ($TerS_{\Phi}$), which forms hetero-oligomers with the phage large terminase (TerL) to

translocate the viral genome into phage heads.[10,11] When a capsid capacity or “headful” has been reached, a non-specific terminal cut is made to complete DNA packaging.[12,13] This process is highly efficient and often results in high titers of infectious phage particles. The SaPIs can hijack this process by employing their own small terminase ($TerS_{SP}$), which pairs with phage TerL to form terminase enzymes that recognize SaPI *pac* sites.[14,15] SaPI DNA is then packaged into phage heads, leading to extremely high frequencies of intra- and intergeneric transfer.[16,17]

Phage lysates resulting from the infection of a sensitive strain, or the induction of a resident prophage, are mostly comprised of infectious phage particles; but they also contain transducing particles, which contain bacterial DNA that can be transferred from one bacterium to another by a process known as genetic transduction. They are formed in the phage lytic cycle by the mechanisms of specialized (ST), generalized (GT), and lateral transduction (LT).[18] Specialized-transducing particles typically contain DNA from prophages that have aberrantly excised from the chromosome with adjacent host genes still attached.[19] Generalized-transducing particles can contain any bacterial DNA (including chromosomal or plasmid DNA), and they are made when DNA packaging initiates from *pac* site homologs in the host genome.[20] In the recently discovered LT, the formation of transducing particles begins when a prophage replicates bidirectionally prior to excision to create multiple integrated phage genomes.[21,22] Some prophages excise and enter the productive lytic cycle to generate infectious particles, while DNA packaging can also initiate in situ from the *pac* site of integrated prophages to generate transducing particles. In this scenario, the first particle is filled with a prophage-bacteria DNA molecule and then the headful packaging machinery continues in the bacterial chromosome for

seven or more successive capsid headfuls. This mechanism only occurs during prophage induction, but it can have a profound impact because it results in the transfer of large spans (several hundred kb) of the bacterial genome at very high frequencies, exceeding that of most mobile genetic elements transferred via conjugation or generalized transduction,[23] without affecting phage production.

Here, we report the discovery of a previously unrecognized stage in SaPI life cycles. While it was assumed that SaPIs excise from the chromosome as the first step after helper phage induction (Figure S1B), we found that induced SaPIs replicate before excision, creating multiple islands on parallel strands that switch genomic tracks to form head-to-tail concatamers while still integrated into the host chromosome. This atypical life cycle allows them to engage in SaPI LT to mobilize large sections of the bacterial chromosome at high frequencies, in addition to a second more sophisticated form of LT that produces transducing particles capable of delivering an intact SaPI element with bacterial DNA. As a result of this second mechanism, which we term lateral cotransduction (LcT), two unrelated pathogenicity islands can be packaged intact in a single infective particle and cotransduced to the same host cell at high frequencies, all in parallel to the normal SaPI life cycle. Moreover, unlike phage-mediated LT, which is limited to prophage induction, we found that SaPI LT and LcT overcome the limitations of phage-mediated LT. Thus, in addition to occurring during the lysogenic induction of strains that carry a SaPI and a helper prophage, SaPI LT and LcT occur after the infection of SaPI-positive strains, and even after the infection of strains that do not carry a SaPI if the infecting lysate contains both phage and SaPI particles. All these features make *S. aureus* PICIs incredibly powerful transducing agents.

Results

SaPIs mediate lateral transduction

SaPIs package their DNA using strategies like those employed by their helper phages and are also capable of GT.[14] Therefore, we initiated these studies to determine if SaPIs could also engage in LT. To test this, we used the prototypical SaPIbov1,[24] which is clinically relevant because it encodes the genes responsible for the expression of the toxic shock syndrome toxin (TSST-1) and staphylococcal enterotoxins C and L (SEC and SEL). Since the SaPIbov1 *pac* site is positioned in the middle of its genome and promotes unidirectional packaging towards the SaPI toxin genes,[14] we hypothesized that if SaPIbov1 engages in LT, this process would mobilize the bacterial DNA localized downstream (in the directionality of the packaging) of the SaPIbov1 attachment site (*att*C) site at very high frequencies. Importantly, this region contains the vSaα genomic island and phenol-soluble modulins (PSM)α group of toxins (Figure 1A). vSaα is a non-self-mobilizable pathogenicity island that carries an array of 11 genes encoding toxins and lipoproteins involved in host-pathogen interactions,[25-27] and the PSMα secreted peptides are highly cytotoxic to a wide variety of host cells.[28,29]

To test for SaPI LT, we constructed a set of strains containing a detoxified SaPIbov1 marked with a tetracycline resistance gene (*tetM*) in which we chromosomally inserted cadmium-resistance cassettes (Cd^R) at 10 kb upstream or 10 kb and 16 kb downstream of the SaPIbov1 *att*C site as selectable proxies for host gene transfer. If SaPI LT occurs, our hypothesis was that headful packaging initiated by SaPI terminase from the *pac* site of an integrated SaPIbov1 would reach a phage capsid capacity (~105% of the genome unit length of the classical helper phages or 46 kb) at approximately 38 kb

downstream of the SaPIbov1 *att*C, which includes vSaα and PSMα. Therefore, if SaPI LT occurs, we would expect high-frequency transfers of the markers localized downstream of the SaPIbov1 *att*C site, while the transfer of the marker localized upstream of the SaPIbov1 *att*C site would be low-frequency and indicative of GT.

These strains were either lysogenized with SaPIbov1 helper phage 80α or with an isogenic non-helper phage (80α Δ*dut*) deleted for its antirepressor gene and unable to induce SaPIbov1.[7] Next, the SaPIbov1-containing lysogenic derivatives were induced with mitomycin C to trigger the SOS response to activate the resident prophages. In parallel, non-lysogenic SaPIbov1-positive strains carrying the different Cd^R markers were infected with either 80α or 80α Δ*dut*. In both scenarios (prophage induction and phage infection), the resulting lysates were tested as donors of cadmium resistance to a non-lysogenic *S. aureus* strain to determine the existence of SaPI LT.

The lysates resulting from prophage induction were first confirmed for SaPI transduction by selection for tetracycline resistance, and as expected, high-frequency SaPIbov1 transfer required wild-type helper phage for induction (Figures S1D and S1E). Remarkably, and in support of the existence of SaPI LT, the transfers of Cd^R markers localized downstream of the SaPIbov1 *att*C site (+10 kb or +16 kb markers), in the directionality of DNA packaging, were approximately three orders of magnitude greater than that observed for the marker localized upstream of the SaPIbov1 *att*C site (-10 kb marker) that was expected to transfer at low frequency by either phage or SaPI GT (Figures 1A and S2A). These results were mirrored with lysates obtained from infecting the non-lysogenic SaPIbov1 strains with either helper phage 80α or non-helper 80α Δ*dut* (Figure 2A), showing that the initiation of DNA packaging (in situ) occurs during the

infection of SaPI-containing strains, which is indicative of the existence of SaPI-LT. Note that this is an important distinction from phage-mediated LT, which is only known to occur during prophage induction and not after phage infection.[21]

Another important observation was that SaPI LT occurred with or without induction of the SaPI life cycle. While the results with the 80α Δ*dut* (non-helper) phage were predictable since we have previously demonstrated that SaPIs remain integrated into the bacterial chromosome and express $TerS_{SP}$ after non-helper prophage induction or phage infection (depicted in Figure S1B),[14,30] the results after SaPI induction with helper phages were unexpected. SaPIs are thought to excise immediately after induction by helper phages (Figure S1B), [1,2,31] and this predicted that SaPI LT would not occur because the mechanism requires the SaPI genomes to remain integrated into the bacterial chromosome at the time of DNA packaging. These results revealed that our current understanding of the SaPI life cycle is not correct and that it likely follows a different sequence of events. Additionally, since clinical strains often contain SaPIs and helper and non-helper phages, these results expand the relevance of SaPI LT.

To confirm that the increased transfer of the markers downstream of the SaPIbov1 *att*C site occurred by SaPI LT, we repeated the induction and infection experiments using SaPIbov1 elements with their *ter*S genes deleted (SaPIbov1 Δ*ter*S). Our hypothesis was that the SaPI $TerS_{SP}$ is absolutely required to specifically initiate in situ packaging from the SaPI *pac* site. This was supported by our results, which showed that when only the phage $TerS_{\Phi}$ was present in the SaPIbov1 Δ*ter*S lysogens, transfers of the markers downstream of the SaPIbov1 *att*C were significantly reduced to the same levels observed for the transfer of the marker located upstream of the SaPIbov1 *att*C site (Figure 1A).

These results suggested that in these mutants, all the markers were mobilized by phage GT.

An alternative explanation for the above results was that a strong SaPI pseudo-*pac* site nearby in the bacterial chromosome directed the packaging of the downstream marker. To confirm that packaging of the downstream markers initiated from the integrated island, $TerS_{SP}$ was expressed under the control of a tetracycline-inducible promoter in strains lysogenic for 80α with its *ter*S gene deleted (80α Δ*ter*S), with or without SaPIbov1 Δ*ter*S, during prophage induction. SaPI *pac* sites are not embedded in their terminase genes like they are in most phage genomes,[14,32] so a SaPIbov1 Δ*ter*S element can still direct DNA packaging. The resulting lysates were tested for transfer of the +10 kb Cd^R marker, and we found that when $TerS_{SP}$ was expressed, the marker was transferred at the low levels of GT without SaPIbov1 Δ*ter*S but was high frequency with SaPIbov1 Δ*ter*S (Figure S3C). These results confirmed that DNA packaging for SaPI LT was initiated from the SaPIbov1 genome.

SaPI LT is widespread and promotes the high-frequency transfer of large sections of the bacterial chromosome

Because the +10 kb and +16 kb markers transferred at high frequencies, we predicted that the processive packaging machinery would continue for many more headfuls before the transfer frequencies dropped to levels that were indistinguishable from GT. Many SaPIs encode proteins CpmA and CpmB that redirect phage capsomeres to form capsids that are one-third their normal size,[30,33] which means that successive headfuls can be any combination of small and large capsids. Here we used the metric of large capsid capacity to measure the maximum coverage of SaPI LT by inserting Cd^R markers into each

successive phage 80α headful, for seven total downstream markers, in non-lysogenic or lysogenic strains that contain SaPIbov1. We found that for lysates generated by induction or infection, strains that expressed $TerS_{SP}$ transferred all seven downstream headful markers at levels well above GT [Figures 1B (normalized by PFU in S3A), 2C, and S3B]. These results show that SaPI LT can occur during the lysogenic induction or infection of SaPI-containing strains to transfer large sections of the *S. aureus* chromosome at high frequency.

Finally, to broaden the scope of our findings, we investigated if other SaPIs also engage in SaPI LT. This was confirmed, as similar observations were made for several other staphylococcal pathogenicity islands (SaPI1, SaPI2, and SaPIbov2) (Figures S2D to S2G and S3B), showing that SaPI LT is not limited to SaPIbov1.

SaPI LT occurs via infection of naïve host cells

Lytic events that activate SaPI life cycles result in the simultaneous release of both phage and SaPI particles in the infecting lysates. Host cells can then be serially infected: first with SaPI, then by phage, or vice versa. In the instances when SaPI reaches a cell first, we reasoned that the island could mediate LT in a naïve cell that has never contained a SaPI. To test this, we first constructed a strain with a mutated SaPIbov1 *att*C site to serve as a control for transient SaPI integration. Non-lysogenic strains (wt and SaPIbov1 *att*C mutant) with downstream Cd^R markers but lacking SaPIs were infected with SaPIbov1 phage lysates, and the resulting particles were assayed for LT. We found that 80α / SaPIbov1 infection transferred the 4 kb Cd^R marker approximately 22-fold more than 80α alone (Figure 2B), in a manner that required an intact SaPIbov1 *att*C site. However, when we repeated this experiment using helper phage ΦNM1 and SaPIbov1, transfer of the 4

kb Cd^R marker by ΦNM1 / SaPIbov1 infection was 3 orders of magnitude greater than GT in the first headful and remained much higher than GT up to the seventh downstream marker (Figures 2B and 2D). In addition, similar observations were made for SaPI1 and SaPI2 (Figures S2I and S2J). Taken together, the above results show that SaPI LT occurs in the lytic events of SaPI-containing strains and even during the infection of naïve host cells, making it much more versatile than phage LT which is limited to lysogenic induction.

Phage and SaPI lateral transduction combine for chromosome hypermobility

Phage 80α is not just a SaPI helper, but it also mediates high-frequency LT,[21] such that phage and SaPI LT can potentially occur in the same cell. To test this, we created strains carrying Cd^R markers downstream of the 80α *att*B site and Cm^R markers downstream of the SaPIbov1 *att*C site, in the directionality of the packaging for both. These 80α (+4 kb Cd^R) / SaPIbov1 (+4 kb Cm^R) lysogens were induced and the lysates were tested for the transfer of each marker. We found that both Cd^R (phage LT) and Cm^R (SaPI LT) markers were transferred at frequencies several orders of magnitude greater than GT (Figure 3A), showing that phage and SaPI LT can combine to transfer two distinct regions of the host chromosome at high frequencies. To further illustrate the potential of LT, Φ85 / SaPIbov1 / SaPI3 lysogenic strains with upstream (indicative of GT) and downstream (indicative of LT) Cd^R markers for each element were induced and the lysates were tested for the transfer of cadmium resistance. As shown in Figure 3B, phage and SaPI LT were again complementary and transferred three distinct regions of the bacterial chromosome at high frequencies in a single lytic event.

For a more direct visualization of phage and SaPI LT, we purified the infective particles resulting from SOS induction of 80α / SaPIbov1 lysogens and extracted the DNA

for sequencing. The reads were then mapped to the reference *S. aureus* genome NCTC 8325 and quantified based on coverage. We found that most of the encapsidated DNA of bacterial origin mapped to the region next to the SaPIbov1 and 80α attachment sites, in the directionality of packaging for SaPI or phage LT (Figure S4). Together, these results confirm that phage and SaPI LT can combine to promote the massive transfer of chromosomal DNA between bacterial strains.

SaPI delayed excision and escape replication

As previously indicated, the observation that SaPIs mediate LT with helper phages suggested that the current model of SaPI excision and episomal replication early upon induction is not correct; rather, delayed excision and replication in the bacterial chromosome are more likely. Bidirectional replication of an integrated prophage creates genomic redundancy that allows for phage maturation and phage LT to proceed in parallel, and we expected the same to occur with the SaPIs. To determine if SaPIs also replicate prior to excision, we checked for escape replication, which is a term normally used to describe when prophages replicate while still attached to the chromosome and amplify the flanking host DNA. To do this, we induced SaPIbov1 strains lysogenic for 80α with mitomycin C or infected non-lysogenic strains with 80α and collected the total chromosomal DNA over time for whole-genome sequencing. At each time point, we quantified the reads corresponding to SaPIbov1 and the adjacent bacterial DNA and represented them as the coverage relative to the average of the whole genome. SOS induction of helper phage lysogens showed the start of SaPIbov1 replication and amplification of the adjacent host DNA by 60 minutes, followed by robust SaPIbov1 episomal replication and clear amplification of the chromosomal DNA by 120 minutes

(Figure 4A), confirming that SaPIbov1 replicates in the chromosome before excision. As expected, in non-helper phage lysogens, SaPIbov1 DNA was in line with the chromosomal average at all time points because SaPI was not induced (Figure 4B). Furthermore, parallel results were observed with the infection of non-lysogenic strains (Figures 4C and 4D). By comparison, the DNA of both helper and non-helper phages showed clear escape replication by 60 to 120 minutes after induction but not by infection (Figure S5). These results confirmed that following helper phage induction, SaPIbov1 initiated bidirectional replication while still attached to the chromosome and amplified the adjacent host DNA, creating the genomic redundancy needed to allow the SaPI life cycle and SaPI LT to proceed in parallel.

SaPI lateral cotransduction

Different types of particles are generated either by the induction of a strain carrying a helper prophage and a SaPI or by the infection of a SaPI-positive strain with a helper phage. Most of these contain either phage or SaPI DNA, but there are also many transducing particles that contain bacterial DNA packaged by phage or SaPI LT. The existence of this mixed population raises the possibility that a recipient can receive DNA from two different types of transducing particles. First, we tested for the frequency of a host cell receiving both types of lateral-transducing particles from a lysate of an 80α (+4 kb Cd^R) / SaPIbov1 *tsst*::*tetM* (+4 kb Cm^R) lysogen. This was done by selecting for recipients of one marker and then scoring for the other. No transductants were obtained that had acquired both chromosomal markers (Table S1), indicating that recipients of both phage (Cd^R) and SaPI (Cm^R) LT events are extremely rare (at this level of detection). Next, we tested for recipients of SaPI transfer and phage or SaPI LT. When we selected

for the tetracycline resistance (Tet^R) of SaPIbov1 *tsst*::*tetM*, we did not obtain any transductants that also received the phage (Cd^R) or SaPI (Cm^R) LT marker. This was expected, given that SaPIbov1 transfer frequencies are generally several orders of magnitude greater than those of phage and SaPI LT (Figures S1D and 3A). Next, when we reversed the order and selected for phage LT first, we still did not observe any transductants with SaPIbov1; but when we selected for SaPI LT (markers +4 or +10 kb Cm^R) first, more than 70% of the transductants had also acquired the island (Figure 5A). Of note, SaPIbov1 cotransduction occurred with a Cm^R marker (+20 kb) inserted after vSaα (Figure S6D), showing that both islands cotransduce to the same recipient cell at high frequencies. Furthermore, lateral cotransduction was also observed with lysates from infections of SaPIbov1-positive strains and naïve infections (Figure 5A). Parallel results were also observed for SaPI1, SaPI2, SaPIbov5, and SaPI PT1028 (Figures S6A and S6B).

Importantly, SaPI cotransduction required a helper phage (Figure 5A), which indicated that induction of the SaPI life cycle was necessary; however, the frequency seemed too high to be the result of two transduction events. To confirm this, we deconstructed the donor lysate to require two events for cotransduction by producing SaPIbov1 or SaPI lateral-transducing particles in separate strains and combining them to form a lysate with both particles in the same ratios as when they are induced from a single lysogenic SaPI-positive strain. The reconstituted lysate was high frequency for SaPIbov1 transfer and SaPI LT, but the SaPI LT transductants were no longer positive for SaPIbov1 (Figure S6C), showing that cotransduction did not occur by two independent events. This result was reiterated when we tested for SaPI cotransduction with Cm^R markers in

additional SaPI LT headfuls (Figure 5A and S6C). Selection for markers in the second or third SaPI LT headful did not result in cotransduction of the island, and because these lysates also contained high titers of both types of particles, they also confirmed that cotransduction does not occur by two events. These results showed that cotransduction occurs by a single particle in the first headful. Therefore, activated SaPIs mediate a form of LT with the added feature of SaPI cotransduction that we henceforth refer to as SaPI lateral cotransduction (LcT).

Molecular basis of SaPI lateral cotransduction

We considered two possible mechanisms that could account for LcT: aberrant excision or DNA packaging from tandem SaPIs. The formation of specialized-transducing particles is a classic example of aberrant excision, which typically occurs at extremely low frequencies and results in defective particles.[18,19] However, SaPI cotransduction was high-frequency and the islands were intact and functional (Figure S6E), so it seemed unlikely that aberrant excision was responsible for LcT.

Phage genomes packaged by the headful mechanism are terminally redundant and contain repeated sequences at each end.[13] Upon injection into a new cell, recombination between DNA containing these sequences generates the circular genome that is important for DNA replication or integration. Based on the importance of terminal repeats to the phage life cycle, we reasoned that LcT could occur by a mechanism in which helper phage induction results in transiently tandem SaPI genomes in the host chromosome (addressed below), whereby terminase initiation from the upstream SaPI element would package roughly 1.5 times a SaPI genome unit length before reaching the adjacent host DNA (Figure 5B). In the case of SaPIbov1, this would fill a large capsid with

one genome unit flanked by redundant sequences (in direct repeat) attached to the entire vSaα before reaching headful capacity. To test for transiently tandem SaPIs, we looked for changes in the headful demarcation by a SaPI-sized insertion. We paired a downstream Cm^R marker (+10 kb) with either of two downstream Cd^R markers (+20 kb and +25 kb) that are well within a headful capacity when there is a single SaPIbov1, but would be in two different headfuls when there are tandem islands, and looked for changes in the genetic linkage of the two markers by SaPI LT. To focus on large capsid headful capacity by SaPI LT, we used 80α Δ*ter*S / SaPIbov1 Δ*cpm*AB lysogens that were not capable of phage GT and small capsid formation. These strains were induced and tested for cotransduction of the two markers. We found that the Cm^R marker was strongly linked to both Cd^R markers with the non-helper phage 80α Δ(*dut*, *ter*S), but not with the helper phage 80α Δ*ter*S (Figure 5C), indicating that the two markers were mostly in different headfuls when the SaPIbov1 life cycle was induced. These results are consistent with an LcT mechanism that involves transiently tandem SaPIs.

Induction of the SaPI life cycle but not the formation of classical SaPI particles was required for LcT, indicating that excision and replication were involved. To confirm this, we tested for LcT of the +4 kb Cm^R marker with SaPIbov1 deletions of primase-replicase Δ(*pri-rep*), excisionase (Δ*xis*), or integrase (Δ*int*) and found that LcT required all three activities (Figure 6A). Of note, LcT was only observed when integrase was supplied in both donor and recipient cells, indicating that the SaPI DNA was sufficiently redundant to circularize in the recipient for site-specific recombination.

Based on these results, we considered two ways tandem SaPI genomes could be formed following escape replication: reintegration of an episomal SaPI in a place that

already contains a SaPI or a bridging excision reaction (illustrated in Figure 6B) in which the *att*R of one SaPI recombines with the *att*L of another SaPI. In the first proposed mechanism, it seemed possible that a SaPI that had excised following escape replication could reintegrate next to an integrated island at an *att*L or *att*R site; although, stably tandem SaPIs have never been observed in any *S. aureus* genome sequenced to date. To test if SaPIs can form tandems by integration, we transduced SaPIbov1 *tsst*::*tetM* into a strain that contains an integrated SaPIbov1 Δ*tsst*::*ermC*. When we selected for the incoming SaPIbov1 *tsst*::*tetM*, only 1 out of 300 transductants was positive for both islands (Table S2). However, whole genome sequencing revealed that the double-positive transductant contained islands at two different locations and not in tandem (Figure S6F). Therefore, SaPIbov1 does not detectably insert into SaPIbov1 *att*L and *att*R sites and it seems unlikely that tandem islands are formed by SaPI reintegration.

The second putative mechanism for tandem SaPI formation is a bridging excision reaction in which the *att*L and *att*R of two different islands in parallel chromosomal tracks are paired so that recombination between the two sites joins two SaPIs rather than excising one from the chromosome. To determine if intermolecular joining occurs, we used polymerase chain reaction (PCR) to amplify the fusion joints of transiently formed tandem SaPIbov1 islands. To distinguish the fusion joints of tandem SaPIs (formed by intermolecular joining) from those of circularized genomes or concatamers generated from rolling-circle replication, we used two different SaPIbov1 genomes with unique primer binding sites: primer 1875 only anneals to SaPIbov1-1875 and elongates toward the *att*R, and primer 1848 only anneals to SaPIbov1-1848 and elongates toward the *att*L. This primer pair was designed to generate a PCR product only when SaPIbov1-1875 and

SaPIbov1-1848 are joined. Next, in a non-lysogenic strain with SaPIbov1-1875 in the native SaPIbov1 *att*C site, we inserted a second SaPIbov1 *att*C site 4 kb downstream. We then integrated SaPIbov1-1848 at the second SaPIbov1 *att*C site so that it has intact *att*L and *att*R sites (Figure 6C). This strain was infected with phage for one hour, the cells were lysed, and the genomic DNA was analyzed by PCR. Primers 1875 and 1848 amplify a 6.2 kb product if no intermolecular joining occurs, and a 1.6 kb product if the two SaPIs are joined. PCR analysis of the infected cells showed that the two SaPIs joined after infection with helper phage 80α, but not with non-helper 80α Δ*dut* or mock infection (Figure 6C). These results confirmed that intermolecular joining occurs between SaPIs; however, they did not distinguish if SaPIs from different genomic tracks were joined.

To determine if SaPIs are joined from different genomic tracks, we used phage LT to deliver bacterial DNA that contains an integrated SaPIbov1 to emulate a parallel DNA strand of an integrated SaPI undergoing escape replication. The SaPIbov1 *att*C site is in the third LT headful of helper prophage Φ52a, so we constructed a strain with SaPIbov1-1958 that has a unique binding site for primer 1958 but is deleted for integrase and is completely unable to excise. This SaPI-positive strain was then lysogenized with a non-helper phage derivative of phage Φ52a (Φ52a Δ*dut*), which is not capable of inducing SaPIbov1 in the donor or recipient strain, and the lysogenic derivative strain was induced to produce a lysate with LT particles containing unexcised SaPIbov1-1958 still attached to bacterial DNA. This lysate was used to infect lysogenic strains carrying SaPIbov1-1848 that were induced for 1 hour prior to infection and the genomic DNA was analyzed by PCR with primers 1958 and 1848. Primers 1958 and 1848 can only make a product if SaPIbov1-1958 and SaPIbov1-1848 are covalently joined. PCR analysis of induced

recipient cells infected with the Φ52a Δ*dut* / SaPIbov1-1958 lysate showed that the two SaPIs were joined in strains lysogenic for helper phage 80α but not with non-helper 80α Δ*dut* (Figure 6D). No PCR product was observed with infections of phage Φ52a Δ*dut* alone, showing that the primers were specific for tandem genomes created by genomic track switching and not rolling-circle replication of a circular SaPI genome.

For additional confirmation of genomic track switching, we next used Nanopore long-read sequencing to capture transiently tandem SaPI genomes in the bacterial chromosome. To avoid inundating the reads with helper phage DNA, we induced the life cycle of SaPIbov1 in a non-lysogenic strain by simultaneously activating the SOS response and expressing 80α dUTPase (the SaPIbov1 antirepressor) from a tetracycline-inducible promoter. Reads that were long enough to capture tandem SaPIs were relatively rare, but we identified 17 individual reads of SaPI concatamers (14 tandem, 2 triple, and 1 quadruple) that were still connected to the bacterial chromosome (Figures S7A to S7C). None of the reads contained host DNA repeated or interspersed between SaPI genomes, indicating they were not the result of rolling-circle replication of aberrantly excised genomes. Taken together, the above results are consistent with the model that bridging excision reactions catalyze genomic track switching that transiently concatamerizes post-replicative SaPI genomes in the bacterial chromosome.

Population analysis reveals genomic signatures of virulence gene transfer by SaPI LT

Our in vitro experimental analysis showed that SaPI LT transferred markers inserted into the genomic island vSaα at high frequencies. vSaα is an integral region of the *S. aureus* genome found in virtually all strains examined.[26] It contains large clusters of genes

involved in innate immune evasion (staphylococcal superantigen-like proteins; SSLs), immune modulation, and invasion (lipoproteins).[34] Of note, the SSLs comprise a large family of proteins with distinct receptor tropisms and functions in evading or inhibiting the innate immune response.[27] Our findings reveal a mechanism of transfer for this key virulence-associated genetic element that was previously considered immobile. To determine if this mode of gene transfer has a broader impact on natural *S. aureus* populations, we looked for elevated levels of variation in gene content and synteny in the regions downstream of SaPI *att*C sites that could result from recombination events between the chromosome and gene fragments transferred by SaPI LT. There are 5 chromosomal sites of integration for SaPIs (SaPI-I to SaPI-V) that are highly conserved across the *S. aureus* species diversity.[35] Here we examined the extent of allelic variation at the three chromosomal regions flanking SaPI-II, SaPI-III/SaPI-IV, and SaPI-V. A pangenome analysis of 235 *S. aureus* genome sequences representative of the species diversity was carried out followed by graphical visualization of each region (Figure 7). The resulting networks represent a summary of the variation in gene content and organization that occurs at each region across the *S. aureus* species diversity.

Extensive variation in the regions downstream of each site was observed, particularly in the genomic island vSaα. Notably, these regions displayed distinct combinations of genes encoding proteins involved in host-pathogen interactions, indicating that they represent hot spots for genomic diversification. The presence of loops or reticulation in the network implies that rearrangements, insertions, or deletions have occurred in regions of the genome impacted by SaPI-LT. Of note, regions downstream of SaPI-III/SaPI-IV (Fig 7 C) and SaPI-V (Fig 7 D) also contain phage integration sites and

resulted in highly complex networks reflecting variation in gene content in integrated phages. We propose that SaPI LT may promote the recombination and reassortment of integrated phage sequences between strains, thereby accelerating phage diversification. Taken together, these data are consistent with the idea that the observed differences in gene content and synteny, as well as the reassortment of virulence gene combinations among natural populations of clinical *S. aureus* isolates, can be attributed to recombination events between the chromosome and DNA transferred by SaPI LT.

Discussion

SaPI life cycles are thought to occur above the chromosome, where rolling-circle replication generates the concatemers needed to package terminally redundant genomic DNA into capsids to form mature SaPI particles.[31] Here we have discovered an unrecognized stage in the SaPI lifecycle that occurs in the chromosome and is complexed with a form of lateral transduction. In our model (Figure S7D), replication prior to excision creates SaPI genomes on parallel tracks that are identical and thus indistinguishable to SaPI excisionase proteins. The pairing of SaPI *att*L and *att*R repeats on the same strand results in an excision event, while recombination between repeats on different tracks joins SaPI genomes to form tandems and concatamers in the chromosome. From these polymeric structures, LT initiates to mobilize large sections of the genome while producing mature SaPI particles with intact genomes joined to host accessory genes – all in parallel to the normal SaPI life cycle that occurs above the chromosome after late excision. For LcT by SaPIbov1, roughly 1.5 SaPIbov1 genomes connected to the vSaα island are packaged and transferred together in a single particle. Upon injection of the hybrid DNA into a new cell (Figure S7E), SaPIbov1 DNA undergoes circularization through a single

crossover event between repeated sequences and integrates into a SaPIbov1 *att*C site, whereas the vSaα island can be acquired or exchanged via homologous recombination with the host chromosome.

Recent studies have demonstrated that GT benefits temperate phages by providing adaptive power to their hosts.[36,37] However, most phages do not benefit directly from their actions since their genomes are rarely delivered intact to the recipients of host genes. This is because bacterial DNA carried in transducing particles usually replaces all or part of the viral genome; though there are special exceptions, such as phage Mu, whose genome is packaged as a monomer flanked by short bits of host DNA.[38,39] By comparison, SaPI LT drives the massive mobility of large sections of the chromosome at extremely high frequencies to provide adaptive power to host cells, while LcT enables SaPI elements to benefit directly from their own host gene transfer by delivering their genomes intact and attached to chromosomal DNA in the same particle. Furthermore, SaPIs are common in *S. aureus* genomes and most of them occupy one of five chromosomal attachment sites (Table S3);[2,40] therefore, LcT can pair many different SaPIs with the same chromosomal region, creating diverse combinations of virulence and accessory genes that can be mobilized as single genetic units.

For the SaPIs, size matters, and maintaining a small genome appears to be more of a strategy than a coincidence. Many SaPIs encode proteins that divert a percentage of phage virion proteins to form SaPI-sized capsids that are too small for the larger helper phage genomes.[30,33] Now with LcT, small SaPI genomes can package more than one unit length in a phage capsid and still leave room for over 20 kb of bacterial accessory genes; as in the case of SaPIbov1, which is small enough to include the entire vSaα

island from the chromosome so that both elements are mobilized intact in the same infective SaPI particle. Then upon injection into a new host cell, the expanded SaPI genomes circularize by recombining between the repeated sequences and integrate into an *att*C site, regaining their original genome size. Thus, LcT enables SaPIs to exploit the genetic capacity of the host chromosome to store accessory and virulence genes so that they can remain small.

Transduction is driven by phages, or so we thought. Here we identified and characterized a powerful mechanism of transduction mediated by pathogenicity islands, showing that transduction is no longer the exclusive domain of phages. We found that SaPI LT and LcT occur during lysogenic induction, infection of SaPI-containing strains, and the infection of strains that do not carry a SaPI, which makes them portable and more versatile than phage LT that has only been observed during prophage induction. We note that this study is the first report of a pathogenicity island mediating lateral transduction and the first demonstration of two unrelated pathogenicity islands mobilized together in a single gene transfer event to the same recipient cell, as well as the first to show a functional transducing agent mobilized together with large pieces of chromosomal DNA.

A notable aspect of SaPI regulation is that $TerS_{SP}$ is expressed with both helper and non-helper phages. This means that any lytic interaction with a phage could potentially lead to the high-frequency transmission of hundreds of kb of the host chromosome downstream of a SaPI, regardless of the phage DNA-packaging specificity. Such massive transfers enable core genes and chromosomal islands that are typically immobile to become highly mobile. Furthermore, SaPI LT can be considered analogous to other host-beneficial accessory functions, such as toxins and virulence factors

commonly encoded by pathogenicity islands, since $TerS_{SP}$ expression is not tied to the SaPI life cycle.

Our population genomic analysis provides evidence for the historical impact of SaPI LT on the *S. aureus* genome. Specifically, the co-incidence of SaPI integration sites with downstream chromosomal islands containing arrays of virulence-associated genes has provided the opportunity for the transfer of key mechanisms of innate immune evasion and cellular invasion. SaPI LT-mediated gene re-assortment could lead to the generation of novel combinations of genes that are beneficial to the recipient.[41] Furthermore, hybrid gene variants with attenuated or novel functions may be formed that may confer enhanced fitness in a particular niche.[42] In conclusion, our results show that SaPIs mediate dynamic and powerful forms of gene transfer and they are one of the most important drivers of pathogen evolution.

Limitations of the study

To our knowledge, genomic track switching is the first report of a mechanism that generates DNA concatamers in the bacterial host chromosome. This finding re-writes SaPI life cycles, and we predict it will also apply to the life cycles of many other chromosomal genetic elements. Here we have used SaPIs as our model system, which are prototypical members of the PICIs. However, we now know that PICIs and other phage satellites are widespread and common in gram-positive and gram-negative bacteria.[3-5] It would be important to determine whether other PICIs also engage in PICI lateral and lateral cotransduction. Another point that requires further investigation is to determine both the advantages that SaPIs confer in promoting LT and LcT, as well as the benefits for the SaPIs themselves. Additional studies are required to fully understand the

impact of these processes on the ecology and evolution of the clinically relevant *S. aureus*.

ACKNOWLEDGMENTS:

Funding: This work was supported in part by the Singapore Ministry of Education grants MOE2017-T2-2-163 and MOE2019-T2-2-162 to J.C.; by grants MR/M003876/1, MR/V000772/1, and MR/S00940X/1 from the Medical Research Council (UK), BB/V002376/1 and BB/V009583/1 from the Biotechnology and Biological Sciences Research Council (BBSRC, UK), and EP/X026671/1 from the Engineering and Physical Sciences Research Council (EPSRC, UK) to J.R.P.; by Biotechnology and Biological Sciences Research Council institute strategic grant funding (ISP2) (BB/P013740/1) to J.R.F.; and by Wellcome Trust 201531/Z/16/Z to J.R.P. and J.R.F.

AUTHOR CONTRIBUTIONS: J.C. and J.R.P. conceived the study. M.S.J.C., E.S., and Y.N.C. conducted the experiments. J.H-L., R.B., R.M., and J.R.F. performed the genomic analyses. J.C. and J.R.P. wrote the manuscript.

DECLARATION OF INTERESTS:

The authors declare no competing interests.

INCLUSION AND DIVERSITY:

We support inclusive, diverse, and equitable conduct of research.

MAIN FIGURE TITLES AND LEGENDS

Figure 1. SaPIs transfer large spans of the chromosome at high frequencies by lateral transduction.

(A) Transfer of Cd^R markers (purple) 10 kb upstream or downstream of SaPIbov1 *att*C by prophage induction. SaPIbov1 strains lysogenic for helper 80α or non-helper 80α Δ*dut* phage (Φ represents either phage) were SOS induced to generate lysates (top). Prediction for in situ DNA packaging initiated from the *pac* site (red) of an integrated SaPIbov1 (bottom). DNA packaging is unidirectional to the right and the headful limit is ~38 kb downstream of the SaPIbov1 *att*C and includes vSaα and PSMα.
(B) Transfer of Cd^R markers (purple) in seven successive headfuls by prophage induction. SaPIbov1 strains lysogenic for 80α were SOS induced to generate lysates.
(A and B) Lysogenic SaPIbov1 (Sb1) strains or *ter*S deletion (Δ*ter*S) derivatives were induced with mitomycin C and the resulting lysates were tested for transduction into *S. aureus.* Transduction units (TrU) per milliliter (ml) are represented as the log TrU per milliliter of lysate. TrU per milliliter amounts for all phage / SaPI double *ter*S deletion mutants were <10. Values are means (*n* = 3 independent samples). Error bars indicate standard deviation.

Figure 2. SaPI lateral transduction mobilizes the genome of non-lysogenic host strains.

(A) Transfer of Cd^R markers 10 kb downstream of SaPIbov1 *att*C by phage infection. Non-lysogenic strains without SaPI (No SaPI), carrying SaPIbov1 (Sb1), or a SaPIbov1 *ter*S deletion (Sb1 Δ*ter*S) were infected with helper 80α or non-helper 80α Δ*dut* phage to generate lysates.
(B) Transfer of Cd^R markers 4 kb downstream of the SaPIbov1 *att*C by naïve infection. Non-lysogenic strains without SaPI and intact SaPIbov1 *att*C (Cd^R_1) or mutated *att*C (Cd^R_1*) were infected with helper phage only (80α or ΦNM1) or helper phage / SaPIbov1 (80α / Sb1 or ΦNM1 / Sb1) to generate lysates.
(C) Transfer of Cd^R markers (purple) in seven successive capsid headfuls by infection. Non-lysogenic SaPIbov1 strains were infected with 80α phage to generate lysates.
(D) Transfer of Cd^R markers (purple) in seven successive capsid headfuls by naïve infection. Non-lysogenic strains without SaPI were infected with ΦNM1 phage only or ΦNM1 / SaPIbov1 to generate lysates.
(A to D) The resulting lysates were tested for transduction into *S. aureus.* Transduction units (TrU) per milliliter were normalized by plaque-forming units (PFU) per milliliter and represented as the log TrU of an average phage titer (1×10^{10} PFU). For all panels, values are means (*n* = 3 independent samples). Error bars indicate standard deviation.

Figure 3. SaPI lateral transduction complements phage lateral transduction.

(A) Simultaneous transfer of phage 80α and SaPIbov1 LT markers. SaPIbov1 *tsst*::*tetM* (Sb1) strains lysogenic for helper 80α phage or *ter*S deletion (Δ*ter*S) derivatives with both 80α phage Cd^R lateral transduction markers 4 kb downstream of the 80α *att*B and SaPIbov1 Cm^R lateral transduction markers 4 kb downstream of the SaPIbov1 *att*C site were induced with mitomycin C.

(B) Simultaneous transfer of phage Φ85, SaPIbov1, and SaPI3 LT markers. Strains lysogenic for Φ85 phage or Φ85 / SaPIbov1 *tsst*::*tetM* (Sb1) / SaPI3 *seb*::*ermC* (S3) with Cd^R markers 10 kb upstream and 9 kb downstream of the Φ85 *att*B or 11 kb upstream and 10 kb downstream of the SaPIbov1 *att*C site or 3 kb upstream and 4 kb downstream of the SaPI3 *att*C site were induced with mitomycin C.
(A and B) The resulting lysates were tested for transduction into *S. aureus.* Transduction units (TrU) per milliliter are represented as the log TrU per milliliter of lysate. Values are means (*n* = 3 independent samples). Error bars indicate standard deviation.

Figure 4. Activated SaPIs replicate in the host chromosome prior to excision.
SaPIbov1 escape replication during helper phage induction or infection. Relative abundance of SaPIbov1 DNA and the chromosome flanking the SaPIbov1 *att*C site. The chromosomal position of SaPIbov1 is indicated in grey. Samples were analyzed at 0 (red), 30 (light blue), 60 (green), and 120 minutes (dark blue) after the induction (Ind) of lysogenic strains (A) helper 80α / SaPIbov1 and (B) non-helper 80α Δ*dut* / SaPIbov1 with mitomycin C or the infection (Inf) of non-lysogenic SaPIbov1 strains with (C) 80α or (D) 80α Δ*dut* phage.

Figure 5. SaPIs cotransduce with adjacent bacterial DNA and form transient tandems in the host chromosome.
(A) Cotransduction of SaPIbov1 with Cm^R markers 4 kb, 10 kb, or headful 2 (HF2) downstream of the SaPIbov1 *att*C. SaPIbov1 *tsst*::*tetM* (Sb1) lysogenic strains were induced with mitomycin C (Ind), non-lysogenic SaPIbov1 *tsst*::*tetM* strains were infected with phage only (Inf), or non-lysogenic strains without SaPI were infected with helper phage / SaPIbov1 *tsst*::*tetM* (Naïve Inf) and the resulting lysates were tested for cotransduction into *S. aureus*.
(B) Predictions for SaPI LT with SaPIbov1 or SaPIbov1::*tetM* as singles or tandems with headful (HF) limits.
(C) Cotransduction of two markers downstream of SaPIbov1 *att*C. SaPIbov1 *tsst*::*tetM* Δ*cpmAB* strains lysogenic for 80α Δ*ter*S or 80α Δ(*dut, ter*S) phage with a Cm^R marker at 10 kb and a Cd^R marker at 20 kb or 25 kb were induced with mitomycin C and the lysates tested for cotransduction. Headful limits for a single [HF(Sb1)] or tandem [HF(Sb1-Sb1)] island are indicated.
(A and C) For each replicate, 100 Cm^R transductants were tested for Tet^R or Cd^R and the percent cotransduction frequency was represented as (Tet^R or Cd^R / Cm^R) x 100. Values are means (*n* = 3 independent samples). Error bars indicate standard deviation.

Figure 6. Activated SaPIs undergo genomic track switching to form concatamers in the host chromosome.
(A) Cotransduction of SaPIbov1 mutants with Cm^R markers 4 kb downstream of the SaPIbov1 *att*C. SaPIbov1 *tsst*::*tetM* Δ(*pri-rep*), Δ*xis, and* Δ*int* mutants lysogenic for 80α were induced with mitomycin C and anhydrotetracycline (ATc) was added for complementation by P_{tet}-*pri-rep*$^+$, P_{tet}-*xis*$^+$, or P_{tet}-*int*$^+$, respectively. The cells were mechanically lysed, and the lysates were tested for cotransduction into *S. aureus* or a recipient that constitutively expresses SaPIbov1 integrase (Δ*int*-c). For each replicate,

100 Cm^R transductants were tested for Tet^R and the percent cotransduction frequency was represented as (Tet^R / Cm^R) x 100. Values are means (*n* = 3 independent samples). Error bars indicate standard deviation.
(B) Two types of excision reactions. The SaPIbov1 genome (light blue) replicates in the host chromosome creating parallel DNA tracks. Normal excision occurs between the *att*L and *att*R on the same strand (bottom). Bridging excision occurs between the *att*L and *att*R on different strands, resulting in track switching that joins two SaPIs head to tail (top).
(C and D) Genomic track switching forms tandem SaPIs. Lane 1 is the 1 kb DNA ladder for both.
(C) Non-lysogenic strains with SaPIbov1-1875 at SaPIbov1 *att*C and SaPIbov1-1848 at the engineered +4 kb SaPIbov1 *att*C site were infected with 80α, 80α Δ*dut,* or mock. PCR analysis with primers 1848 and 1875 amplifies a 1.6 kb product for tandems and 6.2 kb for no tandems.
(D) SaPIbov1-1848 lysogens were induced and infected with lysates from Φ52A Δ*dut* or Φ52A Δ*dut* / SaPIbov1-1958 induced lysogens. SaPIbov1-1958 is deleted for integrase. PCR analysis with primers 1848 and 1958 amplifies a 2.0 kb product if track switching occurs. Primers 1845 and 1848 amplifies a 1.1 kb control.

Figure 7. Gene synteny networks demonstrating allelic variation downstream of SaPI integration sites.
(A) Schematic representation of the *S. aureus* genome indicating the SaPI (green) and phage (red) integration sites analyzed in B to D. Arrows indicate the regions included in the network analysis and the direction of packaging by SaPI LT.
(B) Gene synteny network for the region SaPI-II to the pathogenicity island vSaα.
(C) Gene synteny network for the region SaPI-III/SaPI-IV, encompassing phage integration sites Sa1 and Sa4 (red). Note that the region start (*) is prior to SaPI-III (at 801,747 bp, RF122), but thresholds applied to the network have resulted in a division of this section at a high multiplicity node within SaPI-III (see Methods).
(D) Gene synteny network for the region SaPI-V, encompassing phage integration sites Sa3 and Sa5 (red).
(B to D) Each node represents an allelic variant as defined at the 95% identity threshold, with node size representative of the number of genomes in which the allele is present. Edge thickness represents the number of genomes in which a given pair of alleles neighbor one another. Colors represent the key genomic features, as labelled, which were identified with reference to the strain RF122. Network visualization was created using Graphia v3.0. The distribution of SaPI elements at each SaPI integration site can be found in Table S3.

Supplemental figure titles and legends 1 to 7

Figure S1. High-frequency SaPI transfer requires helper phages, related to Figure 1.

(A) Prophages in lysogenic strains are maintained under repression by their CI repressor proteins (top). The phage lytic cycle (bottom). Phage infection of a sensitive host strain or prophage induction by the SOS response activates the lytic cycle (progresses left to right). Upon induction, prophages first replicate bi-directionally in the host chromosome. The phage genome circularizes episomally and undergoes DNA replication to form long head-to-tail concatemers. The phage DNA-packaging machinery is comprised of the small terminase (TerS), large terminase (TerL), and portal proteins.
(B) SaPI elements in lysogenic strains are repressed by the SaPI Stl master repressor and the host LexA protein (top). The current model for SaPI life cycles (progresses left to right). Helper phages express antirepressor proteins in their lytic cycles (full lytic cycle shown in S1A) that activate SaPI life cycles, resulting in the production of both phage and SaPI particles in the same host cell (middle). The SaPI small terminase ($TerS_{SP}$) proteins complex with phage TerL proteins to form terminase enzymes that now recognize SaPI *pac* sites. Non-helper phages do not encode antirepressor proteins and are unable to activate the SaPI life cycle, so only phage particles are produced (bottom). Of note, the SOS response removes LexA repression, and $TerS_{SP}$ proteins are expressed with helper and non-helper phages.
(C) Model for in situ DNA packaging initiated from the *pac* site of an integrated SaPIbov1. The first phage headful limit is ~38 kb downstream of the SaPIbov1 *att*C and includes vSaα and PSMα. Chromosomal markers were inserted 4 kb, 10 kb, 20 kb, and 25 kb downstream of the SaPIbov1 *att*C.
(D) SaPIbov1 *tsst*::*tetM* strains lysogenic for helper 80α or non-helper 80α △*dut* phage were induced with mitomycin C.
(E) Non-lysogenic SaPIbov1::*tetM* strains were infected with 80α or 80α △*dut* phage.
(D and E) The resulting lysates were tested for plaque formation or SaPI transduction into *S. aureus.* The *ter*S genotypes are indicated as WT (+) and deletion (Δ). No SaPI (NS) is indicated. The results are represented as SaPI-specific transductants (SPST) per milliliter or plaque-forming units (PFU) per milliliter. PFU per milliliter for all phage *ter*S deletion mutants or SPST per milliliter amounts for all phage / SaPI double *ter*S deletion mutants were <10. Values are means (n = 3 independent samples). Error bars indicate standard deviation.

Figure S2. SaPIs mediate lateral transduction during prophage induction, phage infection, and naïve infection, related to Figure 2.

(A to E) SaPI lateral transduction by prophage induction.
(A) SaPIbov1 *tsst*::*tetM* strains lysogenic for helper 80α or non-helper 80α △*dut* phage (Φ represents either phage) with Cd^R markers 16 kb downstream of the SaPIbov1 *att*C were induced with mitomycin C.
(B) SaPIbov1 *tsst*::*tetM* strains lysogenic for 80α or 80α △*dut* with Cm^R markers 4 kb downstream of the SaPIbov1 *att*C were induced with mitomycin C.
(C) SaPIbov1 Δ*tsst*::*tetM* Δ(*sec-sel*) strains lysogenic for 80α or 80α △*dut* with Cm^R markers 20 kb downstream of the SaPIbov1 *att*C were induced with mitomycin C.

(D) SaPI1 *tsst*::*tetM* strains lysogenic for helper 80α tested for the transfer of Cd^R markers 3 kb upstream or 4 kb downstream of the SaPIbov1 *att*C were induced with mitomycin C.
(E) SaPI2 *tsst*::*tetM* strains lysogenic for 80α tested for the transfer of Cd^R markers 4 kb downstream of the SaPIbov1 *att*C were induced with mitomycin C.
(F and G) SaPI lateral transduction by infection.
(F) SaPI1 *tsst*::*tetM* non-lysogenic strains with Cd^R markers 3 kb upstream or 4 kb downstream of the SaPIbov1 *att*C were infected with 80α.
(G) SaPI2 *tsst*::*tetM* non-lysogenic strains with Cd^R markers 4 kb downstream of the SaPIbov1 *att*C were infected with 80α.
(H to J) SaPI lateral transduction by naïve infection. Non-lysogenic strains without SaPI were infected with (H) ΦNM1 or ΦNM1 / SaPIbov1, (I) 80α or 80α / SaPI1, and (J) 80α or 80α / SaPI2.
(A and D to G) The resulting lysates were tested for transduction into *S. aureus.* Transduction units (TrU) per milliliter are represented as the log TrU per milliliter of lysate. TrU per milliliter amounts for all phage / SaPI double *ter*S deletion mutants (gray) were <10. Values are means (*n* = 3 independent samples). Error bars indicate standard deviation.
(B, C, H to J) The resulting lysates were tested for transduction into *S. aureus.* TrU per milliliter were normalized by plaque-forming units (PFU) per milliliter and represented as the log TrU of an average phage titer (1×10^{10} PFU). For all panels, values are means (*n* = 3 independent samples). Error bars indicate standard deviation.

Figure S3. SaPI lateral transduction mobilizes large regions of the host chromosome and SaPI terminase is essential for high-frequency SaPI lateral transduction, related to Figure 3.
(A and B) Strains lysogenic for 80α tested for the transfer of Cd^R markers in seven successive headfuls for (A) SaPIbov1 and (B) SaPIbov2. Strains were induced with mitomycin C and the resulting lysates were tested for transduction into *S. aureus.* Transduction units (TrU) per milliliter were normalized by plaque-forming units (PFU) per milliliter and represented as the log TrU of an average phage titer (1×10^{10} PFU). For all panels, values are means (*n* = 3 independent samples). Error bars indicate standard deviation.
(C) Strains lysogenic for helper 80α △*ter*S or non-helper 80α △(*dut, ter*S) phage with or without SaPIbov1 *tsst*::*tetM* △*ter*S and Cd^R markers 10 kb downstream of the SaPIbov1 *att*C were induced with mitomycin C and the resulting lysates were tested for transduction into *S. aureus.* Anhydrotetracycline (ATc) was added at the same time for complementation by P_{tet}-*ter*S_{Sb1}. The resultant lysates were tested for transduction into *S. aureus.* Transduction units (TrU) per milliliter are represented as the log TrU per milliliter of lysate. TrU per milliliter amounts for no complementation (-ATc) were <10. Values are means (*n* = 3 independent samples). Error bars indicate standard deviation.

Figure S4. A direct visualization of lateral transduction by analyzing the capsid DNA extracted from purified phage and SaPI particles, related to Figure 4.

(A and B) SaPIbov1 strains lysogenic for helper 80α or non-helper 80α Δ*dut* phage were induced (Ind) with mitomycin C and the resulting phage and SaPI particles were purified.
(C and D) Non-lysogenic strains carrying SaPIbov1 were infected (Inf) with 80α or 80α Δ*dut* phage and the resulting phage and SaPI particles were purified.
(A to D) The DNA from the phage and SaPI particles were extracted and sequenced. The coverage of chromosomal DNA is represented for (A) 80α and 80α Δ*dut* inductions, (B) SaPIbov1 with helper phage (SaPIbov1) and non-helper phage [SaPIbov1(Δ*dut*)] inductions, (C) 80α and 80α Δ*dut* infections, and (D) SaPIbov1 with helper phage (SaPIbov1) and non-helper phage [SaPIbov1(Δ*dut*)] infections.

Figure S5. Phages replicate in the bacterial chromosome following prophage induction and not during infection, related to Figure 5.
(A to D) Relative abundance of (A and C) helper 80α or (B and D) non-helper 80α Δ*dut* phage genomic DNA and the chromosomal regions adjacent to the 80α *att*B site for (A and B) induction (Ind) or (C and D) infection (Inf) of non-lysogenic strains. Samples were analyzed at 0 (red), 30 (light blue), 60 (green), and 120 min (dark blue) after induction with mitomycin C or phage infection.

Figure S6. Lateral cotransduction occurs when an intact SaPI genome and adjacent host chromosomal DNA are packaged together in a single phage capsid, related to Figure 6.
(A and B) The SaPI family carries out lateral cotransduction.
(A) Cotransduction of SaPI1 *tsst*::*tetM* or SaPI2 *tsst*::*tetM* and their *cpmAB* deletion (Δ*cpmAB*) derivatives with Cm^R markers 4 kb downstream of the SaPI1 *att*C site or SaPI2 *att*C site, respectively. Strains lysogenic for helper 80α phage were induced with mitomycin C (Ind), non-lysogenic SaPI1 *tsst*::*tetM* or SaPI2 *tsst*::*tetM* strains were infected with 80α only (Inf), and non-lysogenic strains without SaPI were infected with 80α / SaPI1 *tsst*::*tetM* or 80α / SaPI2 *tsst*::*tetM* for naïve infections (Naïve Inf).
(B) Cotransduction of SaPIbov5 *vwb*::*ermC* or SaPI PT1028::*ermC* with Cm^R or Cd^R markers 4 kb downstream of the SaPIbov1 *att*C or SaPI4 *att*C, respectively. SaPIbov1 and SaPIbov5 (Sb5) share the same SaPIbov1 *att*C site and SaPI PT1028 inserts into the SaPI4 *att*C site. Strains lysogenic for helper 80α phage were induced with mitomycin C (Ind).
(C) Cotransduction of SaPIbov1 *tsst*::*tetM* with Cm^R markers 4 kb, 10 kb, or capsid headful 3 (HF3) downstream of the SaPIbov1 *att*C. Strains lysogenic for non-helper 80α Δ*dut* (teal) or helper 80α (dark blue) phage were induced with mitomycin C. A cotransduction assay with a deconstructed (DC, gray) lysate comprised of two independent donor strain lysates was also tested. A SaPIbov1 *tsst*::*tetM* strain lysogenic for 80α phage was the SaPI donor, while a SaPIbov1 Δ*tsst*::*ermC* strain lysogenic for 80α Δ*dut* with a Cm^R marker 10 kb downstream of the SaPIbov1 *att*C was the lateral marker donor. Both strains were induced with mitomycin C individually and the resultant lysates were combined equally. Cotransduction of the SaPIbov1 *tsst*::*tetM* with the Cm^R marker 10 kb downstream of the SaPIbov1 *att*C was tested.

(D) Cotransduction of SaPIbov1 Δ*tsst*::*tetM* Δ(*sec-sel*) strains lysogenic for 80α or 80α Δ*dut* with Cm^R markers 20 kb downstream of the SaPIbov1 *att*C site were induced with mitomycin C.
(A to D) The resulting lysates were tested for cotransduction into *S. aureus*. For each replicate, 100 Cm^R or Cd^R transductants were tested for Em^R or Tet^R and the cotransduction frequency was represented as a percentage, calculated as (Em^R or Tet^R / Cm^R or Cd^R) x 100. Values are means (*n* = 3 independent samples). Error bars indicate standard deviation.
(E) SaPIbov1 *tsst*::*tetM* cotransduction with a Cm^R marker 4 kb downstream of the SaPIbov1 *att*C into a *S. aureus* strain lysogenic for 80α. Tet^R and Cm^R transductants and the original donor strain (80α / SaPIbov1 *tsst*::*tetM* with a Cm^R marker 4 kb downstream) were induced with mitomycin C. The resulting lysates were tested for SaPIbov1 *tsst*::*tetM* transduction into *S. aureus.* The results are represented as SaPI-specific transductants (SPST) per milliliter. Values are means for the original donor strain (*n* = 3 independent samples). Error bars indicate standard deviation.
(F) One Em^R and Tet^R isolate from Table S2 retained the recipient SaPIbov1::*ermC* after acquiring the donor SaPIbov1::*tetM*. This isolate was sequenced, and the results showed that the second SaPIbov1::*tetM* was not in tandem with SaPIbov1::*ermC* but was located at a second site. PCR analysis with primer set 1364 and 1878 confirmed the presence of the second SaPIbov1 at a secondary *att*C site. Lane 1 is the 1 kb DNA ladder and lane 2 is the 100 bp DNA ladder.

Figure S7. SaPIs form genomic tandems and concatamers in the host chromosome, related to Figure 7.
Non-lysogenic SaPIbov1 *tsst*::*tetM* strains were induced with mitomycin C and anhydrotetracycline was added at the same time for SaPIbov1 de-repression by P_{tet}-*dut*. The high molecular weight genomic DNA was prepared and sequenced by Nanopore long-read sequencing. From over 2 million total reads, 17 unique reads with at least tandem SaPIs attached to bacterial DNA were recovered. Reads shown here are alignments with the (A) tandem SaPIbov1 *tsst*::*tetM* reference genome, (B) triple SaPIbov1 *tsst*::*tetM* reference genome, and (C) quadruple SaPIbov1 *tsst*::*tetM* reference genome. The quality scores and conservation are shown. Unique reads were aligned using Qiagen CLC Workbench.
(D) Model for SaPI lateral cotransduction in the donor cell. The induced SaPIbov1 genome (light blue) replicates in the host chromosome (1) and amplifies the adjacent bacterial chromosome including vSaα (light red) and PSMα (green). Normal excision (2) occurs between the *att*L and *att*R sites on the same strand, while bridging excision (3) between the *att*L and *att*R sites on different strands results in track switching that joins two SaPIs head to tail. SaPI terminase initiates DNA packaging (4) and a transducing particle containing intact SaPIbov1 and vSaα is formed (5). Lateral transduction then proceeds to mobilize several hundred kb of the chromosome by headful units (6).
(E) Model for SaPI lateral cotransduction in the recipient cell. Approximately 1.5 SaPIbov1 genomes attached to the vSaα island are injected into a new cell (1). SaPIbov1 circularizes through a single crossover event between repeated sequences (2). The circular SaPIbov1 genome integrates at a SaPIbov1 *att*C site (3). The vSaα

island is acquired or exchanged via homologous recombination with the host chromosome (4). Each “X” indicates a crossover event.

STAR METHODS

KEY RESOURCES TABLE

REAGENT or RESOURCE	SOURCE	IDENTIFIER
Bacterial and virus strains		
Bacterial strains, see Table S4		
Phage 80α	[43]	NC_009526
Phage 85	[44]	NC_007050.1
Phage ΦNM1	[45]	DQ530359
Chemicals, peptides, and recombinant proteins		
Mitomycin C	Sigma-Aldrich	Cat# M0503
Anhydrotetracycline Hydrochloride	Sigma-Aldrich	Cat# 94664
Calcium Chloride	Fisher	Cat# BP510-500
Sodium Citrate	Sigma-Aldrich	Cat# W302600
Ampicillin Sodium Salt	Sigma-Aldrich	Cat# A9518
Chloramphenicol	Fisher	Cat# BP904-100
Erythromycin	Fisher	Cat# BP920-25
Streptomycin Sulfate	Fisher	Cat# BP910-50
Cadmium Chloride	Sigma-Aldrich	Cat# 655198
Tetracycline Hydrochloride	Fisher	Cat# BP912-100
LB Broth	BD Difco	Cat# 244620
Tryptic Soy Broth	Sigma-Aldrich	Cat# 22092
Agar	Fisher	Cat# BP2641-1
Sucrose	Sigma-Aldrich	Cat# 84097
Beadbug Silica Beads	Sigma-Aldrich	Cat# Z763721
Phusion High-Fidelity DNA Polymerase	New England Biolabs	Cat# M0530L
T4 Polynucleotide Kinase	New England Biolabs	Cat# M0201S
dNTPs	Promega	Cat# U1240
Rapid DNA Ligation	Roche	Cat# 11635379001
Lysostaphin Endopeptidase	AMBI Products LLC	Cat# LSPN-50
Critical commercial assays		
Epicenter Tissue & Cell Lysis Solution	Lucigen	Cat# MTC096H
Epicenter MPC Protein Precipitation Buffer	Lucigen	Cat# MMP095H
GenElute Bacterial Genomic DNA Kit	Sigma-Aldrich	Cat# NA2110
Monarch Genomic DNA purification Kit	New England Biolabs	Cat# T3010L
QIAprep Spin miniprep Kit	Qiagen	Cat# 27106
QIAquick gel extraction Kit	Qiagen	Cat# 28706
Deposited data		
Data for the main and supplemental figures and long-read sequencing.	Mendeley Data	DOI:10.17632/yxfmv6ps4c.1
Oligonucleotides		
Primers, see Table S6		
Recombinant DNA		
Plasmids, see Table S5		
Software and algorithms		
Assembly_dereplicator	[46]	https://github.com/rrwick/Assembly-Dereplicator

Artemis	[47]	https://github.com/sanger-pathogens/Artemis
Bedtools v2.30.0	[48]	https://github.com/arq5x/bedtools2
Biorender	BioRender Software	https://www.biorender.com/
BLAST v.2.12.0	[49]	https://ncbi.nlm.nih.gov/
Burrows-Wheeler Alignment Tool v0.7.17	[50]	https://github.com/lh3/bwa
FastQC v0.11.8	Babraham Bioinformatics	http://www.bioinformatics.babraham.ac.uk/projects/fastqc/
Chromatiblock v1	[51]	https://github.com/mjsull/chromatiblock/
Graphia v3.0	[52]	https://github.com/JDHarlingLee/GraPPLE
GraPPLE	[53]	https://github.com/JDHarlingLee/GraPPLE
GraphPad Prism	GraphPad Software	https://www.graphpad.com/scientific-software/prism/
ncbi-genome-download	NCBI-genome-download, GitHub Program	https://github.com/kblin/ncbi-genome-download
Picard-tools v2.1.1	The Picard Toolkit, Broad Institute	http://broadinstitute.github.io/picard/
PIRATE v1.0.4	[54]	https://github.com/SionBayliss/PIRATE
Prokka v1.14.6	[55]	https://github.com/tseemann/prokka
SAMtools v1.11	[56]	https://github.com/samtools/samtools
SeqKit v2.3.1	[57]	https://github.com/shenwei356/seqkit
Trimmomatic v0.39	[58]	https://github.com/usadellab/Trimmomatic

1

RESOURCE AVAILABILITY

Lead contact

Further information and requests for resources and reagents should be directed to and will be fulfilled by the lead contact, John Chen (miccjy@nus.edu).

Materials availability

All unique/stable reagents generated in this study are available from the Lead Contact with a completed Materials Transfer Agreement.

Data and code availability

All data reported in this paper will be shared by the lead contacts upon request or through Mendeley Data (DOI: 10.17632/yxfmv6ps4c.1). This paper does not report original code. Any additional information required to reanalyze the data reported in this paper is available from the lead contacts upon request.

Experimental Model and Study Participant Details

Phages, bacterial strains, and growth conditions

The phages used in this study are listed in the key resources table. The bacterial strains used in this study are listed in Table S4. *S. aureus* strains were grown in tryptic soy broth (TSB) and tryptic soy agar (TSA) plates. *E. coli* strains were grown in Luria-Bertani (LB) broth or on LB agar plates. Antibiotic-resistant *S. aureus* strains were selected and maintained on 5 μg ml^{-1} erythromycin, 5 μg ml^{-1} tetracycline, 10 μg ml^{-1} chloramphenicol, 300 μg ml^{-1} streptomycin, or 0.1 mM $CdCl_2$ during the strain construction or testing process. For inducible-promoter induction, 31.25 or 62.5 ng ml^{-1} anhydrotetracycline was used. Antibiotic-resistant *E. coli* were selected and maintained on 100 μg ml^{-1} ampicillin.

METHOD DETAILS

DNA methods

Plasmids and oligonucleotides used in this study are listed in Tables S5 and S6, respectively. The sequences of all phages, SaPIs, and strains were previously accessed from NCBI GenBank. The primers used for cloning and screening in this study were obtained from Integrated DNA Technologies. Sequencing was outsourced to external vendors 1st Base (Singapore) and Macrogen (Singapore). Sequence data were aligned against appropriate reference DNA sequences using SnapGene (GSL Biotech LLC, San Diego, CA). Phusion High-Fidelity DNA polymerase, restriction enzymes, and ligase were purchased from New England Biolabs.

S. aureus chromosomal DNA preparation

Cultures of *S. aureus* were inoculated and incubated overnight. Overnight cultures were centrifuged, and cell pellets were washed and resuspended in Buffer P1 (Qiagen, Singapore). Cell suspensions were incubated with 5 µg lysostaphin until cell lysis, 37°C, 1 hour, followed by the addition of 5 µg of proteinase K, 37°C, 1 hour. Cell lysis buffer (Epicenter), and MPC protein precipitation buffer (Epicenter) were added to each tube in a stepwise manner and mixed gently prior to centrifugation in pre-chilled centrifuges, 4°C, 15000 rpm, 15 minutes. Supernatants were harvested and precipitated with isopropanol. DNA pellets were then collected and washed with 70% ethanol before being air-dried. Once dry, the DNA pellets were gently resuspended in water and left to stand at 4°C overnight.

Allelic exchange

For the generation of insertions in the *S. aureus* chromosome, allelic exchange was performed as previously described.[14,21,59]

Phage titers and SaPI transductions

Preparations of phage lysates, transduction, and titrations were performed as previously described.[7,14,21,60] For phage only, or phage and SaPI lysates, lysogens were grown to the mid-logarithmic stage in TSB, normalized to OD_{600}=0.5, and adjusted to 2 μg ml^{-1} MC (Sigma) until complete lysis. Phage infection lysates were made by infecting the same density of naive cells with an MOI = 0.1 or MOI = 1.0 until complete lysis. Lysates were then adjusted to 1 μg ml^{-1} DNase I and 1 μg ml^{-1} RNase and filter sterilized (0.2 μm pore) before use. Phage titers were determined by plaque formation on bacterial lawns of RN450 plated on phage agar. Phage titration results are reported as the number of plaque-forming units (PFU) ml^{-1}. For transductions, RN450 cells were infected for 30 minutes and then adjusted to 100 mM sodium citrate. 3 ml of top agar was added to each reaction and plated by pouring the molten mixture on the appropriate selective agar. The results are reported as the number of transduction units (TrU) ml^{-1}.

Lateral cotransduction analysis

Lysates from a phage infection or lysogen induction of strains containing both a SaPI *tsst*::*tetM* and a chromosomal marker (Cd^R or Cm^R) at varying distances from the SaPI *att*C site were used to determine SaPI cotransduction frequencies. Chromosomal marker transduction was first selected by plating on appropriate selective agar. The Cd^R or Cm^R transductants of three independent lysates (100 transductants each) were then tested for Tet^R and the frequency was represented as the (Tet^R / Cd^R or Cm^R) x 100%.

Inducible complementation of SaPIbov1 mutants

Lysogens of 80α or with SaPIbov1 *tsst*::*tetM*, SaPIbov1 *tsst*::*tetM* Δ(*pri-rep*), SaPIbov1 *tsst*::*tetM* Δ*int,* or SaPIbov1 *tsst*::*tetM* Δ*xis* were grown to mid-logarithmic phase in TSB, normalized to OD_{600} = 0.5, and MC-induced (T = 0 min). Anhydrotetracycline (31.25 ng

ml^{-1}) was added at various time points (0, 30, 60, 90, and 120 minutes or no addition) after mitomycin C for complementation by P_{Tet}-(*pri-rep*)/*int*/*xis*. Complementation results at 60 minutes for P_{tet}-*pri-rep*$^{+}$ or 90 minutes for P_{tet}-*xis*$^{+}$, P_{tet}-*int*$^{+}$ showed the highest lateral cotransduction activity and were represented in this work. All cultures were harvested and mechanically lysed 2 hours (26°C, 100 rpm) post-anhydrotetracycline induction in a Precellys 24 (Bertin) with 0.1 mm Beadbug silica beads (Sigma-Aldrich). All lysates were filter sterilized (0.2 µm pore) before use.

Whole genome sequencing (escape replication)

Samples were induced or infected as described in previous sections. At the indicated time points after MC-induction or phage infection, 12 ml of sample was taken for DNA extraction using GenElute Bacterial Genomic DNA kit (Sigma) following the manufacturer's instructions. The DNA was precipitated by 0.3 M NaOAc and 2.25 volume of 100% ethanol, then pelleted at 12,000 × g for 30 min at 4 °C and washed once with 1 ml of 70% ethanol. After centrifugation, the DNA pellets were air-dried for 30 min and resuspended in 50 µl nuclease-free water. Quality control of DNA samples was tested using Agilent Bioanalyzer 2100 and whole genome sequencing (WGS) was performed at the University of Glasgow Polyomics Facility using Illumina NextSeq500 obtaining 2 x 75 bp pair-end reads with DNA PCR free libraries. Trimmed reads were mapped to the appropriate genome: 80α (NC_009526.1), SaPIbov1 (AF217235.1), and NTCT 8325 (CP000253).

Whole genome sequencing (capsid DNA)

A total of 100 ml lysates from phage infections or lysogen inductions were produced as described in previous sections. Capsid precipitation and capsid DNA extraction were performed as previously described.[22] Quality control of DNA samples was tested using

Agilent Bioanalyzer 2100 and WGS was performed at the University of Glasgow Polyomics Facility using Illumina TruSeq DNA Nano library prep, obtaining 2 × 75 bp pair-end reads with DNA PCR free libraries. A total of 3000X bacterial genome coverage, 56 M reads, were generated and trimmed reads were mapped to the appropriate genome: 80α (NC_009526.1), SaPIbov1 (AF217235), and NTCT 8325 (CP000253).

Whole genome sequencing analyses

We first used FastQC v0.11.8 to assess the quality of the sequencing reads and Trimmomatic v0.39 to remove adapters and low-quality reads.[58] Sequencing reads from each experiment were mapped to their respective reference genomes using the Burrows-Wheeler Alignment Tool v0.7.17.[50] Picard-tools v2.1.1 (Broad Institute) was next used to obtain the bam files, which were merged with SAMtools v1.11,[56] sorted and indexed; and Bedtools v2.30.0 subcommand *bamtobed* was used to produce the bed files.[48] We computed the relative coverage over 100 sliding windows along the entire chromosome for each of the experiments. For this, we computed the average coverages across the full genome without phages, which were removed using Bedtools subcommand *subtract*. Subsequently, the coverages across the sliding windows were divided by the chromosomal averages. All the bioinformatic analyses were performed using the Cloud Infrastructure for Microbial Bioinformatics (CLIMB).

Detection of transient SaPI concatamers in the bacterial chromosome by PCR analysis

For intermolecular joining (Figure 6C), a non-lysogenic strain with a second SaPIbov1 *att*C site inserted +4 kb downstream of the native SaPIbov1 *att*C was constructed. A SaPIbov1 *sec-sel* deletion mutant [SaPIbov1 Δ*tsst*::*tetM* Δ(*sec-sel*)] or “SaPIbov1-1875”

was integrated at the primary SaPIbov1 *att*C site, and SaPIbov1 with synonymous codon changes in the *int* gene (SaPIbov1 Δ*tsst*::*cat194 int*^{syn}) or "SaPIbov1-1848" was inserted at the +4 kb secondary SaPIbov1 *att*C site. Thus, both SaPIbov1-1875 and SaPIbov1-1848 have intact *att*L and *att*R sites. This double SaPIbov1-positive strain was infected with phage (80α, 80α △*dut,* or mock) for one hour and then the cells were harvested and mechanically lysed in a Precellys 24 (Bertin) with 0.1 mm Beadbug silica beads (Sigma-Aldrich). The genomic DNA was then analyzed by PCR. Primer 1875 elongates toward the *att*R and only anneals to the *sec-sel* deletion joint of SaPIbov1-1875, while primer 1848 elongates toward the *att*L and only binds to synonymous codon changes in the *int* gene of SaPIbov1-1848. Therefore, PCR analysis with primers 1848 and 1875 produces a 1.6 kb product for tandems and 6.2 kb for no tandems.

For track switching (Figure 6D), a non-helper mutant of Φ52A (Φ52A △*dut*) was constructed. Of note, the Φ52A △*dut* mutant does not induce SaPIbov1 in the donor or recipient strains. A SaPIbov1 integrase deletion mutant (SaPIbov1 *tsst*::*tetM* △*int*) or "SaPIbov1-1958" that is unable to excise was integrated into the SaPIbov1 *att*C site, which is located in the third lateral headful of Φ52A. This lysogenic strain was induced to generate Φ52A lateral-transducing particles that contain SaPIbov1-1958 still integrated into bacterial DNA. This lysate was used to infect lysogenic strains carrying SaPIbov1-1848 that were induced for 1 hour prior to infection and the genomic DNA was analyzed by PCR with primers 1958 and 1848. Primer 1958 elongates toward *att*R and anneals to the *sel* gene of SaPIbov1-1958 and it can only make a product with primer 1848 if SaPIbov1-1958 and SaPIbov1-1848 are covalently joined. PCR analysis with primers 1848 and 1958 produces a 2.0 kb product if track switching occurs. Primers 1845 and 1848 produce a 1.1 kb control.

Detection of transient SaPI concatamers in the bacterial chromosome by long-read Nanopore sequencing

Bacterial cultures were grown and adjusted to OD_{600}=0.5 before MC treatment. Anhydrotetracycline was added to these mixtures after 1 hour. The cells were then harvested by centrifugation 1 or 2 hours after anhydrotetracycline addition. Chromosomal DNA was prepared from the bacterial pellets accordingly as described above. At least six sample replicates from each time point were prepared and analyzed. Microbial Genome Sequencing Centre (USA) performed long-read Nanopore sequencing. The Nanopore reads were mapped to an appropriate template comprising tandem SaPIbov1 (AF217235), flanked by +/- 10 kb of *S. aureus* NTCT 8325 (CP000253) chromosomal DNA at the SaPIbov1 *att*C site using Qiagen CLC Genomics Workbench and SnapGene.

Pangenome synteny network analysis

All complete *S. aureus* assemblies were downloaded from RefSeq (January 2022) using NCBI-genome-download v0.2.9, giving an initial dataset of 693 genomes. This was dereplicated using Assembly_dereplicator v0.1.0 at a threshold of 0.001, reducing the dataset to 236 genomes; 1 further genome was excluded based on mash distance. The remaining 235 genomes were annotated using Prokka v1.14.6 and the pangenome was established using PIRATE v1.0.4 with default thresholds.[54,55] The synteny map of genes at the 95% identity threshold was recreated as described in,[53] and the resulting network was visualized using Graphia v3.0.[52] Edges of weight 1 were removed from the network, and the network was clustered using the Weighted Louvain Clustering algorithm (granularity = 0.800) to define regions for visualization; some specific nodes were also removed for visual clarity of the resulting network. This network was used to visualize

the synteny after the SaPI-I and SaPI-II integration sites (Figure 7B). Flanking coordinates for core genes are taken from the reference genome RF122 (AJ938182).

Regions downstream of SaPI-III/IV and SaPI-V were investigated in this network, but due to the complexity of these regions, they were extracted and analyzed individually via the following method. After orientating the 235 genomes to begin at *dnaA* and visualizing their structure via Chromatiblock v1 with RF122 as the reference genome,[51] 22 genomes were excluded from the dataset for the synteny analysis of the SaPI V and SaPI III regions due to large-scale chromosomal rearrangements. Flanking core genes of either end of each individual region was identified by manually inspecting the Prokka-annotated GFF file of the whole RF122 genome in Artemis.[47] The positions of these flanking genes in the remaining 213 genomes were obtained by BLAST v.2.12.0 and then used to extract the regions within each pair of flanking genes from the whole genomes via SeqKit v2.3.1.[49,57] Reference co-ordinates from RF122 are 1,793,187 bp - 2,056,198 bp for SaPI V and 801,747 bp and 1,136,250 bp for SaPI III. The two extracted regions were annotated with Prokka and processed by PIRATE and GraPPLE as above. The resulting synteny networks were visualised in Graphia, and simplified as follows: edges with weight <3 were removed, and nodes with node degree >35 were removed. This greatly reduces complexity in the network, retaining only the best-represented syntenic connections. For graphical presentation, only the first part of each region is shown, with coordinates as noted in Figure 7.

Distribution of SaPIs across the genome dataset.

For each SaPI integration site, 1000 bp sequences that included integrase and contiguous chromosomal flanking sequence were used to interrogate the database of *S. aureus* genome sequences using BLAST v.2.12.0.[49]

Image creation

Some images were created with BioRender. Agreement numbers PW23WE7MCW, AB23WE7VUA, MT23WE8HRL, DW23WE9005, KC23X8TLLK, and BD25G4PYX2.

QUANTIFICATION AND STATISTICAL ANALYSIS

The statistical details for each experiment are found in the figure legends. Data are presented as means ± standard deviation. Individual data points are superimposed onto bar graphs. Statistical analyses were performed with GraphPad Prism (version 9.5.1) and Microsoft Excel (version 16.69.1).

EXCEL DATA TABLES

Table S4. Strains used in this study, related to STAR Methods Phages, bacterial strains, and growth conditions.

Table S5. Plasmids used in this study, related to STAR DNA methods.

Table S6. Oligonucleotides used in this study, related to STAR DNA methods.

REFERENCES

1. Novick, R.P., Christie, G.E., and Penades, J.R. (2010). The phage-related chromosomal islands of Gram-positive bacteria. Nat Rev Microbiol *8*, 541-551. 10.1038/nrmicro2393.
2. Penades, J.R., and Christie, G.E. (2015). The Phage-Inducible Chromosomal Islands: A Family of Highly Evolved Molecular Parasites. Annual review of virology *2*, 181-201. 10.1146/annurev-virology-031413-085446.
3. de Sousa, J.A.M., Fillol-Salom, A., Penades, J.R., and Rocha, E.P.C. (2023). Identification and characterization of thousands of bacteriophage satellites across bacteria. Nucleic acids research. 10.1093/nar/gkad123.
4. Fillol-Salom, A., Martinez-Rubio, R., Abdulrahman, R.F., Chen, J., Davies, R., and Penades, J.R. (2018). Phage-inducible chromosomal islands are ubiquitous within the bacterial universe. ISME J *12*, 2114-2128. 10.1038/s41396-018-0156-3.
5. Martinez-Rubio, R., Quiles-Puchalt, N., Marti, M., Humphrey, S., Ram, G., Smyth, D., Chen, J., Novick, R.P., and Penades, J.R. (2017). Phage-inducible islands in the Gram-positive cocci. ISME J *11*, 1029-1042. 10.1038/ismej.2016.163.
6. Ubeda, C., Maiques, E., Barry, P., Matthews, A., Tormo, M.A., Lasa, I., Novick, R.P., and Penades, J.R. (2008). SaPI mutations affecting replication and transfer and enabling autonomous replication in the absence of helper phage. Mol Microbiol *67*, 493-503. 10.1111/j.1365-2958.2007.06027.x.
7. Tormo-Mas, M.A., Mir, I., Shrestha, A., Tallent, S.M., Campoy, S., Lasa, I., Barbe, J., Novick, R.P., Christie, G.E., and Penades, J.R. (2010). Moonlighting bacteriophage proteins derepress staphylococcal pathogenicity islands. Nature *465*, 779-782. 10.1038/nature09065.
8. Court, D.L., Oppenheim, A.B., and Adhya, S.L. (2007). A new look at bacteriophage lambda genetic networks. J Bacteriol *189*, 298-304. 10.1128/JB.01215-06.
9. Susskind, M.M., and Botstein, D. (1978). Molecular genetics of bacteriophage P22. Microbiological reviews *42*, 385-413.
10. Casjens, S.R. (2011). The DNA-packaging nanomotor of tailed bacteriophages. Nat Rev Microbiol *9*, 647-657. 10.1038/nrmicro2632.
11. Rao, V.B., and Feiss, M. (2008). The bacteriophage DNA packaging motor. Annu Rev Genet *42*, 647-681. 10.1146/annurev.genet.42.110807.091545.
12. Streisinger, G., Edgar, R.S., and Denhardt, G.H. (1964). Chromosome Structure in Phage T4. I. Circularity of the Linkage Map. Proc Natl Acad Sci U S A *51*, 775-779.
13. Streisinger, G., Emrich, J., and Stahl, M.M. (1967). Chromosome structure in phage t4, iii. Terminal redundancy and length determination. Proc Natl Acad Sci U S A *57*, 292-295.
14. Chen, J., Ram, G., Penades, J.R., Brown, S., and Novick, R.P. (2015). Pathogenicity island-directed transfer of unlinked chromosomal virulence genes. Molecular cell *57*, 138-149. 10.1016/j.molcel.2014.11.011.
15. Ubeda, C., Olivarez, N.P., Barry, P., Wang, H., Kong, X., Matthews, A., Tallent, S.M., Christie, G.E., and Novick, R.P. (2009). Specificity of staphylococcal phage

and SaPI DNA packaging as revealed by integrase and terminase mutations. Mol Microbiol *72*, 98-108.
16. Chen, J., and Novick, R.P. (2009). Phage-mediated intergeneric transfer of toxin genes. Science *323*, 139-141. 10.1126/science.1164783.
17. Chen, J., Carpena, N., Quiles-Puchalt, N., Ram, G., Novick, R.P., and Penades, J.R. (2015). Intra- and inter-generic transfer of pathogenicity island-encoded virulence genes by cos phages. ISME J *9*, 1260-1263. 10.1038/ismej.2014.187.
18. Chiang, Y.N., Penades, J.R., and Chen, J. (2019). Genetic transduction by phages and chromosomal islands: The new and noncanonical. PLoS Pathog *15*, e1007878. 10.1371/journal.ppat.1007878.
19. Morse, M.L., Lederberg, E.M., and Lederberg, J. (1956). Transduction in Escherichia Coli K-12. Genetics *41*, 142-156.
20. Zinder, N.D., and Lederberg, J. (1952). Genetic exchange in Salmonella. J Bacteriol *64*, 679-699.
21. Chen, J., Quiles-Puchalt, N., Chiang, Y.N., Bacigalupe, R., Fillol-Salom, A., Chee, M.S.J., Fitzgerald, J.R., and Penades, J.R. (2018). Genome hypermobility by lateral transduction. Science *362*, 207-212. 10.1126/science.aat5867.
22. Fillol-Salom, A., Bacigalupe, R., Humphrey, S., Chiang, Y.N., Chen, J., and Penades, J.R. (2021). Lateral transduction is inherent to the life cycle of the archetypical Salmonella phage P22. Nat Commun *12*, 6510. 10.1038/s41467-021-26520-4.
23. Humphrey, S., Fillol-Salom, A., Quiles-Puchalt, N., Ibarra-Chavez, R., Haag, A.F., Chen, J., and Penades, J.R. (2021). Bacterial chromosomal mobility via lateral transduction exceeds that of classical mobile genetic elements. Nat Commun *12*, 6509. 10.1038/s41467-021-26004-5.
24. Fitzgerald, J.R., Monday, S.R., Foster, T.J., Bohach, G.A., Hartigan, P.J., Meaney, W.J., and Smyth, C.J. (2001). Characterization of a putative pathogenicity island from bovine Staphylococcus aureus encoding multiple superantigens. J Bacteriol *183*, 63-70. 10.1128/JB.183.1.63-70.2001.
25. Baba, T., Takeuchi, F., Kuroda, M., Yuzawa, H., Aoki, K., Oguchi, A., Nagai, Y., Iwama, N., Asano, K., Naimi, T., et al. (2002). Genome and virulence determinants of high virulence community-acquired MRSA. Lancet *359*, 1819-1827. 10.1016/s0140-6736(02)08713-5.
26. Fitzgerald, J.R., Reid, S.D., Ruotsalainen, E., Tripp, T.J., Liu, M., Cole, R., Kuusela, P., Schlievert, P.M., Jarvinen, A., and Musser, J.M. (2003). Genome diversification in Staphylococcus aureus: Molecular evolution of a highly variable chromosomal region encoding the Staphylococcal exotoxin-like family of proteins. Infection and immunity *71*, 2827-2838. 10.1128/IAI.71.5.2827-2838.2003.
27. Fraser, J.D., and Proft, T. (2008). The bacterial superantigen and superantigen-like proteins. Immunol Rev *225*, 226-243. 10.1111/j.1600-065X.2008.00681.x.
28. Cheung, G.Y., Joo, H.S., Chatterjee, S.S., and Otto, M. (2014). Phenol-soluble modulins--critical determinants of staphylococcal virulence. FEMS Microbiol Rev *38*, 698-719. 10.1111/1574-6976.12057.
29. Peschel, A., and Otto, M. (2013). Phenol-soluble modulins and staphylococcal infection. Nat Rev Microbiol *11*, 667-673. 10.1038/nrmicro3110.
30. Ubeda, C., Maiques, E., Tormo, M.A., Campoy, S., Lasa, I., Barbe, J., Novick, R.P., and Penades, J.R. (2007). SaPI operon I is required for SaPI packaging

and is controlled by LexA. Mol Microbiol *65*, 41-50. 10.1111/j.1365-2958.2007.05758.x.
31. Mir-Sanchis, I., Martinez-Rubio, R., Marti, M., Chen, J., Lasa, I., Novick, R.P., Tormo-Mas, M.A., and Penades, J.R. (2012). Control of Staphylococcus aureus pathogenicity island excision. Mol Microbiol *85*, 833-845. 10.1111/j.1365-2958.2012.08145.x.
32. Bento, J.C., Lane, K.D., Read, E.K., Cerca, N., and Christie, G.E. (2014). Sequence determinants for DNA packaging specificity in the S. aureus pathogenicity island SaPI1. Plasmid *71*, 8-15. 10.1016/j.plasmid.2013.12.001.
33. Poliakov, A., Chang, J.R., Spilman, M.S., Damle, P.K., Christie, G.E., Mobley, J.A., and Dokland, T. (2008). Capsid size determination by Staphylococcus aureus pathogenicity island SaPI1 involves specific incorporation of SaPI1 proteins into procapsids. J Mol Biol *380*, 465-475. 10.1016/j.jmb.2008.04.065.
34. Tribelli, P.M., Luqman, A., Nguyen, M.T., Madlung, J., Fan, S.H., Macek, B., Sass, P., Bitschar, K., Schittek, B., Kretschmer, D., and Gotz, F. (2020). Staphylococcus aureus Lpl protein triggers human host cell invasion via activation of Hsp90 receptor. Cell Microbiol *22*, e13111. 10.1111/cmi.13111.
35. Subedi, A., Ubeda, C., Adhikari, R.P., Penades, J.R., and Novick, R.P. (2007). Sequence analysis reveals genetic exchanges and intraspecific spread of SaPI2, a pathogenicity island involved in menstrual toxic shock. Microbiology *153*, 3235-3245. 10.1099/mic.0.2007/006932-0.
36. Fillol-Salom, A., Alsaadi, A., Sousa, J.A.M., Zhong, L., Foster, K.R., Rocha, E.P.C., Penades, J.R., Ingmer, H., and Haaber, J. (2019). Bacteriophages benefit from generalized transduction. PLoS Pathog *15*, e1007888. 10.1371/journal.ppat.1007888.
37. Haaber, J., Leisner, J.J., Cohn, M.T., Catalan-Moreno, A., Nielsen, J.B., Westh, H., Penades, J.R., and Ingmer, H. (2016). Bacterial viruses enable their host to acquire antibiotic resistance genes from neighbouring cells. Nat Commun *7*, 13333. 10.1038/ncomms13333.
38. George, M., and Bukhari, A.I. (1981). Heterogeneous host DNA attached to the left end of mature bacteriophage Mu DNA. Nature *292*, 175-176. 10.1038/292175a0.
39. Groenen, M.A., and van de Putte, P. (1985). Mapping of a site for packaging of bacteriophage Mu DNA. Virology *144*, 520-522. 10.1016/0042-6822(85)90292-2.
40. Novick, R.P., and Ram, G. (2016). The Floating (Pathogenicity) Island: A Genomic Dessert. Trends in genetics : TIG *32*, 114-126. 10.1016/j.tig.2015.11.005.
41. Power, J.J., Pinheiro, F., Pompei, S., Kovacova, V., Yuksel, M., Rathmann, I., Forster, M., Lassig, M., and Maier, B. (2021). Adaptive evolution of hybrid bacteria by horizontal gene transfer. Proc Natl Acad Sci U S A *118*. 10.1073/pnas.2007873118.
42. Chen, S., Krinsky, B.H., and Long, M. (2013). New genes as drivers of phenotypic evolution. Nat Rev Genet *14*, 645-660. 10.1038/nrg3521.
43. Christie, G.E., Matthews, A.M., King, D.G., Lane, K.D., Olivarez, N.P., Tallent, S.M., Gill, S.R., and Novick, R.P. (2010). The complete genomes of Staphylococcus aureus bacteriophages 80 and 80alpha--implications for the specificity of SaPI mobilization. Virology *407*, 381-390. 10.1016/j.virol.2010.08.036.

44. Kwan, T., Liu, J., DuBow, M., Gros, P., and Pelletier, J. (2005). The complete genomes and proteomes of 27 Staphylococcus aureus bacteriophages. Proc Natl Acad Sci U S A *102*, 5174-5179. 10.1073/pnas.0501140102.
45. Bae, T., Baba, T., Hiramatsu, K., and Schneewind, O. (2006). Prophages of Staphylococcus aureus Newman and their contribution to virulence. Mol Microbiol *62*, 1035-1047. 10.1111/j.1365-2958.2006.05441.x.
46. Wick, R., and Holt, K. (2019). rrwick/Assembly-Dereplicator: Assembly Dereplicator v0.1.0. 10.5281/ZENODO.3365572.
47. Carver, T., Harris, S.R., Berriman, M., Parkhill, J., and McQuillan, J.A. (2012). Artemis: an integrated platform for visualization and analysis of high-throughput sequence-based experimental data. Bioinformatics *28*, 464-469. 10.1093/bioinformatics/btr703.
48. Quinlan, A.R., and Hall, I.M. (2010). BEDTools: a flexible suite of utilities for comparing genomic features. Bioinformatics *26*, 841-842. 10.1093/bioinformatics/btq033.
49. Camacho, C., Coulouris, G., Avagyan, V., Ma, N., Papadopoulos, J., Bealer, K., and Madden, T.L. (2009). BLAST+: architecture and applications. BMC Bioinformatics *10*, 421. 10.1186/1471-2105-10-421.
50. Li, H., and Durbin, R. (2009). Fast and accurate short read alignment with Burrows-Wheeler transform. Bioinformatics *25*, 1754-1760. 10.1093/bioinformatics/btp324.
51. Sullivan, M.J., and van Bakel, H. (2020). Chromatiblock: scalable whole-genome visualization of structural differences in prokaryotes. J Open Source Softw *5*. 10.21105/joss.02451.
52. Freeman, T., Horsewell, S., Patir, A., Harling-Lee, J., Regan, T., Shih, B., Prendergast, J., Hume, D., and Angus, T. (2020). Graphia: A platform for the graph-based visualisation and analysis of complex data. http://biorxiv.org/lookup/doi/10.1101/2020.09.02.279349.
53. Harling-Lee, J.D., Gorzynski, J., Yebra, G., Angus, T., Fitzgerald, J.R., and Freeman, T.C. (2022). A graph-based approach for the visualisation and analysis of bacterial pangenomes. BMC Bioinformatics *23*, 416. 10.1186/s12859-022-04898-2.
54. Bayliss, S.C., Thorpe, H.A., Coyle, N.M., Sheppard, S.K., and Feil, E.J. (2019). PIRATE: A fast and scalable pangenomics toolbox for clustering diverged orthologues in bacteria. Gigascience *8*. 10.1093/gigascience/giz119.
55. Seemann, T. (2014). Prokka: rapid prokaryotic genome annotation. Bioinformatics *30*, 2068-2069. 10.1093/bioinformatics/btu153.
56. Li, H., Handsaker, B., Wysoker, A., Fennell, T., Ruan, J., Homer, N., Marth, G., Abecasis, G., Durbin, R., and Genome Project Data Processing, S. (2009). The Sequence Alignment/Map format and SAMtools. Bioinformatics *25*, 2078-2079. 10.1093/bioinformatics/btp352.
57. Shen, W., Le, S., Li, Y., and Hu, F. (2016). SeqKit: A Cross-Platform and Ultrafast Toolkit for FASTA/Q File Manipulation. PLoS One *11*, e0163962. 10.1371/journal.pone.0163962.
58. Bolger, A.M., Lohse, M., and Usadel, B. (2014). Trimmomatic: a flexible trimmer for Illumina sequence data. Bioinformatics *30*, 2114-2120. 10.1093/bioinformatics/btu170.

59. Bruckner, R. (1997). Gene replacement in Staphylococcus carnosus and Staphylococcus xylosus. FEMS microbiology letters *151*, 1-8. 10.1111/j.1574-6968.1997.tb10387.x.
60. Novick, R.P. (1991). Genetic systems in staphylococci. Methods in enzymology *204*, 587-636.
61. Novick, R. (1967). Properties of a cryptic high-frequency transducing phage in Staphylococcus aureus. Virology *33*, 155-166.
62. Kreiswirth, B.N., Lofdahl, S., Betley, M.J., O'Reilly, M., Schlievert, P.M., Bergdoll, M.S., and Novick, R.P. (1983). The toxic shock syndrome exotoxin structural gene is not detectably transmitted by a prophage. Nature *305*, 709-712.
63. Humphrey, S., San Millan, A., Toll-Riera, M., Connolly, J., Flor-Duro, A., Chen, J., Ubeda, C., MacLean, R.C., and Penades, J.R. (2021). Staphylococcal phages and pathogenicity islands drive plasmid evolution. Nat Commun *12*, 5845. 10.1038/s41467-021-26101-5.
64. Fernandez, L., Gonzalez, S., Quiles-Puchalt, N., Gutierrez, D., Penades, J.R., Garcia, P., and Rodriguez, A. (2018). Lysogenization of Staphylococcus aureus RN450 by phages varphi11 and varphi80alpha leads to the activation of the SigB regulon. Sci Rep *8*, 12662. 10.1038/s41598-018-31107-z.
65. Yanisch-Perron, C., Vieira, J., and Messing, J. (1985). Improved M13 phage cloning vectors and host strains: nucleotide sequences of the M13mp18 and pUC19 vectors. Gene *33*, 103-119.

Figure 1

Click here to access/download;Figure;Figure 1.pdf

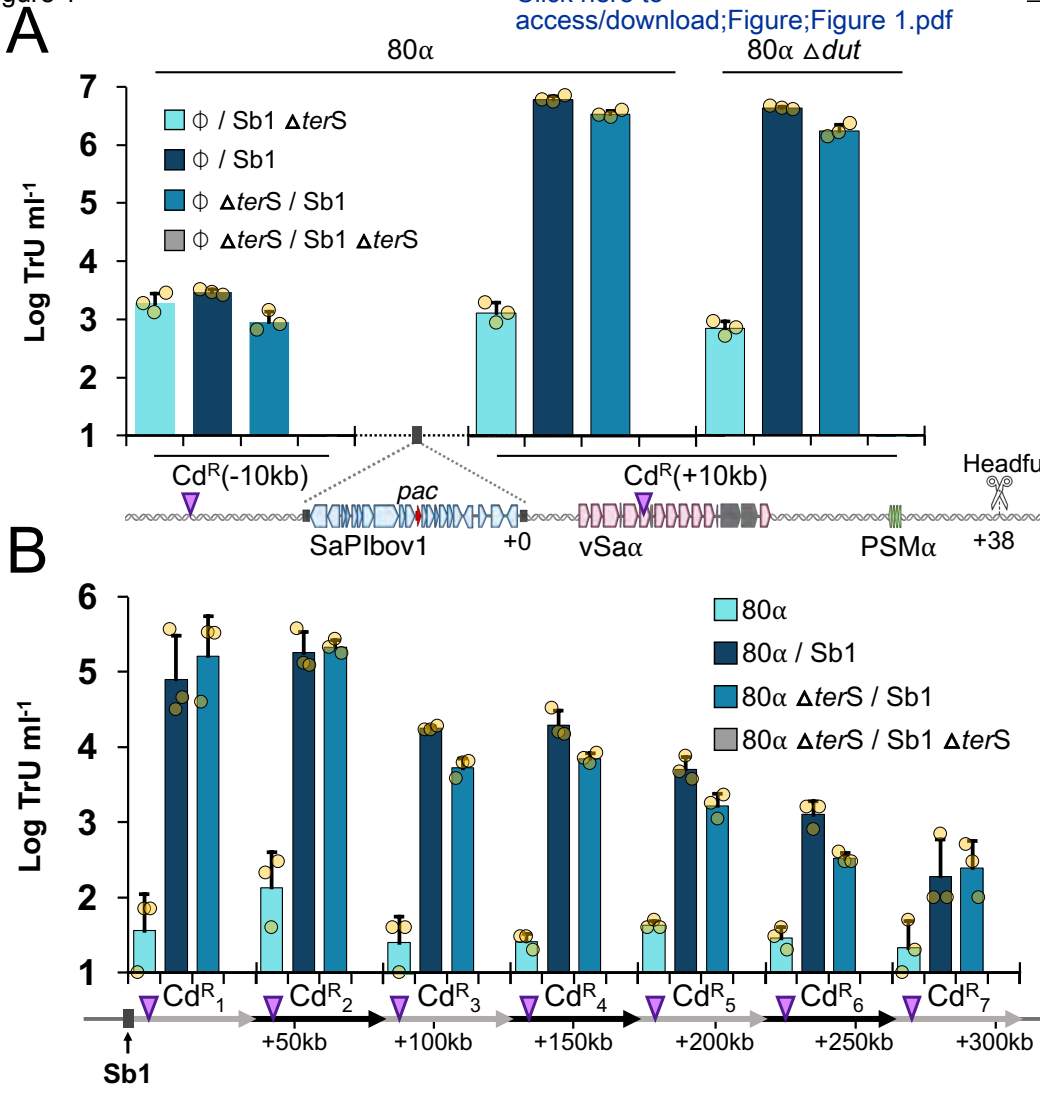

Figure 2

Click here to access/download;Figure;Figure 2.pdf

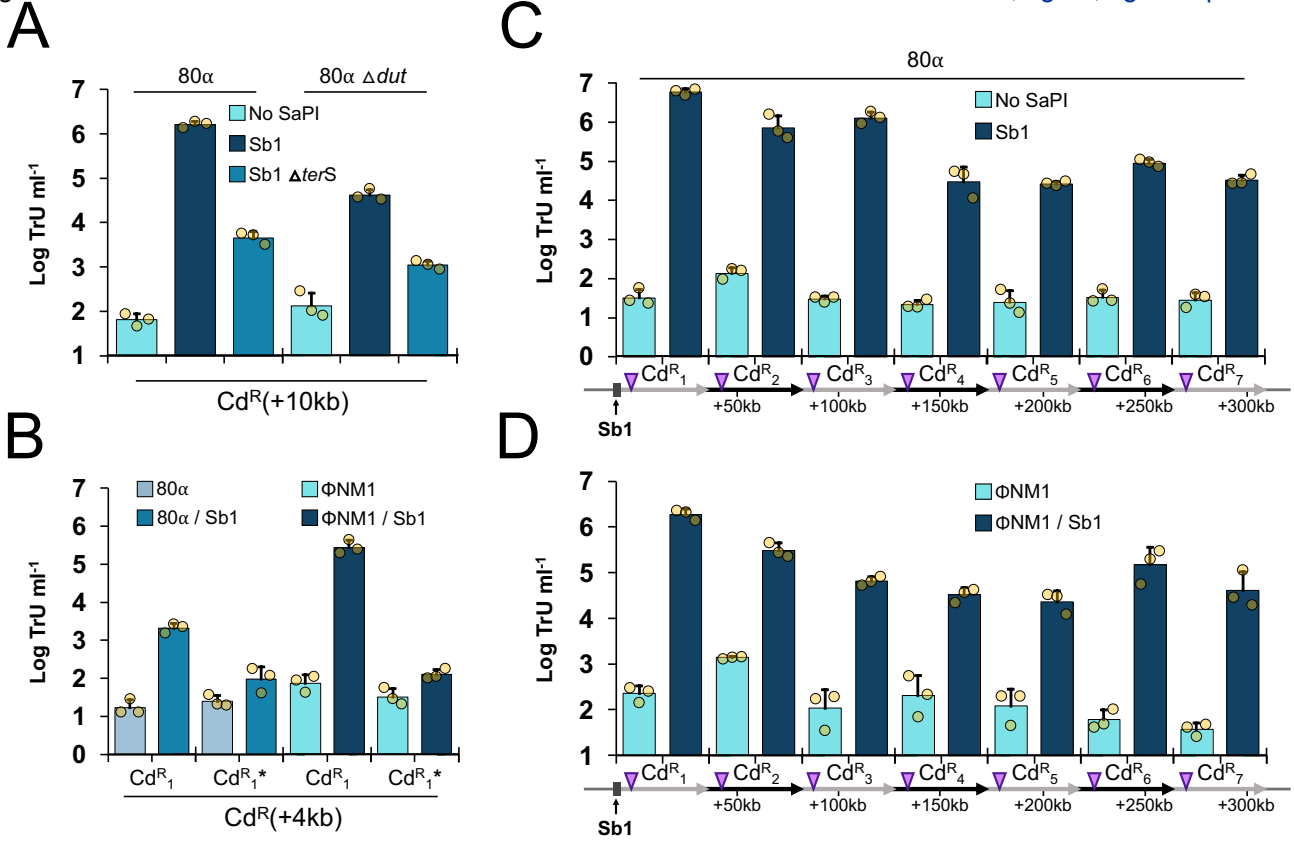

Figure 3

Click here to access/download;Figure;Figure 3.pdf

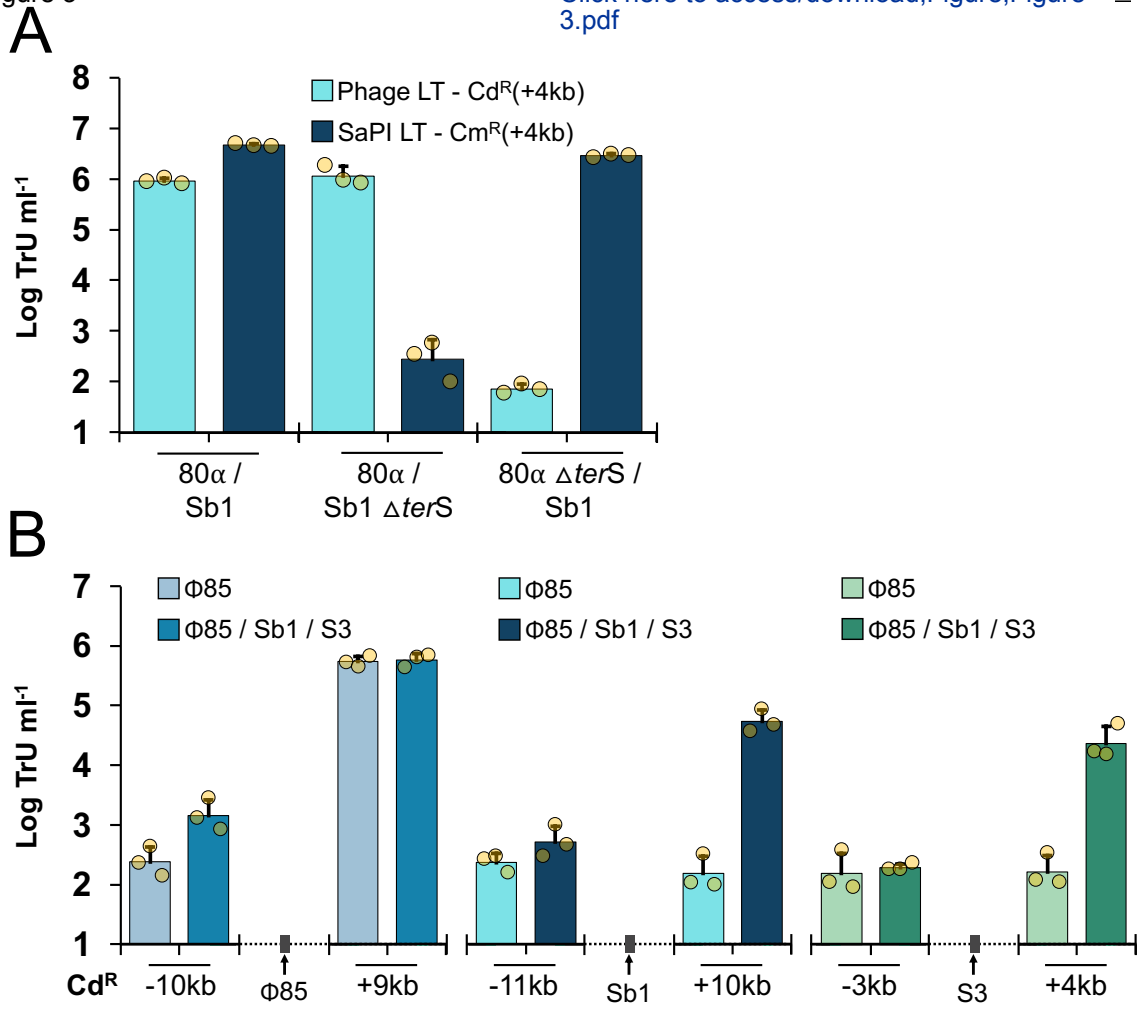

Figure 4

Click here to access/download;Figure;Figure 4.pdf

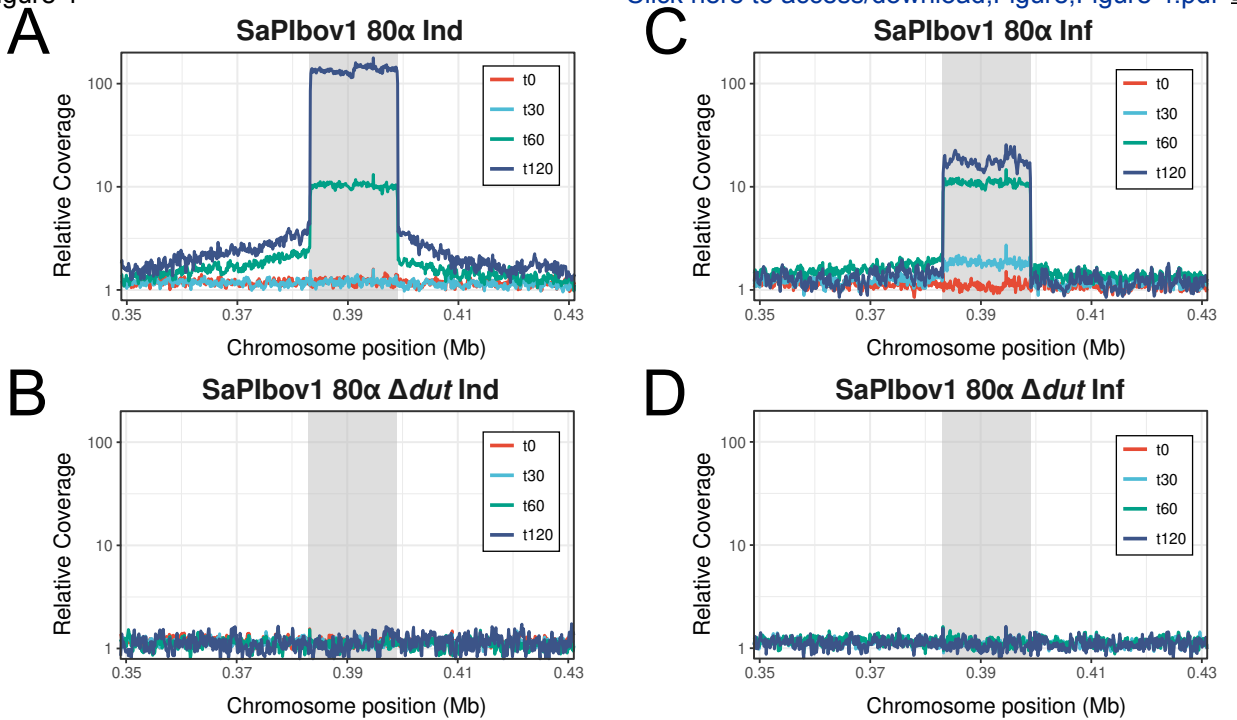

Figure 5

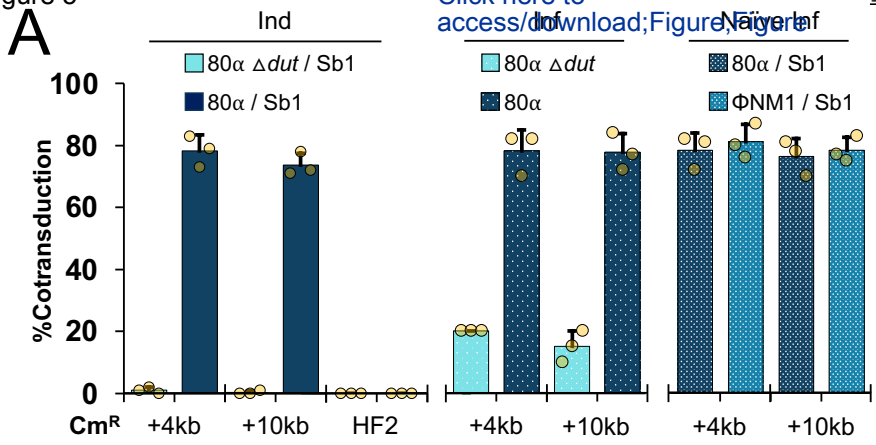

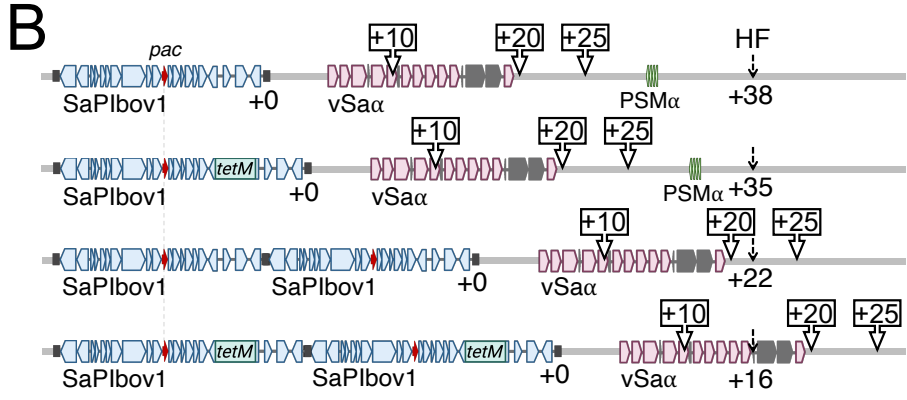

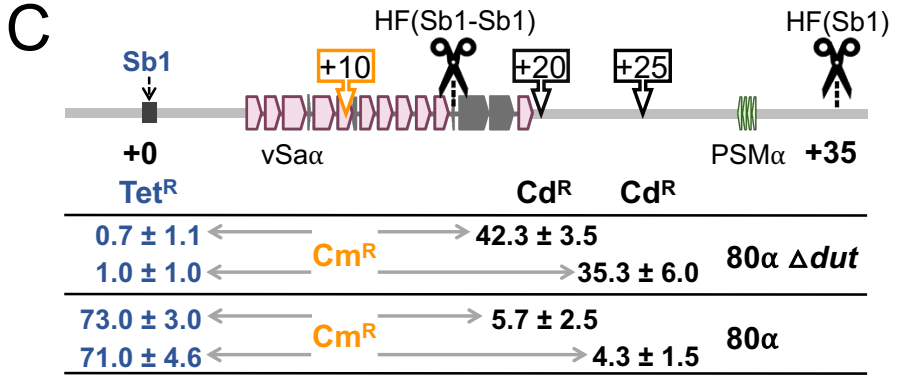

Figure 6

Click here to access/download;Figure;Figure 6.pdf

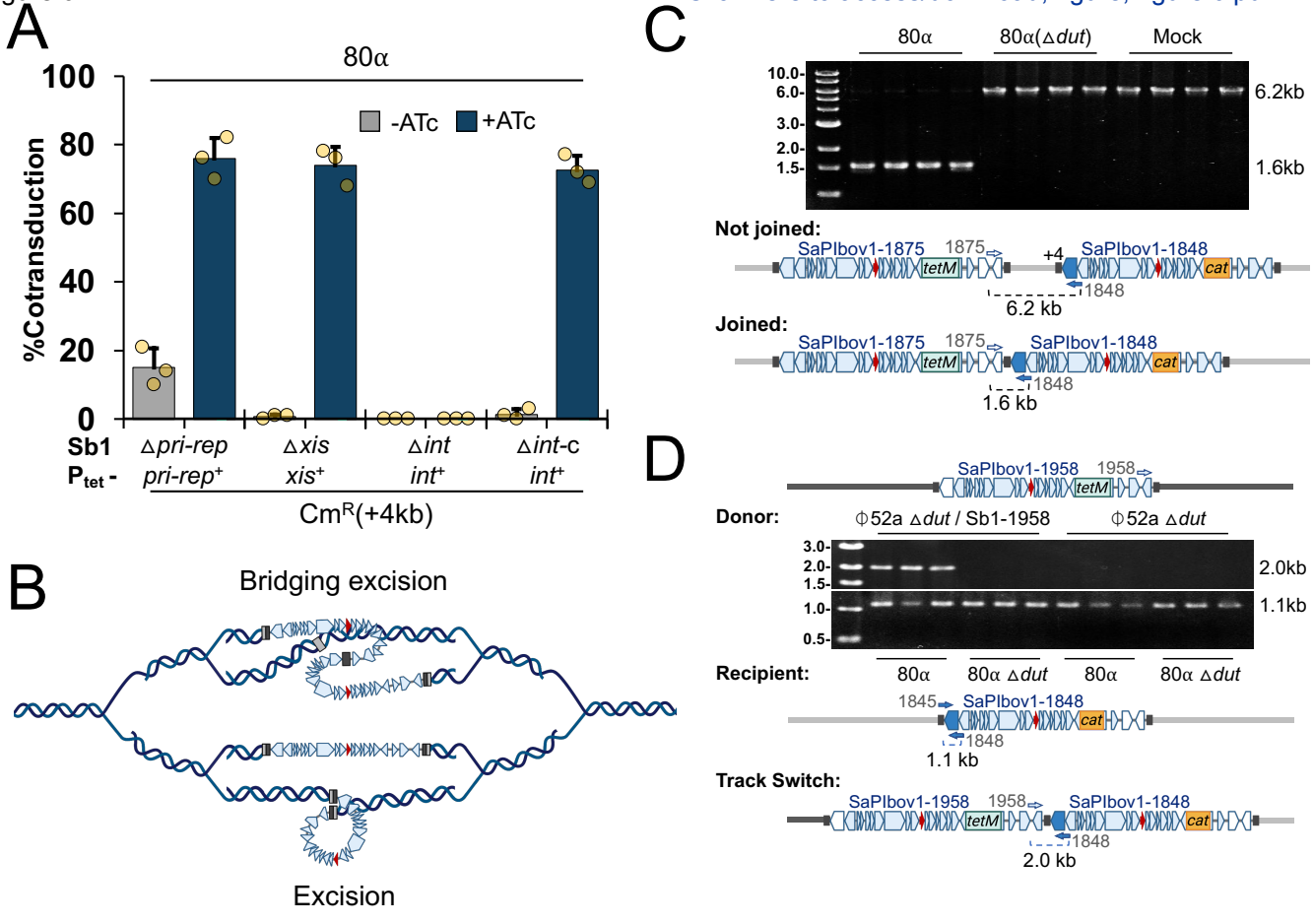

Figure 7

Click here to access/download;Figure;Figure 7.pdf

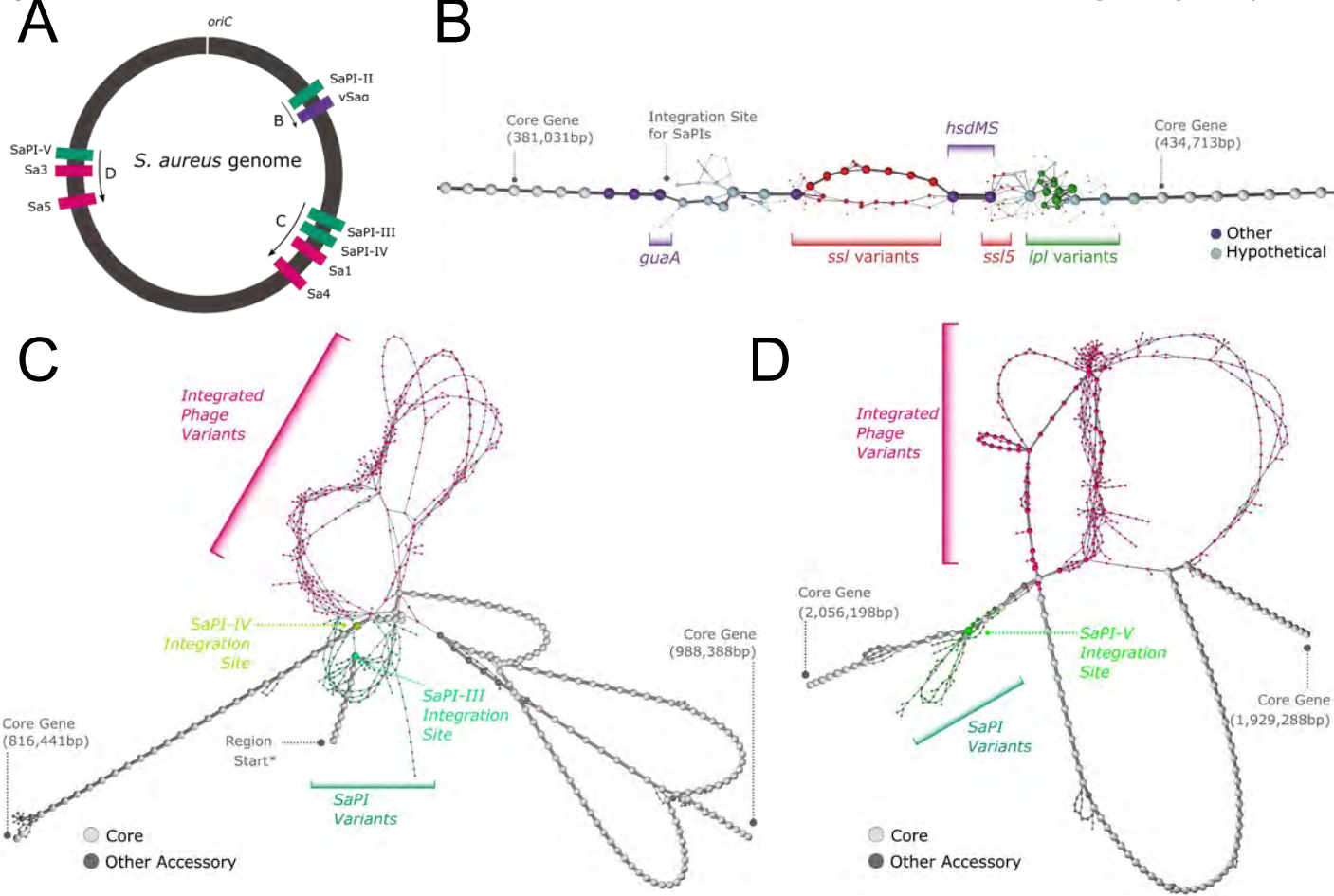

Table S4. Strain

Strains
S. aureus
RF122
RN450
RN4220
RN10616
JP12871
JP13536
JP13950
JP21092
JP21093
JP21100
JP21101
JP22013
JP22014
JP22015
JP22016

JP22017

JP22018

JP22019

JP22020

JP22278

JP22279

JP22280

JP22281

JP2392

JP22294

JP14151

JP13797

JP14153

JP22534

JP22535

JP22536

JP22537

JP22538

JP22539

JP22548

JP22549

JP22550

JP22551

JP22552

JP22553

JCSA17

JCSA438

JCSA534

JCSA631

JCSA643

JCSA651

JCSA652

JCSA653

JCSA654

JCSA657

JCSA667

JCSA668

JCSA669

JCSA671

JCSA672

JCSA673

JCSA911

JCSA913

JCSA917

JCSA918

JCSA919

JCSA920

JCSA1067

JCSA1085

JCSA1086

JCSA1087

JCSA1089

JCSA1196

JCSA1487

JCSA1488

JCSA1199

JCSA1200

JCSA1201

JCSA1202

JCSA1203

JCSA1204

JCSA1205

JCSA1206

JCSA1207

JCSA1208

JCSA1209

JCSA1210

JCSA1211

JCSA1212

JCSA1213

JCSA1214

JCSA1215

JCSA1216

JCSA1217

JCSA1218

JCSA1219

JCSA1220

JCSA1221

JCSA1222

JCSA1223

JCSA1224

JCSA1225

JCSA1226

JCSA1243

JCSA1244

JCSA1245

JCSA1246

JCSA1247

JCSA1248

JCSA1249

JCSA1250

JCSA1305

JCSA1430

JCSA1431

JCSA1487

JCSA1488

JCSA1794

JCSA1795

JCSA1796

JCSA1797

JCSA1798

JCSA1799

JCSA1800

JCSA1801

JCSA1802

JCSA1803

JCSA1816

JCSA1829

JCSA1830

JCSA1831

JCSA1832

JCSA1833

JCSA1834

JCSA1835

JCSA1836

JCSA1837

JCSA1838

JCSA1839

JCSA1840

JCSA1841

JCSA1842

JCSA1843

JCSA1844

JCSA1845

JCSA1846

JCSA1847

JCSA1848

JCSA1849

JCSA1850

JCSA1851

JCSA1852

JCSA1853

JCSA1854

JCSA1855

JCSA1856

JCSA1857

JCSA1858

JCSA1859

JCSA1860

JCSA1861

JCSA1862

JCSA1863

JCSA1913

JCSA1978

JCSA1979

JCSA1980

JCSA1981

JCSA1982

JCSA1983

JCSA1984

JCSA2013

JCSA2014

JCSA2015

JCSA2016

JCSA2018

JCSA2019

JCSA2020

JCSA2021

JCSA2034

JCSA2035

JCSA2036

JCSA2037

JCSA2038

JCSA2039

JCSA2040

JCSA2041

JCSA2042

JCSA2043

JCSA2044

JCSA2045

JCSA2046

JCSA2047

JCSA2049

JCSA2050

JCSA2051

JCSA2052

JCSA2053

JCSA2054

JCSA2055

JCSA2056

JCSA2057

JCSA2058

JCSA2059

JCSA2060

JCSA2061

JCSA2062

JCSA2068

JCSA2070

JCSA2072

JCSA2074

JCSA2076

JCSA2078

JCSA2105

JCSA2106

JCSA2109

JCSA2110

JCSA2111

JCSA2112

JCSA2113

JCSA2115

JCSA2117

JCSA2118

JCSA2119

JCSA2130

JCSA2136

JCSA2137

JCSA2140

JCSA2141

JCSA2149

JCSA2150

JCSA2202

JCSA2203

JCSA2211

JCSA2212

JCSA2215

JCSA2216

JCSA2217

JCSA2218

JCSA2219

JCSA2220

JCSA2221

JCSA2222

JCSA2223

JCSA2224

JCSA2233

JCSA2234

JCSA2235

JCSA2248

JCSA2249

JCSA2250

JCSA2251

JCSA2253

JCSA2254

JCSA2255

JCSA2287

JCSA2293

JCSA2294

JCSA2295

JCSA2316

JCSA2317

JCSA2319

JCSA2320

JCSA2321

JCSA2322

JCSA2323

JCSA2324

JCSA2325

Strains
JCSA2326
JCSA2327
JCSA2328
JCSA2329
JCSA2330
JCSA2345
JCSA2346
JCSA2347
JCSA2348
JCSA2349
JCSA2350
JCSA2351

s used in this study, related to STAR Methods Phages, bacterial strains, and growth conditions.

Description
Bovine mastitis isolate, SaPIbov1
NCTC8325 cured of Φ11, Φ12, and Φ13
Restriction-defective derivative of RN450
RN4220, 80α
RN4220 lysogenic for 80α Δ*ter* S
RN4220 SAOUHSC_00841::*cadCA* ; Cd^R marker 3 kb upstream SaPI type IV *att* C
RN4220 SAOUHSC_00848::*cadCA* ; Cd^R marker 4 kb downstream SaPI type IV *att* C
JP13536 lysogenic for 80α
JP13950 lysogenic for 80α
JP21092, SaPI1 *tsst* ::*tetM*
JP21093, SaPI1 *tsst::tetM*
JP21092, SaPI1 *tsst::tetM* Δ*ter* S
JP21093, SaPI1 *tsst::tetM* Δ*ter* S
JP13536 lysogenic for 80α Δ*ter* S
JP13950 lysogenic for 80α Δ*ter* S

JP22015, SaPI1 *tsst::tetM*

JP22016, SaPI1 *tsst::tetM*

JP22015, SaPI1 *tsst::tetM* Δ*ter* S

JP22016, SaPI1 *tsst::tetM* Δ*ter* S

JP13536, SaPI1 *tsst::tetM*

JP13950, SaPI1 *tsst::tetM*

JP13536, SaPI1 *tsst::tetM* Δ*ter* S

JP13950, SaPI1 *tsst::tetM* Δ*ter* S

RN450 lysogenic for Φ85

RN4220 SAOUHSC_00365::*cadCA* ; Cd^R marker 11 kb upstream SaPI type II *att* C

RN4220 SAOUHSC_00390::*cadCA* ; Cd^R marker 10 kb downstream SaPI type II *att* C

RN4220 SAOUHSC_01064::*cadCA* ; Cd^R marker 10 kb upstream Sa7 *att* B

RN4220 SAOUHSC_01091::*cadCA* ; Cd^R marker 9 kb downstream Sa7 *att* B

JP13536 lysogenic for Φ85

JP13950 lysogenic for Φ85

JP22294 lysogenic for Φ85

JP14151 lysogenic for Φ85

JP13797 lysogenic for Φ85

JP14153 lysogenic for Φ85

JP22534, SaPIbov1 *tsst::tetM* , SaPI3 *seb* ::*erm* C

JP22535, SaPIbov1 *tsst::tet* M, SaPI3 *seb* ::*erm* C

JP22536, SaPIbov1 *tsst::tetM* , SaPI3 *seb* ::*erm* C

JP22537, SaPIbov1 *tsst::tetM* , SaPI3 *seb* ::*erm* C

JP22538, SaPIbov1 *tsst::tetM* , SaPI3 *seb* ::*erm* C

JP22539, SaPIbov1 *tsst::tetM* , SaPI3 *seb* ::*erm* C

RN4220 (*rpsL**)

RN450, 80α

JCSA17, SaPIbov1 *tsst* ::*tetM*

RN4220, pJC1693 (SaPI4 *int* +)

JCSA438, 80α Δ*ter* S

JCSA438, SaPI1 *tsst* ::*tetM*

JCSA438, SaPI2 *tsst* ::*tetM*

JCSA438, SaPIbov1 *tsst* ::*tetM*

JCSA438 , SaPIbov2 *bap* ::*tetM*

JCSA438, SaPIbov1 *tsst* ::*tetM* Δ*ter* S

JCSA643, SaPI1 *tsst* ::*tetM*

JCSA643, SaPI2 *tsst* ::*tetM*

JCSA643, SaPIbov1 *tsst* ::*tetM*

JCSA643, SaPI1 *tsst*::*tetM* Δ*ter*S

JCSA643, SaPI2 *tsst*::*tetM* Δ*ter*S

JCSA643, SaPIbov1 *tsst*::*tetM* Δ*ter*S

JCSA438, 80α Δ*dut*

JCSA911, 80α Δ(*dut, ter*S*)*

JCSA911, SaPIbov1 *tsst*::*tetM*

JCSA911, SaPIbov1 *tsst*::*tetM* Δ*ter*S

JCSA913, SaPIbov1 *tsst*::*tetM*

JCSA913, SaPIbov1 *tsst*::*tetM* Δ*ter*S

JCSA17, *cadCA* 4kb downstream SaPI4 *att*C

RN450, SaPI1 *tsst*::*tetM*

RN450, SaPI2 *tsst*::*tetM*

RN450, SaPIbov1 *tsst*::*tetM*

RN450, SaPIbov1 *tsst*::*tetM* Δ*ter*S

RN450, Φ52a

JCSA438, *cadCA* 4 kb downstream 80α *att*C

JCSA643, *cadCA* 4 kb downstream 80α *att*C

JCSA438, *cadCA* 10 kb downstream SaPIbov1 *att*C

RN450, *cadCA* 10 kb downstream SaPIbov1 *att*C

JCSA1087, *cadCA* 10 kb downstream SaPIbov1 *att*C

JCSA1089, *cadCA* 10 kb downstream SaPIbov1 *att*C

JCSA438, *cadCA* 16 kb downstream SaPIbov1 *att*C

RN450, *cadCA* 16 kb downstream SaPIbov1 *att*C

JCSA1087, *cadCA* 16 kb downstream SaPIbov1 *att*C

JCSA1089, *cadCA* 16 kb downstream SaPIbov1 *att*C

JCSA653, *cadCA* 10 kb downstream SaPIbov1 *att*C

JCSA657, *cadCA* 10 kb downstream SaPIbov1 *att*C

JCSA669, *cadCA* 10 kb downstream SaPIbov1 *att*C

JCSA673, *cadCA* 10 kb downstream SaPIbov1 *att*C

JCSA653, *cadCA* 16 kb downstream SaPIbov1 *att*C

JCSA657, *cadCA* 16 kb downstream SaPIbov1 *att*C

JCSA669, *cadCA* 16 kb downstream SaPIbov1 *att*C

JCSA673, *cadCA* 16 kb downstream SaPIbov1 *att*C

JCSA917, *cadCA* 10 kb downstream SaPIbov1 *att*C

JCSA918, *cadCA* 10 kb downstream SaPIbov1 *att*C

JCSA919, *cadCA* 10 kb downstream SaPIbov1 *att*C

JCSA920, *cadCA* 10 kb downstream SaPIbov1 *att*C

JCSA917, *cadCA* 16 kb downstream SaPIbov1 *att*C

JCSA918, *cadCA* 16 kb downstream SaPIbov1 *att*C

JCSA919, *cadCA* 16 kb downstream SaPIbov1 *att*C

JCSA920, *cadCA* 16 kb downstream SaPIbov1 *att*C

JCSA643, *cadCA* 10 kb downstream SaPIbov1 *att*C

JCSA643, *cadCA* 16 kb downstream SaPIbov1 *att*C

JCSA913, *cadCA* 10 kb downstream SaPIbov1 *att*C

JCSA913, *cadCA* 16 kb downstream SaPIbov1 *att*C

JCSA1223, SaPI4 *att*C::pJC1746

JCSA1210, SaPI4 *att*C::pJC1746

JCSA1225, SaPI4 *att*C::pJC1746

JCSA1218, SaPI4 *att*C::pJC1746

JCSA1224, SaPI4 *att*C::pJC1746

JCSA1214, SaPI4 *att*C::pJC1746

JCSA1226, SaPI4 *att*C::pJC1746

JCSA1222, SaPI4 *att*C::pJC1746

RN4220, Δ*recA* pJC2094 allele exchanged

RF122, SaPIbov1 Δ*tsst*::*tetM* pJC2127 allele exchange

JCSA1430, SaPIbov1 Δ*tsst*::*tetM* Δ(*sel-sec*) pJC2126 allele exchange

JCSA438, *cadCA* 4 kb downstream 80α *att*B

JCSA643, *cadCA* 4 kb downstream 80α *att* B

RN450, *cadCA* 4 kb downstream SaPI1 *att* C pJC2485 allele exchange

JCSA438, *cadCA* 4 kb downstream SaPI1 *att* C

JCSA651, *cadCA* 4 kb downstream SaPI1 *att* C

JCSA667, *cadCA* 4 kb downstream SaPI1 *att* C

JCSA671, *cadCA* 4 kb downstream SaPI1 *att* C

RN450, *cadCA* 4 kb downstream SaPI2 *att* C pJC2489 allele exchange

JCSA438, *cadCA* 4 kb downstream SaPI2 *att* C

JCSA651, *cadCA* 4 kb downstream SaPI2 *att* C

JCSA667, *cadCA* 4 kb downstream SaPI2 *att* C

JCSA671, *cadCA* 4 kb downstream SaPI2 *att* C

JCSA534, SaPIbov1 Δ*tsst*::*cat194* pJC2674 allele exchange

RN450, *cadCA* 1st headful downstream of SaPIbov1 *att* C pJC2247 allele exchange

RN450, *cadCA* 2nd headful downstream of SaPIbov1 *att* C pJC2300 allele exchange

RN450, *cadCA* 3rd headful downstream of SaPIbov1 *att* C pJC2616 allele exchange

RN450, *cadCA* 4th headful downstream of SaPIbov1 *att* C pJC2617 allele exchange

RN450, *cadCA* 5th headful downstream of SaPIbov1 *att* C pJC2618 allele exchange

RN450, *cadCA* 6th headful downstream of SaPIbov1 *att* C pJC2301 allele exchange

RN450, *cadCA* 7th headful downstream of SaPIbov1 *att* C pJC2302 allele exchange

JCSA438, *cadCA* 1st headful downstream of SaPIbov1 *att* C

JCSA438, *cadCA* 2nd headful downstream of SaPIbov1 *att* C

JCSA438, *cadCA* 3rd headful downstream of SaPIbov1 *att* C

JCSA438, *cadCA* 4th headful downstream of SaPIbov1 *att* C

JCSA438, *cadCA* 5th headful downstream of SaPIbov1 *att* C

JCSA438, *cadCA* 6th headful downstream of SaPIbov1 *att* C

JCSA438, *cadCA* 7th headful downstream of SaPIbov1 *att* C

JCSA653, *cadCA* 1st headful downstream of SaPIbov1 *att* C

JCSA653, *cadCA* 2nd headful downstream of SaPIbov1 *att* C

JCSA653, *cadCA* 3rd headful downstream of SaPIbov1 *att* C

JCSA653, *cadCA* 4th headful downstream of SaPIbov1 *att* C

JCSA653, *cadCA* 5th headful downstream of SaPIbov1 *att* C

JCSA653, *cadCA* 6th headful downstream of SaPIbov1 *att* C

JCSA653, *cadCA* 7th headful downstream of SaPIbov1 *att* C

JCSA669, *cadCA* 1st headful downstream of SaPIbov1 *att* C

JCSA669, *cadCA* 2nd headful downstream of SaPIbov1 *att* C

JCSA669, *cadCA* 3rd headful downstream of SaPIbov1 *att* C

JCSA669, *cadCA* 4th headful downstream of SaPIbov1 *att* C

JCSA669, *cadCA* 5th headful downstream of SaPIbov1 *att* C

JCSA669, *cadCA* 6th headful downstream of SaPIbov1 *att*C

JCSA669, *cadCA* 7th headful downstream of SaPIbov1 *att*C

JCSA673, *cadCA* 1st headful downstream of SaPIbov1 *att*C

JCSA673, *cadCA* 2nd headful downstream of SaPIbov1 *att*C

JCSA673, *cadCA* 3rd headful downstream of SaPIbov1 *att*C

JCSA673, *cadCA* 4th headful downstream of SaPIbov1 *att*C

JCSA673, *cadCA* 5th headful downstream of SaPIbov1 *att*C

JCSA673, *cadCA* 6th headful downstream of SaPIbov1 *att*C

JCSA673, *cadCA* 7th headful downstream of SaPIbov1 *att*C

JCSA653, SaPIbov1 *tsst*::*tetM* Δ(*pri-rep*) pJC2772 allele exchange

JCSA1829, SaPIbov1 *tsst*::*tetM*

JCSA1830, SaPIbov1 *tsst*::*tetM*

JCSA1831, SaPIbov1 *tsst*::*tetM*

JCSA1832, SaPIbov1 *tsst*::*tetM*

JCSA1833, SaPIbov1 *tsst*::*tetM*

JCSA1834, SaPIbov1 *tsst*::*tetM*

JCSA1835, SaPIbov1 *tsst*::*tetM*

JCSA1487, SaPIbov1 *tsst*::*tetM*, *cat194* 4 kb downstream of SaPIbov1 *att*C pJC2909 allele exchange

JCSA1487, SaPIbov1 *tsst*::*tetM* Δ*ter*S, *cat194* 4 kb downstream of SaPIbov1 *att*C pJC2909 allele exchange

JCSA1488, SaPIbov1 *tsst:* :*tetM* , *cat194* 4 kb downstream of SaPIbov1 *att* C, pJC2909 allele exchange

JCSA1488, SaPIbov1 *tsst* ::*tetM* Δ*ter* S, cat194 4 kb downstream of SaPIbov1 *att* C, pJC2909 allele exchange

JCSA438, *cat194* 10 kb downstream of SaPIbov1 *att* C pJC2884 allele exchange

JCSA2018, SaPIbov1 *tsst* ::*tetM*

JCSA911, *cat194* 10 kb downstream of SaPIbov1 *att* C pJC2884 allele exchange

JCSA2020, SaPIbov1 *tsst* ::*tetM*

RN450, *cadCA* 1st headful upstream of SaPIbov1 *att* C pJC2869 allele exchange

JCSA438, *cadCA* 1st headful upstream of SaPIbov1 *att* C

JCSA643, *cadCA* 1st headful upstream of SaPIbov1 *att* C

JCSA653, *cadCA* 1st headful upstream of SaPIbov1 *att* C

JCSA657, *cadCA* 1st headful upstream of SaPIbov1 *att* C

JCSA669, *cadCA* 1st headful upstream of SaPIbov1 *att* C

JCSA673, *cadCA* 1st headful upstream of SaPIbov1 *att* C

RN450, *cadCA* 4 kb downstream of SaPIbov1 *attC* pJC2247 allele exchange

JCSA438, *cadCA* 4 kb downstream of SaPIbov1 *att* C

JCSA643, *cadCA* 4 kb downstream of SaPIbov1 *att* C

JCSA653, *cadCA* 4 kb downstream of SaPIbov1 *att* C

JCSA657, *cadCA* 4 kb downstream of SaPIbov1 *att* C

JCSA667, *cadCA* 4 kb downstream of SaPIbov1 *att* C

JCSA673, *cadCA* 4 kb downstream of SaPIbov1 *att*C

RN450, SaPIbov1 *att*C* synonymous mutations pJC2626 allele exchange

JCSA2049, *cadCA* 4 kb downstream of SaPIbov1 *att*C

JCSA438, *cat194* 4 kb downstream of SaPIbov1 *att*C

JCSA911, *cat194* 4 kb downstream of SaPIbov1 *att*C

JCSA438, *cat194* 2nd headful downstream of SaPIbov1 *att*C

JCSA911, *cat194* 2nd headful downstream of SaPIbov1 *att*C

JCSA438, *cat194* 3rd headful downstream of SaPIbov1 *att*C

JCSA911, *cat194* 3rd headful downstream of SaPIbov1 *att*C

JCSA2051, SaPIbov1 *tsst*::*tetM*

JCSA2052, SaPIbov1 *tsst*::*tetM*

JCSA2053, SaPIbov1 *tsst*::*tetM*

JCSA2054, SaPIbov1 *tsst*::*tetM*

JCSA2055, SaPIbov1 *tsst*::*tetM*

JCSA2056, SaPIbov1 *tsst*::*tetM*

JCSA438, *cat194* 4 kb downstream of SaPI1 *att*C

JCSA438, *cat194* 4 kb downstream of SaPI2 *att*C

JCSA2068, SaPI1 *tsst*::*tetM*

JCSA2068, SaPI1 *tsst*::*tetM* Δ*cpmAB*

JCSA2070, SaPI2 *tsst*::*tetM*

JCSA2070, SaPI2 *tsst*::*tetM* Δ*cpmAB*

JCSA2051, SaPIbov5 *vwb*::*ermC*

JCSA2052, SaPIbov5 *vwb*::*ermC*

JCSA438, *cadCA* 4 kb downstream SaPI4 *att* C

JCSA911, *cadCA* 4 kb downstream SaPI4 *att* C

JCSA2109, SaPIpT1028::*ermC*

JCSA2110, SaPIpT1028::*ermC*

JCSA2051, SaPIbov1 *tsst*::*tetM* Δ*int*

JCSA2051, SaPIbov1 *tsst*::*tetM* Δ*xis*

JCSA1085, *cat194* 4 kb downstream of SaPI1 *att* C

JCSA1086, *cat194* 4 kb downstream of SaPI2 *att* C

JCSA1087, *cat194* 4 kb downstream of SaPIbov1 *att* C

JCSA2051, SaPIbov1 *tsst*::*tetM* Δ(*pri-rep)*

JCSA643, *cat194* 10 kb downstream of SaPIbov1 *attC* pJC2884 allele exchange

JCSA913, *cat194* 10 kb downstream of SaPIbov1 *attC* pJC2884 allele exchange

JCSA2136, *cadCA* 25 kb downstream of SaPIbov1 *attC* pJC2922 allele exchange

JCSA2137, *cadCA* 25 kb downstream of SaPIbov1 *attC* pJC2922 allele exchange

JCSA2040, SaPIbov1 *tsst*::*tetM* Δ*cpmAB*

JCSA2041, SaPIbov1 *tsst*::*tetM* Δ*cpmAB*

JCSA2136, SaPIbov1 *tsst*::*tetM* Δ*cpmAB*, *cadCA* 20 kb downstream of SaPIbov1 *attC* pJC2921 allele exchange

JCSA2137, SaPIbov1 *tsst*::*tetM* Δ*cpmAB*, *cadCA* 20 kb downstream of SaPIbov1 *attC* pJC2921 allele exchange

JCSA2051, SaPIbov1 Δ*tsst*::*tetM* Δ(*sel-sec*)

JCSA2052, SaPIbov1 Δ*tsst*::*tetM* Δ(*sel-sec*)

JCSA2211, (4 kb downstream of SaPIbov1 *att*C)::(SaPI Bov1 *att*C site) pJC2964 allele exchange

JCSA2212, (4 kb downstream of SaPIbov1 *att*C)::(SaPI Bov1 *att*C site) pJC2964 allele exchange

JCSA1305, SaPIbov1 Δ*tsst*::*ermC*

RN450, *cat194* 4 kb downstream of SaPI1 *att*C

JCSA2218, SaPI1 *tsst*::*tetM*

RN450, *cat194* 4 kb downstream of SaPI2 *att*C

JCSA2220, SaPI2 *tsst*::*tetM*

RN450, *cat194* 4 kb downstream of SaPIbov1 *att*C

JCSA2222, SaPIbov1 *tsst*::*tetM*

JCSA1816, SaPIbov1 Δ*tsst*::*cat194 int*^{syn} synonymous mutations pJC2984 allele exchange

JCSA2222, SaPIbov1 Δ*tsst*::*tetM* Δ(*sel-sec*)

JCSA2233, (4 kb downstream of SaPIbov1 *att*C)::(SaPI Bov1 *att*C site) pJC2964 allele exchange

JCSA2234, (4 kb downstream of SaPIbov1 *att*C)::(SaPI Bov1 *att*C site)::SaPIbov1 Δ*tsst*::*cat194 int*^{syn} synonymous mutatio

RF122, SaPIbov1 Δ*tsst*::*cat194 int*^{syn} synonymous mutations

JCSA2248, SaPIbov1 Δ*tsst*::*cat194* *int*^{syn} synonymous mutations, Δ(*sel-sec*) allele exchange pJC2126

JCSA2223, (4 kb downstream of SaPIbov1 *att*C)::(SaPI Bov1 *att*C site) pJC2964 allele exchange

JCSA2250, (4 kb downstream of SaPIbov1 *att*C)::(SaPI Bov1 *att*C site)::SaPIbov1 Δ*tsst:*:*cat194* *int*^{syn} synonymous mutatio

JCSA17, SaPIbov1 Δ*tsst*::*tetM* Δ(*sel-sec*)

JCSA2253, SaPIbov1 Δ*tsst*::*cat194* Δ(*sel-sec*) pJC2847 allele exchange

JCSA2254, SaPIbov1 Δ*tsst*::*cat194* *int*^{syn} synonymous mutations, Δ(*sel-sec*) pJC2984 allele exchange

RN450, pJC3056 (SaPIbov1 *int*+)

JCSA2130, SaPIbov1 *tsst*::*tetM* Δ(*pri-rep*), SaPI1 *att*C::pJC2791 (SaPIbov1 *pri-rep*+)

JCSA2115, SaPIbov1 *tsst*::*tetM* Δ*xis*, SaPI1 *att*C::pJC2786 (SaPIbov1 *xis*+)

JCSA2130, SaPIbov1 *tsst*::*tetM* Δ*int*, SaPI1 *att*C::pJC3038 (SaPIbov1 *int*+)

JCSA1196, Φ52a Δ*dut* pJC3067 allele exchange

JCSA2316, SaPIbov1 *tsst*::*tetM* Δ*int*

JCSA438, SaPIbov1 Δ*tsst*::*cat194* *int*^{syn} synonymous mutations, Δ(*sel-sec*)

JCSA911, SaPIbov1 Δ*tsst*::*cat194 int*^{syn} synonymous mutations, Δ(*sel-sec*)

RN450, *cat194* 10 kb downstream of SaPIbov1 *att*C

JCSA232, SaPIbov1 *tsst*::*tetM*

RN450, *cat194* 20 kb downstream of SaPIbov1 *att*C pJC2945 allele exchange

RN438, *cat194* 20 kb downstream of SaPIbov1 *att*C

RN911, *cat194* 20 kb downstream of SaPIbov1 *att*C

JCSA2323, SaPIbov1 Δ*tsst* ::*tetM* Δ(*sel-sec*)

JCSA2324, SaPIbov1 Δ*tsst* ::*tetM* Δ(*sel-sec*)

JCSA2325, SaPIbov1 Δ*tsst* ::*tetM* Δ(*sel-sec*)

JCSA2049, *cat194* 10 kb downstream of SaPIbov1 *att* C

JCSA2049, *cat194* 20 kb downstream of SaPIbov1 *att* C

JCSA1836 , SaPIbov2 *bap* ::*tetM*

JCSA1837 , SaPIbov2 *bap* ::*tetM*

JCSA1838 , SaPIbov2 *bap* ::*tetM*

JCSA1839 , SaPIbov2 *bap* ::*tetM*

JCSA1840 , SaPIbov2 *bap* ::*tetM*

JCSA1841 , SaPIbov2 *bap* ::*tetM*

JCSA1842 , SaPIbov2 *bap* ::*tetM*

Description

Reference
24
61
62
30
63
This work
This work
This work
This work
This work
This work
This work
This work
This work
This work

This work

This work

This work

This work

This work

This work

This work

This work

64

This work

63

This work

21

This work

This work

This work

This work

This work

This work

This work

This work

This work

This work

This work

This work

16

14

This work

14

14

14

14

14

14

14

14

14

14

14

14

14

14

This work

This work

This work

This work

This work

This work

21

This work

This work

This work

This work

21

21

21

This work

This work

This work

This work

This work

This work

This work

This work

This work

This work

This work

This work

This work

This work

This work

This work

This work

This work

This work

This work

This work

This work

This work

This work

This work

This work

This work

This work

This work

This work

This work

This work

This work

This work

This work

This work

This work

This work

This work

This work

This work

This work

21

This work

This work

This work

This work

This work

This work

This work

This work

This work

This work

This work

This work

This work

This work

This work

This work

This work

This work

This work

This work

This work

This work

This work

This work

This work

This work

This work

This work

This work

This work

This work

This work

This work

This work

This work

This work

This work

This work

This work

This work

This work

This work

This work

This work

This work

This work

This work

This work

This work

This work

This work

This work

This work

This work

This work

This work

This work

This work

This work

This work

This work

This work

This work

This work

This work

This work

This work

This work

This work

This work

This work

This work

This work

This work

This work

This work

This work

This work

This work

This work

This work

This work

This work

This work

This work

This work

This work

This work

This work

This work

This work

This work

This work

This work

This work

This work

This work

This work

This work

This work

This work

This work

This work

This work

This work

This work

This work

This work

This work

This work

This work

This work

This work

This work

This work

This work

This work

This work

This work

This work

This work

This work

This work

This work

This work

This work

This work

This work

This work

This work

This work

This work

This work

This work

This work

This work

This work

This work

This work

This work

This work

This work

This work

This work

This work

This work

This work

This work

This work

This work

This work

This work

This work

This work

This work

This work

This work

This work

Reference
This work
This work
This work
This work
This work
This work
This work
This work
This work
This work
This work

Table S5. Plasmids used in this study, related to STAR DNA methods.

Plasmid	Description
pBT2	Vector for allelic replacement
pUC18	*E. coli* cloning vector
pJP1872	pBT2-*cadCA*
pJP1850	pJP1872 allele exchange SAOUHSC_00841::*cadCA* ; Cd^R marker 3 kb upstream SaPI type IV *att* C
pJP1847	pJP1872 allele exchange SAOUHSC_00848::*cadCA* ; Cd^R marker 4 kb downstream SaPI type IV *att* C
pJP2803	pJP1872 allele exchange SAOUHSC_00365::*cadCA* ; Cd^R marker 11 kb upstream SaPI type II *att* C
pJP1853	pJP1872 allele exchange SAOUHSC_01064::*cadCA* ; Cd^R marker 10 kb upstream Sa7 *att* B
pJC1213	pT181 replicon, *cat194*
pJC1600	Allelic exchange vector, *cat194*
pJC1630	pUC18, PCR JCO445 + JCO446 SaPIbov1 *ter* S
pJC1691	SaPI1 *att* C integration vector, Ptet promoter, *ermC*
pJC1673	SaPI4 *att* C integration vector, Ptet promoter, *ermC*
pJC1693	pJC1213 (SaPI4 Integrase+)
pJC1706	Allelic exchange vector, *ermC*
pJC1746	pJC1673, pJC1630 (PstI-BamHI) SaPIbov1 *ter* S
pJC1950	Allelic exchange vector, *cat194*

pJC1992	pUC18, PCR JCO814 + JCO815 RN450, *cadCA* 10 kb downstream SaPIbov1 *att* C
pJC1993	pUC18, PCR JCO818 + JCO819 RN450, *cadCA* 16 kb downstream SaPIbov1 *att* C
pJC1994	Inverse PCR of pJC1992 JCO816 + JCO817 10 kb downstream SaPIbov1 *att* C
pJC1995	Inverse PCR of pJC1993 JCO820 + JCO821 16 kb downstream SaPIbov1 *att* C
pJC2002	pJC1706, pJC1994 (KpnI-SpHI) 10 kb downstream SaPIbov1 *att* C
pJC2003	pJC1706, pJC1995 (KpnI-SpHI) 16 kb downstream SaPIbov1 *att* C
pJC2004	pJC2002, *cadCA* (PstI-BamHI) 10 kb downstream SaPIbov1 *att* C
pJC2005	pJC2003, *cadCA* (PstI-BamHI) 16 kb downstream SaPIbov1 *att* C
pJC2094	pJC1950, Δ*recA*
pJC2122	pUC18, PCR JCO928 + JCO930 SaPIbov1 Δ(*sel-sec*)
pJC2123	pUC18, PCR JCO929 + JCO931 SaPIbov1 Δ(sel-sec)
pJC2124	pUC18, PCR JCO932 + JCO934 SaPIbov1 Δ*tsst* ::*tetM*
pJC2125	pUC18, PCR JCO933 + JCO935 SaPIbov1 Δ*tsst* ::*tetM*
pJC2126	pJC1706, pJC2122 (SphI-XhoI) + pJC2123 (XhoI-KpnI) SaPIbov1 Δ(*sel-sec*)
pJC2127	pJC1706, pJC2124 (SphI-PstI) + *tetM* (PstI-BamHI) + pJC2125 (BamHI-KpnI) SaPIbov1 Δ*tsst* ::*tetM*
pJC2244	pUC18, PCR JCO1016 + JCO1017 4 kb downstream SaPIbov1 *att* C
pJC2245	Inverse PCR of pJC2244 JCO1018 + JCO1019 4 kb downstream SaPIbov1 *att* C
pJC2246	pJC1706, pJC2245 (KpnI-SphI) 4 kb downstream SaPIbov1 *att* C
pJC2247	pJC2246, *cadCA* (PstI-BamHI) 4 kb downstream SaPIbov1 *att* C

pJC2278	pUC18, PCR JCO1112 + JCO1113 2nd headful downstream SaPIbov1 *att* C
pJC2279	pUC18, PCR JCO1114 + JCO1115 6th headful downstream SaPIbov1 *att* C
pJC2280	pUC18, PCR JCO1116 + JCO1117 7th headful downstream SaPIbov1 *att* C
pJC2281	Inverse PCR of pJC2278 JCO1120 + JCO1121 2nd headful downstream SaPIbov1 *att* C
pJC2282	Inverse PCR of pJC2279 JCO1122 + JCO1123 6th headful downstream SaPIbov1 *att* C
pJC2283	Inverse PCR of pJC2280 JCO1124 + JCO1125 7th headful downstream SaPIbov1 *att* C
pJC2284	pJC1706, pJC2281 (KpnI-SphI) 2nd headful downstream SaPIbov1 *att* C
pJC2285	pJC1706, pJC2282 (KpnI-SphI) 6th headful downstream SaPIbov1 *att* C
pJC2286	pJC1706, pJC2283 (KpnI-SphI) 7th headful downstream SaPIbov1 *att* C
pJC2300	pJC2284, *cadCA* (PstI-BamHI) 2nd headful downstream SaPIbov1 *att* C
pJC2301	pJC2285, *cadCA* (PstI-BamHI) 6th headful downstream SaPIbov1 *att* C
pJC2302	pJC2286, *cadCA* (PstI-BamHI) 7th headful downstream SaPIbov1 *att* C
pJC2311	pUC18, PCR JCO1141 + JCO1142 *sarA* P1 promoter
pJC2343	pJC1213, pJC2311 (PstI-BamHI) *sarA* P1 promoter
pJC2346	pUC18, PCR JCO1109 + JCO1170 SaPIbov1 *att* C
pJC2358	pUC18, PCR JCO1187 + JCO1188 SaPIbov1 Δ*tsst* ::*ermC*
pJC2359	pUC18, PCR JCO1189 + JCO1190 SaPIbov1 Δ*tsst* ::*ermC*
pJC2360	pJC1600, pJC2358 (KpnI-BamHI) + *ermC* (BamHI-PstI) + pJC2359 (PstI-SphI) SaPIbov1 Δ*tsst* ::*ermC*
pJC2482	pUC18, PCR JCO1312 + JCO1313 4 kb downstream SaPI1 *att* C

pJC2483	Inverse PCR of pJC2482 JCO1314 + JCO1315 4 kb downstream SaPI1 *att* C
pJC2484	pJC1600, pJC2483 (KpnI-SphI) 4 kb downstream SaPI1 *att* C
pJC2485	pJC2484, *cadCA* (PstI-BamHI) 4 kb downstream SaPI1 *att* C
pJC2486	pUC18, PCR JCO1316 + JCO1317 4 kb downstream SaPI2 *att* C
pJC2487	Inverse PCR of pJC2486 JCO1318 + JCO1319 4 kb downstream SaPI2 *att* C
pJC2488	pJC1600, pJC2487 (KpnI-SphI) 4 kb downstream SaPI2 *att* C
pJC2489	pJC2488, *cadCA* (PstI-BamHI) 4 kb downstream SaPI2 *att* C
pJC2602	pUC18, PCR JCO1329 + JCO1330 3rd headful downstream SaPIbov1 *att* C
pJC2603	pUC18, PCR JCO1331 + JCO1332 4th headful downstream SaPIbov1 *att* C
pJC2604	pUC18, PCR JCO1133 + JCO1134 5th headful downstream SaPIbov1 *att* C
pJC2610	Inverse PCR of pJC2602 JCO1335 + JCO1336 3rd headful downstream SaPIbov1 *att* C
pJC2611	Inverse PCR of pJC2603 JCO1337 + JCO1338 4th headful downstream SaPIbov1 *att* C
pJC2612	Inverse PCR of pJC2604 JCO1339 + JCO1340 5th headful downstream SaPIbov1 *att* C
pJC2613	pJC1706, pJC2610 (KpnI-SphI) 3rd headful downstream SaPIbov1 *att* C
pJC2614	pJC1706, pJC2611 (KpnI-SphI) 4th headful downstream SaPIbov1 *att* C
pJC2615	pJC1706, pJC2612 (KpnI-SphI) 5th headful downstream SaPIbov1 *att* C
pJC2616	pJC2613, *cadCA* (PstI-BamHI) 3rd headful downstream SaPIbov1 *att* C
pJC2617	pJC2614, *cadCA* (PstI-BamHI) 4th headful downstream SaPIbov1 *att* C
pJC2618	pJC2615, *cadCA* (PstI-BamHI) 5th headful downstream SaPIbov1 *att* C

pJC2619	Inverse PCR of pJC2482 JCO1341 + JCO1342 4 kb downstream SaPI1 *att* C
pJC2620	pJC1706, pJC2619 (KpnI-SphI) 4 kb downstream SaPI1 *att* C
pJC2625	Inverse PCR of pJC2346 JCO1214 + JCO1215 SaPIbov1 *attC** synonymous mutations
pJC2626	pJC1706, pJC2625 (KpnI-SphI) SaPIbov1 attC* synonymous mutations
pJC2658	pUC18, PCR JCO1388 + JCO1389 SaPIbov1 Δ*tsst* ::*cat194*
pJC2659	pUC18, PCR JCO1390 + JCO1384 SaPIbov1 Δ*tsst* ::*cat194*
pJC2674	pJC1600, pJC2658 (SphI-AvrII) + *cat194* (AvrII-SacII) + pJC2659 (SacII-KpnI) SaPIbov1 Δ*tsst* ::*cat194*
pJC2736	pUC18, PCR JCO1511 + JCO1513 SaPIbov1 Δ(*pri-rep*)
pJC2737	pUC18, PCR JCO1512 + JCO1514 SaPIbov1 Δ(*pri-rep*)
pJC2746	pUC18, PCR JCO1507 + JCO1508 SaPIbov1 *xis* +
pJC2786	pJC1691, pJC2746 (PstI-BamHI) SaPIbov1 *xis* +
pJC2772	pJC1706, pJC2636 (SphI-XhoI) + pJC2637 (XhoI-KpnI) SaPIbov1 Δ(*pri-rep*)
pJC2774	pUC18, PCR JCO1533 + JCO1510 SaPIbov1 *pri-rep* +
pJC2775	pUC18, PCR JCO1534 + JCO1509 SaPIbov1 *pri-rep* +
pJC2791	pJC1691, pJC2774 (BamHI-NheI) + pJC2775 (NheI-PstI) SaPIbov1 *pri-rep* +
pJC2847	pJC1600, pJC2658 (SphI-AvrII) + *cat194* (SacII-AvrII) + pJC2659 (SacII-KpnI) SaPIbov1 Δ*tsst* ::*cat194* (reve
pJC2852	pUC18, PCR JCO1657 + JCO1660 10 kb upstream SaPIbov1 *att* C
pJC2853	pUC18, PCR JCO1658 + JCO1659 10 kb upstream SaPIbov1 *att* C
pJC2854	pJC2852, pJC2853 (EcoRI-BamHI) 10 kb upstream SaPIbov1 *attC*

pJC2868	pJC1706, pJC2854 (SphI-EcoRI) 10 kb upstream SaPIbov1 *att* C
pJC2869	pJC2868, *cadCA* (PstI-BamHI) 10 kb upstream SaPIbov1 *att* C
pJC2884	pJC2002, *cat194* (PstI-BamHI) 10 kb downstream SaPIbov1 *att* C
pJC2903	pJC2284, *cat194* (PstI-BamHI) 2nd headful downstream SaPIbov1 *att* C
pJC2904	pJC2613, *cat194* (PstI-BamHI) 3rd headful downstream SaPIbov1 *att* C
pJC2909	pJC2246, *cat194* (PstI-BamHI) 4 kb downstream SaPIbov1 *att* C
pJC2915	pUC18, PCR JCO1714 + JCO1715 20 kb downstream SaPIbov1 *att* C
pJC2916	pUC18, PCR JCO1718 + JCO1719 25 kb downstream SaPIbov1 *att* C
pJC2917	Inverse PCR of pJC2915 JCO1716 + JCO1717 20 kb downstream SaPIbov1 *attC*
pJC2918	Inverse PCR of pJC2916 JCO1720 + JCO1721 25 kb downstream SaPIbov1 *attC*
pJC2919	pJC1706, pJC2917 (KpnI-SphI) 20 kb downstream SaPIbov1 *attC*
pJC2920	pJC1706, pJC2918 (KpnI-SphI) 25 kb downstream SaPIbov1 *attC*
pJC2921	pJC2919, *cadCA* (PstI-BamHI) 20 kb downstream SaPIbov1 *attC*
pJC2922	pJC2920, *cadCA* (PstI-BamHI) 25 kb downstream SaPIbov1 *attC*
pJC2945	pJC2929, *cat194* (PstI-BamHI) 20 kb downstream SaPIbov1 *attC*
pJC2962	pUC18, PCR JCO1842 + JCO1843 (4 kb downstream of SaPIbov1 *attC*)::(SaPI Bov1 *att* C site)
pJC2963	pUC18, PCR JCO1844 + JCO1845 SaPIbov1 int^{syn} synonymous mutations
pJC2964	pJC2246, pJC2962 (PstI-BamHI) (4 kb downstream of SaPIbov1 *att* C)::(SaPI Bov1 *att* C site)
pJC2983	Inverse PCR of pJC2963 JCO1846 + JCO1847 SaPIbov1 int^{syn} synonymous mutations

pJC2988	Allelic exchange vector, *ermC*
pJC2984	pJC1706, pJC2983 (KpnI-SphI) SaPIbov1 *int*^{syn} synonymous mutations
pJC2901	pJC2620, *cat194* (PstI-BamHI) 4 kb downstream SaPI1 *att* C
pJC2902	pJC2488, *cat194* (PstI-BamHI) 4 kb downstream SaPI2 *att* C
pJC3037	pUC18, PCR JCO1944 + JCO1945 SaPIbov1 *int*+
pJC3038	pJC1691, pJC3037 (PstI-BamHI) SaPIbov1 *int* +
pJC3054	pT181 replicon, *ermC* , *sarA* P1 promoter
pJC3056	pJC3054, pJC3037 (PstI-BamHI) SaPIbov1 *int* +
pJC3063	pUC18, PCR JCO1951 + JCO1952 Φ52a Δ*dut*
pJC3066	Inverse PCR of pJC3063 JCO1953 + JCO1954 Φ52a Δ*dut*
pJC3067	pJC2988, 3066 (PstI-BamHI) Φ52a Δ*dut*

Plasmid	**Description**

Reference
59
65
21
This work
This work
This work
This work
14
14
14
This work
14
14
14
This work
21

This work

This work

This work

This work

This work

This work

This work

This work

21

This work

This work

This work

This work

This work

This work

This work

This work

This work

This work

This work

This work

This work

This work

This work

This work

This work

This work

This work

This work

This work

This work

This work

This work

This work

This work

This work

This work

This work

This work

This work

This work

This work

This work

This work

This work

This work

This work

This work

This work

This work

This work

This work

This work

This work

This work

This work

This work

This work

This work

This work

This work

This work

This work

This work

This work

This work

This work

This work

This work

This work

This work

This work

This work

This work

This work

This work

This work

This work

This work

This work

This work

This work

This work

This work

This work

This work

This work

This work

This work

This work

This work

This work

This work

This work

This work

This work

This work

This work

This work

Reference
This work
This work
This work
This work
This work
This work
This work
This work
This work
This work

Table S6. Oligonucleotides used in this study, related to STAR DNA methods.

Oligonucleotides	Sequence (5'-3')	Reference
JCO444	GGATCCGCGTTCTCCCTTTTATCTTTATAACGC	14
JCO445	CTGCAGTTGTAGAGGTGATAGAATGAGTGAGTTAACG	14
JCO814	GCATGCGTAGAAGCACCGCAACAAACAGC	This work
JCO815	GGTACCCACCAGTAGCTAACAATCCCAATACTAATGTTGCTTTAGC	This work
JCO816	GAGCTGCAGCTGTCATTTTCATAGTTGTATGCTCCATTCG	This work
JCO817	GAGGGATCCCAATTGCGAAAGCAAGTTTAGCATTAGGTATTTTAGC	This work
JCO818	GCATGCCAGAGTAACATCATCAGTTGTAGTAAACGATAATCCGG	This work
JCO819	GGTACCGCAGTCCATTTCGCACTATACGGTG	This work
JCO820	GAGCTGCAGAGTAATAGACATGTGATTCCTCCGCC	This work
JCO821	GAGGGATCCGAAAAACAACGTCAGCAACAAGCTG	This work
JCO928	GCATGCGTCATACAACAAGTTGGTGGC	This work
JCO929	GGTACCCAACGCTCATGCTGAAC	This work
JCO930	CTCGAGCGTTAATTATGAAGTGATGTTAATTGATGTGAAG	This work
JCO931	CTCGAGAAGGAGAAACAGAGGATTTCTAAGCATC	This work
JCO932	GCATGCGTTCAGCATGAGCGTTG	This work
JCO933	GGTACCCATGAGCGAACTAGAAGTGATG	This work

JCO934	CTGCAGAATTAGAAAGTGTTTGTTACATAGGGAGC	This work
JCO935	GGATCCGTGTTCTCCCTTTTATCTTTATAACGC	This work
JCO1016	GCATGCGGAAACAGAGGCAACGCTAC	This work
JCO1017	GGTACCCGCTTGTACTGATTGTACATTCGATGTAATTACACC	This work
JCO1018	GAGCTGCAGACTTAAACCATATTTACCAGAATTGATGAATATGC	This work
JCO1019	GAGGGATCCATGTACATTGCCATTCTTACATACGTATAGTC	This work
JCO1109	CTGCAGAAGGCGCGCCTAAACCCTCCGATCTCTATCAC	This work
JCO1112	GCATGCGTACGATACCTATACCACCTGTTAGTGCG	This work
JCO1113	GGTACCAAAACACTCATTTTTGGAGGTGCCTATATCGC	This work
JCO1114	GCATGCGGGAGGTTGAGTAATGAATAAAGTAGAAGCG	This work
JCO1115	GGTACCTCGCAATAACACCAACAAACACGATAGC	This work
JCO1116	GCATGCTTGTTTTTGAAAGAGCGAGACGGTTCG	This work
JCO1117	GGTACCATTTTGCCTACTAGTGGTTCTGGCTTTAGC	This work
JCO1120	GAGCTGCAGCTTTGAAAATAAAAAATTAAGGGCGTATAATCACC	This work
JCO1121	GAGGGATCCATATTACTGCTAAGTGTAAAACGAAAATCATCATTGATAGC	This work
JCO1122	GAGCTGCAGGGATAAATATTGAGTTGCATAGAAGAATACTGC	This work
JCO1123	GAGGGATCCTCTCGAAAAGACAATTTACCAAGG	This work
JCO1124	GAGCTGCAGTACTTTTTAGTATTTTCAAAATAATTTTAAATGACCACATCTACAACG	This work
JCO1125	GAGGGATCCGTGTGTTTTCAATTGGATAGTTTAATTAAACTGACTACATC	This work

JCO1141	CGGGCATGCGCTGATATTTTTGACTAAACCAAATGC	This work
JCO1142	TTCCTGCAGGATGCATCTTGCTCGATACATTTGC	This work
JCO1170	GGTACCACGAATCGGTGCTAAATCTAACAGC	This work
JCO1187	GGTACCCTCGCTATCTCCTCAGAACGTTGTG	This work
JCO1188	GGATCCGACCCACTACTATACCAGTCTAGCAAATCC	This work
JCO1189	CTGCAGAAAAAACACAGATGGCAGCATCAGCC	This work
JCO1190	GCATGCGAAGTTGTAGTCAAGCGTGGG	This work
JCO1214	GAGAATTTGAGTAGTTGGAAAATTACAATAAGGACGG	This work
JCO1215	GAGTCACTCCCATTCGATAGTGCTTGGTGGTTTTGATG	This work
JCO1312	GCATGCGCGTACACACAAGTTGATGATAATGC	This work
JCO1313	GGTACCGTCGCCACCGAACTCAATC	This work
JCO1314	GAGGGATCCATAGTAAAGTTGATCTGGATCAACACGACC	This work
JCO1315	GAGCTGCAGTTAATGAGTCGTGGTATTTCTCAAAGAGAAGC	This work
JCO1316	GCATGCCTGGCTTGTCCCCAGTTGATATAG	This work
JCO1317	GGTACCGTGCATAATGCCGGGAATGATGTAAAACTG	This work
JCO1318	GAGGGATCCGGGCACCACCAATAAACATAAGTAGC	This work
JCO1319	GAGCTGCAGCTCTCAGTGCAGCTGGAG	This work
JCO1329	GCATGCGGCGTTGTCGTGTTAACTGC	This work
JCO1330	GGTACCGTCGCATCTAACAGTGTGAAGCCATC	This work

JCO1331	GCATGCGCGACGATACATTATCACCTGGTGTAAACC	This work
JCO1332	GGTACCATAACTGAACGTCCTGAATAGTCAACACG	This work
JCO1333	GCATGCGAGATTGTGCCAGGACAATTAGTGAG	This work
JCO1334	GGTACCGCCGGTTCTGACACAAGTG	This work
JCO1335	GAGCTGCAGTTAATTAATCCTATTCCCGCTGCTGTAC	This work
JCO1336	GAGGGATCCTTTATTGCCTTTAATGAACGGTGTGTTTTTTAAGACG	This work
JCO1337	GAGCTGCAGCGTATTAATCAGTAACTTCTTTTTGTGTTTCAGGAGCAT	This work
JCO1338	GAGGGATCCCAATTTACAAAACAGGCAAAAAGATACTAAGCTGAAT	This work
JCO1339	GAGCTGCAGTGTGGCTAATAATGTTGATTTATAGATGAACCGCC	This work
JCO1340	GAGGGATCCCCACTTAAATTGGGTATGAACTCAATTTATGTGATGTGG	This work
JCO1341	GAGGGATCCGAAAATAAAAGTTTGTAATAGATATAGACTGTCGATATTGG	This work
JCO1342	GAGCTGCAGAAAATATTATTTAGAAACTTTGCGTTCAATTACTTCTCTC	This work
JCO1364	GGTCACGGGGACATCAAGACAACTATG	This work
JCO1384	CCGCGGTTTACCACTTTTTCTGTAATAATTATTAATAAAGGG	This work
JCO1388	GCATGCCCATTACAAGAGAAGATCCTGC	This work
JCO1389	CCTAGGTTTTAATTCTCCTTCATTTAAATGTGTAAACGTTTACGC	This work
JCO1390	GGTACCGTGAGTTAACGGCAAAACAAG	This work
JCO1507	CTGCAGAATTAGAGATAAAATGGTAGGAGAGGAATAATATGAGCC	This work
JCO1508	GGATCCCCATTTCTAAACACGCAACTTGAAC	This work

JCO1509	CTGCAGTTTTACTCTGTGAATCACTAGAGGTGC	This work
JCO1510	GGATCCCTACTCAATAATTAGAATTAGGATTGTATGAATTGG	This work
JCO1511	GCATGCGCTGTTCATCATCACATAAACCATATC	This work
JCO1512	GGTACCCAGGAGAGATTACAACGTGCG	This work
JCO1513	CTCGAGGGTGAAAAAGACAGGTTACAAAAACAGG	This work
JCO1514	CTCGAGCATTTTTTGCACCTCTAGTGATTCACAG	This work
JCO1533	GGCAATCGTAACAATGCACTAGCTAGC	This work
JCO1534	GCCCAACTAAGCTAGCTAGTGCATTG	This work
JCO1657	GCATGCGTCAGAACATGTATATAATCTTGTGAAAAAGCATC	This work
JCO1658	GAATTCCAGCACATACGTTACCACAACAAATTTTGG	This work
JCO1659	GAGCTGCAGGGCGGGTATTTCTTGCAATG	This work
JCO1660	GAGGGATCCCCCTCTAGCTATACTTATCATTTTAAGCTAGAGG	This work
JCO1714	GGTACCGTGAAGCACGACCATTGCTC	This work
JCO1715	GCATGCCCACTTTAGTATGGTCATATTTAGTTTCTGC	This work
JCO1716	GAGCTGCAGTGCTTGTCCGTTTGTCATAATATATAACATTG	This work
JCO1717	GAGGGATCCGAAGCATCTGAAAATCAAAACGCTTTAATCTC	This work
JCO1718	GGTACCGGGATGTGGAAATATGAAAGATGAACAG	This work
JCO1719	GCATGCCACTTGACCTTCATCTAAAGCATTG	This work
JCO1720	GAGCTGCAGGTGTAACTATCAACATATTCAAGATTAGAAGGG	This work

JCO1721	GAGGGATCCTGATTCTCTTACTGGAGTAACAACTTCTGC	This work
JCO1842	CTGCAGCACACCACAATGTTGGTGGATTAC	This work
JCO1843	GGATCCGGACGATACACACTCGTTCAATAGG	This work
JCO1844	GCATGCTTGGATGGAAGGAGCTGGTCAAATGGC	This work
JCO1845	GGTACCTGATGTATTTTGCGAATTTATCAGCCACCTG	This work
JCO1846	ACTGCCATCCTTTTTCTTATATTTTTTAATCATATAAATCAATC	This work
JCO1847	ACTGCGTACATGTTCGTGGCCTATTTAGGTACTGAT	This work
JCO1848	CAGTACTGCGTACATGTTCGTGGCC	This work
JCO1875	GAAATCCTCTGTTTCTCCTTCTCGAGCG	This work
JCO1878	ACTTTTCGCCATACATTTCTGGCTCATAAGAGCG	This work
JCO1945	GGATCCGTAATTACGCGGTTTCCAGCC	This work
JCO1946	CTGGACCTACATCGCCGTTAGATAAGACTG	This work
JCO1951	CTGCAGCAGAAGTTGAATATCATCATTTCGATGATGTG	This work
JCO1952	GGATCCGAGTTAGGCATCTTCTTGATAATCGC	This work
JCO1953	GAGTGTGTTAGTCACTTTCCTGCTCCTCC	This work
JCO1954	GAGGGAAGTAGCGGAGTATAAAGACATCTTAGATCG	This work
JCO1958	GTGCCGTATTCTTTACCTTTACCAGTATCATTGTGTCC	This work
Oligonucleotides	**Sequence (5'-3')**	**Reference**

Plasmid	Oligonucleotides	Sequence (5'-3')	Reference
pJP1850	Cd-IV-SaPI1-1mB	CGCGGATCCTTTGACTTAGCCTTTGTCTGC	This work
	Cd-IV-SaPI1-2cX	GCTCTAGAGTCAATAACTATTTTAAATTTTCTAAC	This work
	Cd-IV-SaPI1-3mS	ACGCGTCGACGAAATTTTACTAAGGTGTTAGG	This work
	Cd-IV-SaPI1-4cP	AACTGCAGGAATGACATGCATTTCATGCG	This work
pJP1847	Cd-I-SaPI1-1mB	CGCGGATCCATGTAGTTGTAGAACATCCAG	This work
	Cd-I-SaPI1-2cX	GCTCTAGAATATTATTTAGAAACTTTGCGTTC	This work
	Cd-I-SaPI1-3mS	ACGCGTCGACTTGAAAATAAAAGTTTGTAATAGAT	This work
	Cd-I-SaPI1-4cP	AACTGCAGCCAAATAATACGCCAATACCTG	This work
pJP2803	Cd-XVI-1mB	CGCGGATCCGACGATTGACTGAGAAACTTGG	This work
	Cd-XVI-2cX	GCTCTAGAATGTAATAATGCTAACTAAGAGATTAG	This work
	Cd-XVI-3mS	ACGCGTCGACTTTGATCCAGAATAGTCAACTGG	This work
	Cd-XVI-4cP	AACTGCAGCTACTGCCATACCAAATACCG	This work
pJP1853	Cd-IV-80alpha-1mB	CGCGGATCCTAAAGTAGTTGGTGATATGGC	This work
	Cd-IV-80alpha-2cX	GCTCTAGACATTTTAGTCAGTTGCTTTTTC	This work
	Cd-IV-80alpha-3mS	ACGCGTCGACATTAAAATAAAACGAGATTACACAAC	This work
	Cd-IV-80alpha-4cP	AACTGCAGTAGAGCCGTTTCAGCTTTGTC	This work

Plasmid	Oligonucleotides	Sequence (5’-3’)	Reference

Supplemental Figure 1

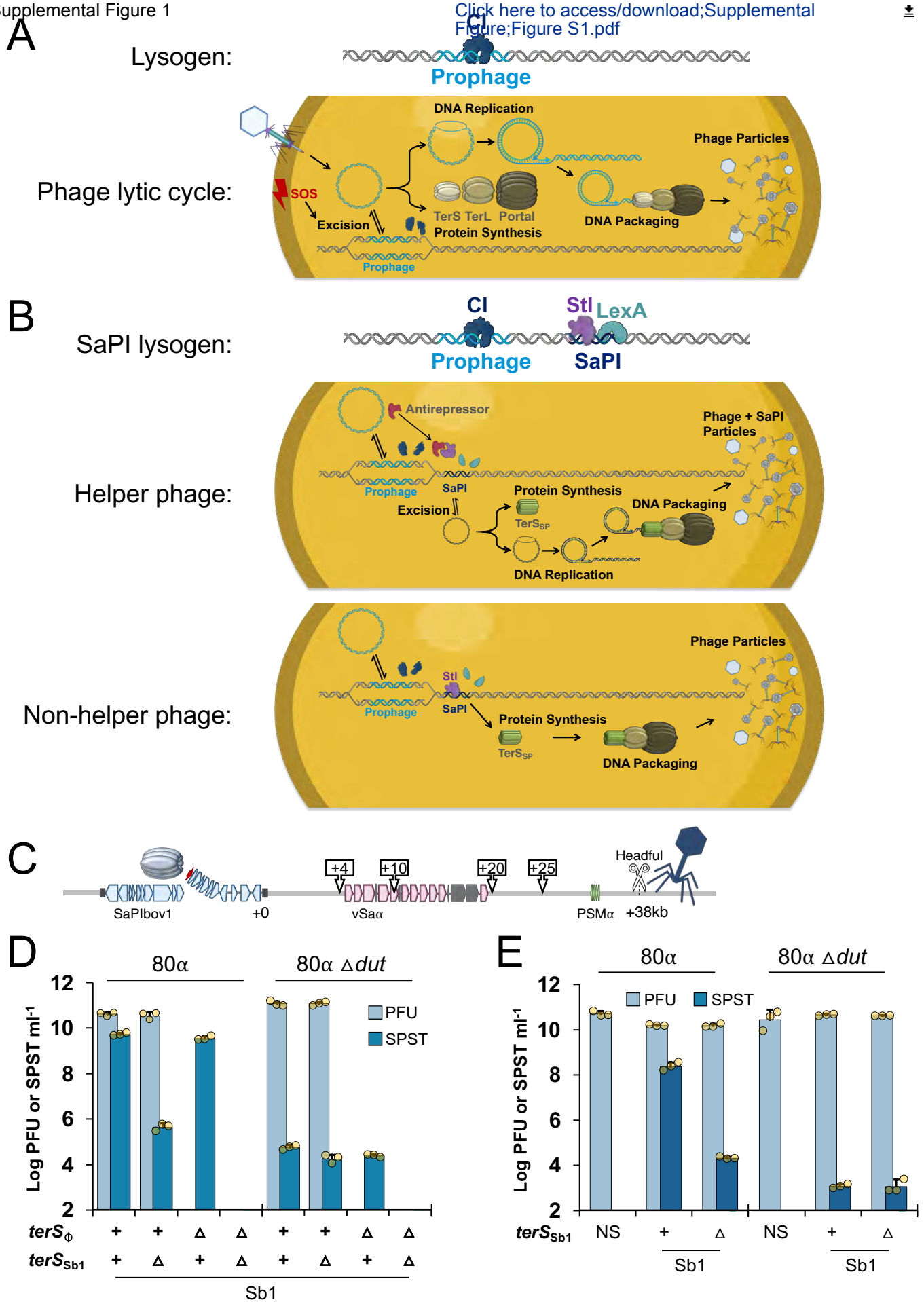

Supplemental Figure 2

Click here to access/download;Supplemental Figure;Figure S2.pdf

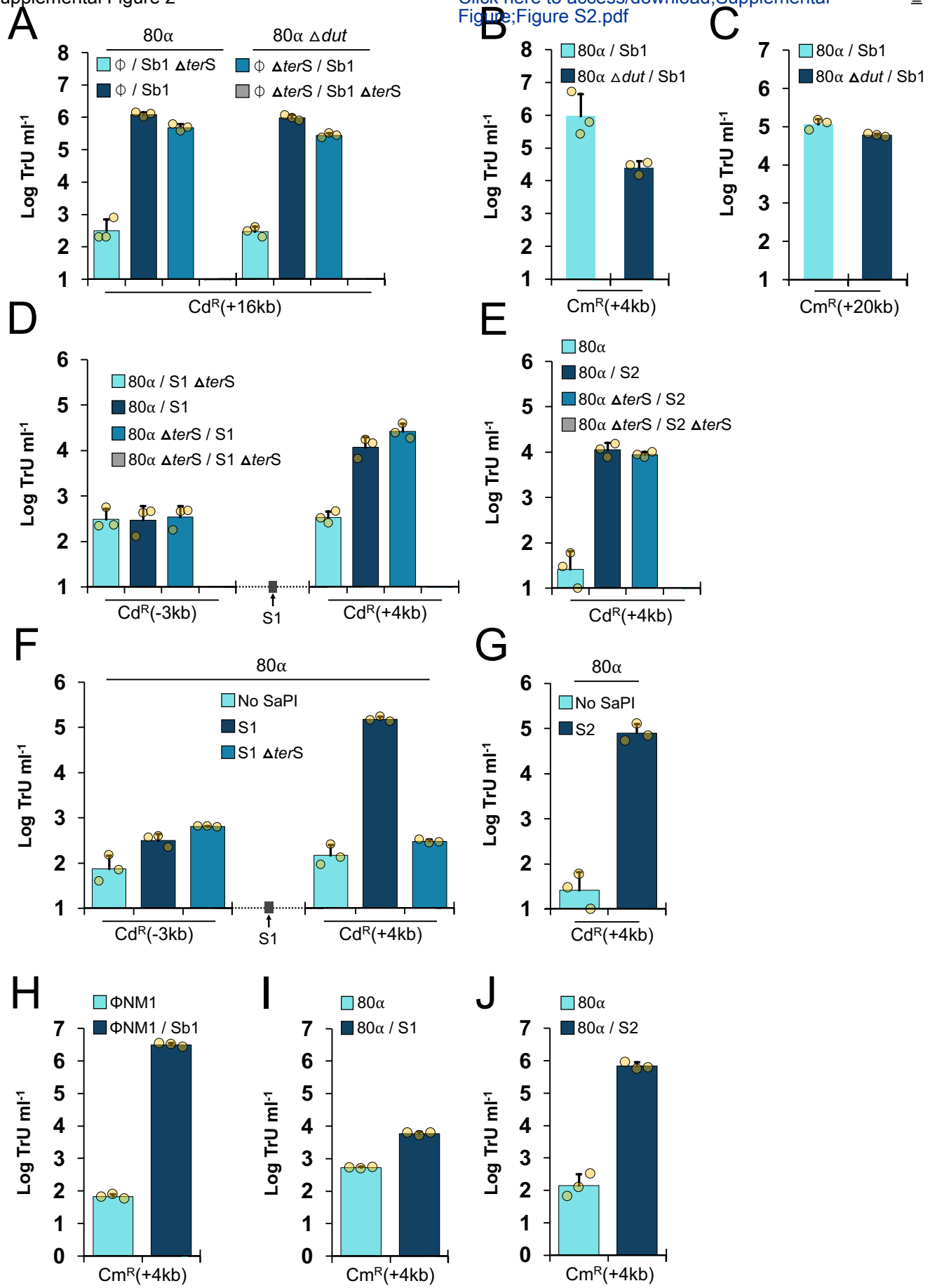

Supplemental Figure 3

Click here to access/download;Supplemental

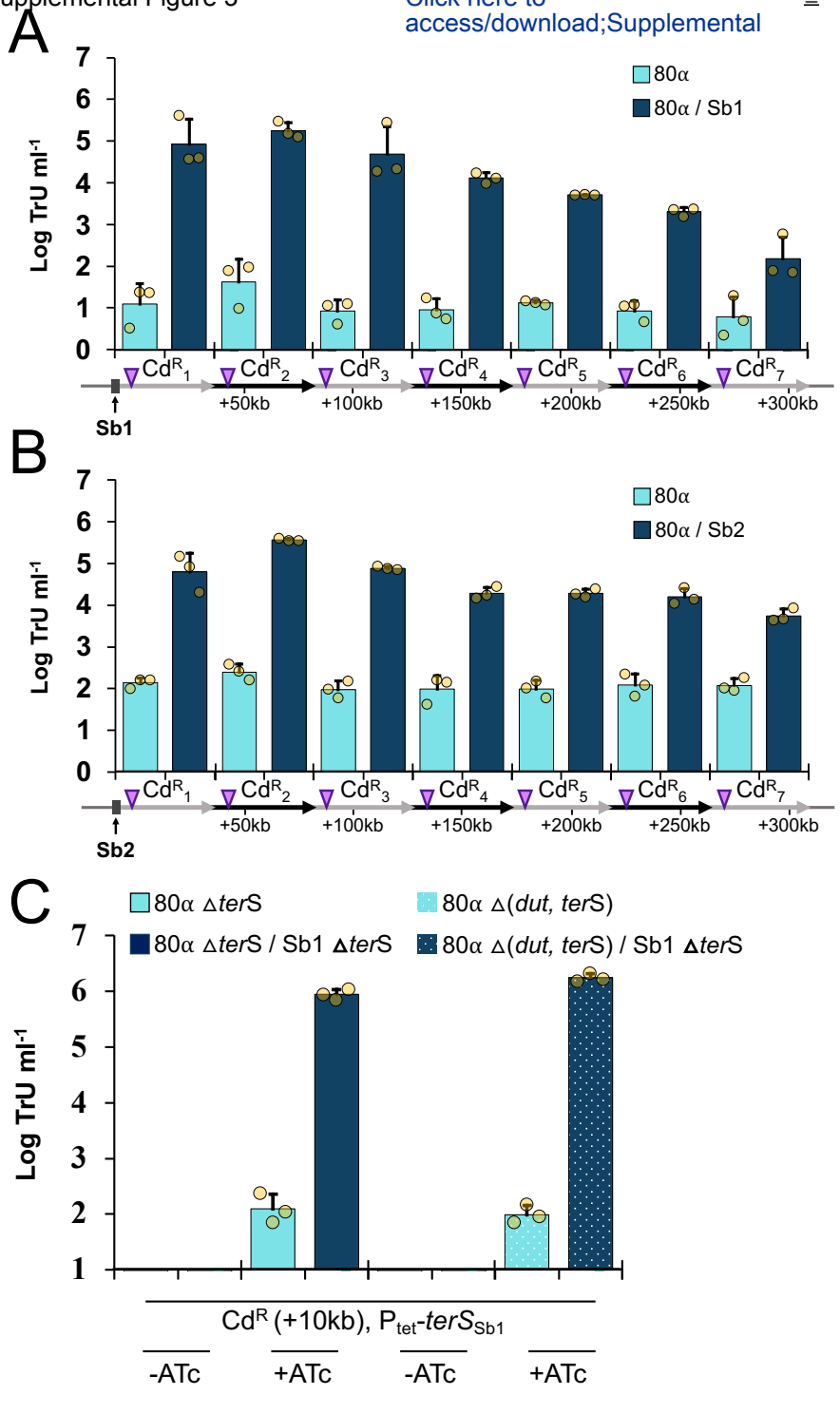

Supplemental Figure 4

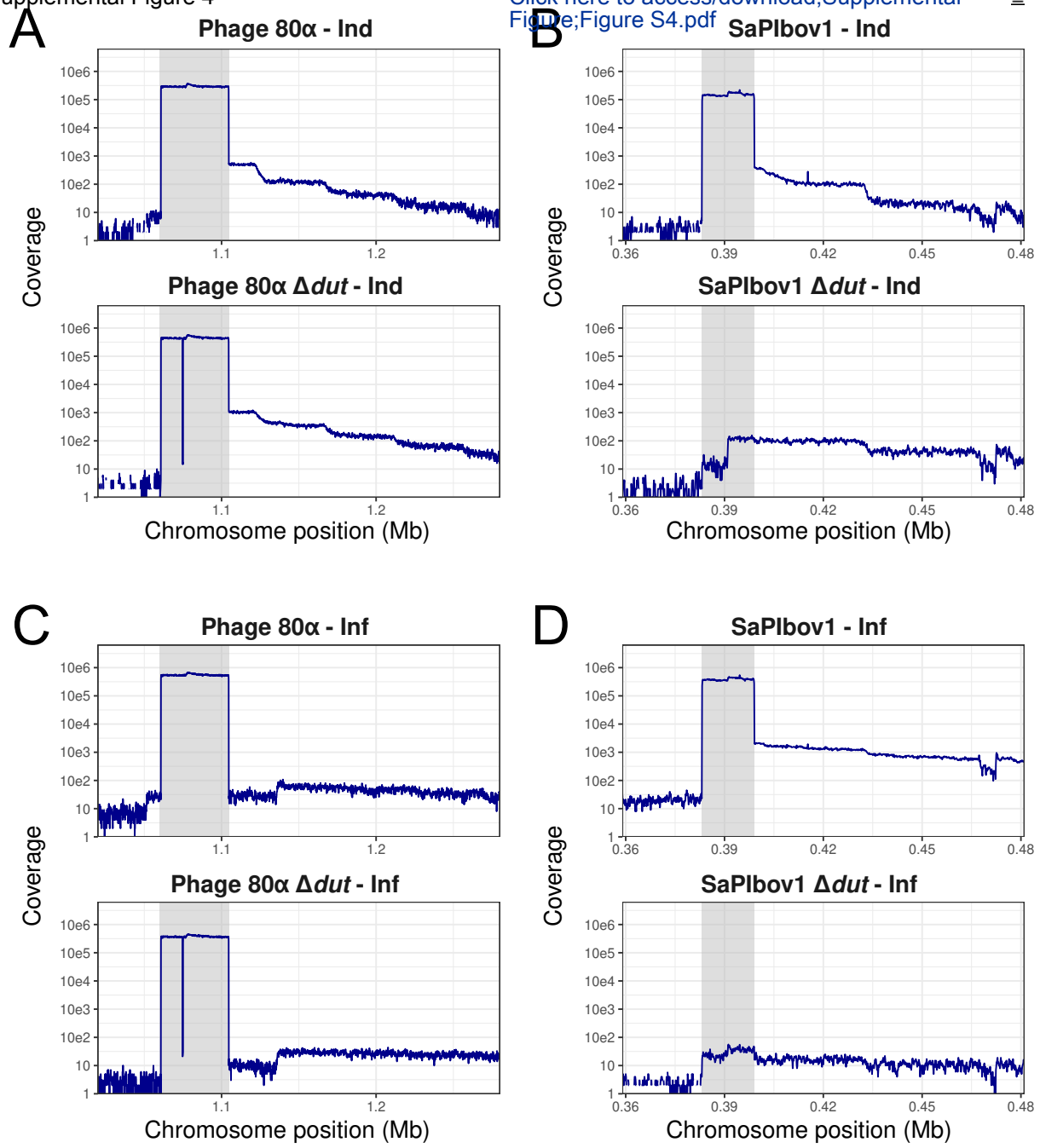

Supplemental Figure 5

Click here to access/download;Supplemental Figure;Figure S5.pdf

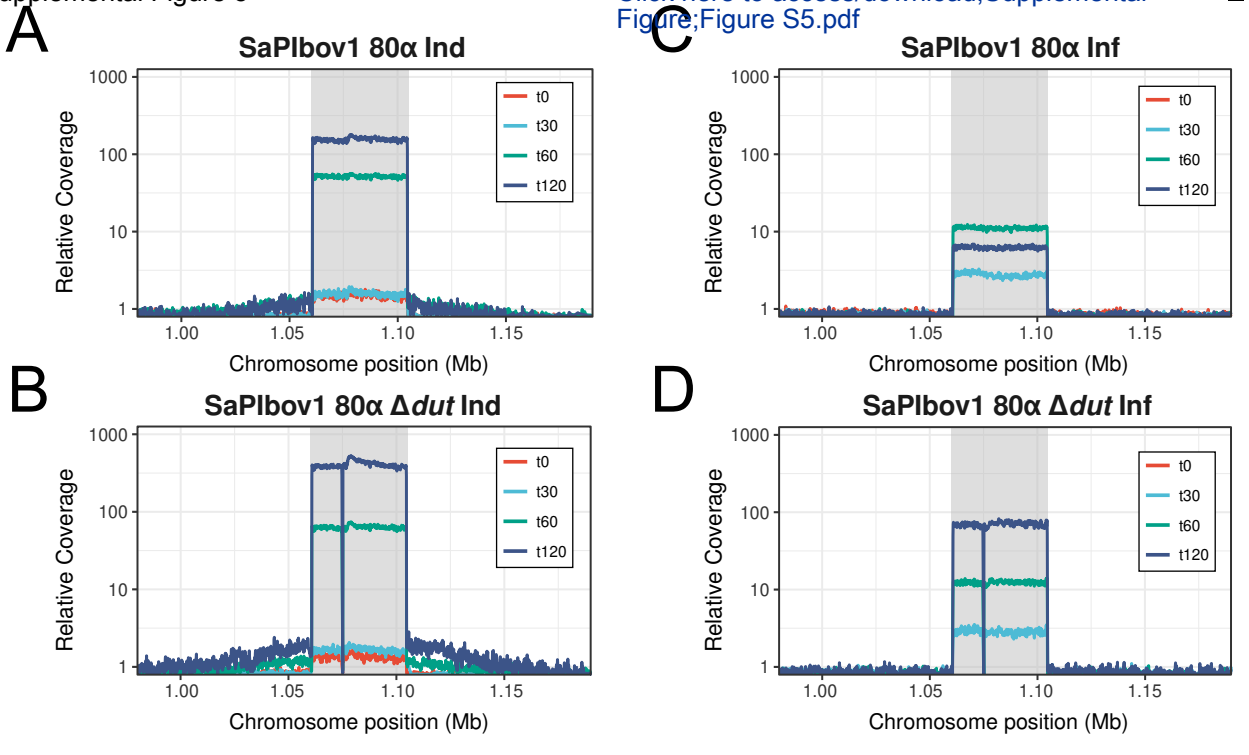

Supplemental Figure 6

Click here to access/download;Supplemental Figure;Figure S6.pdf

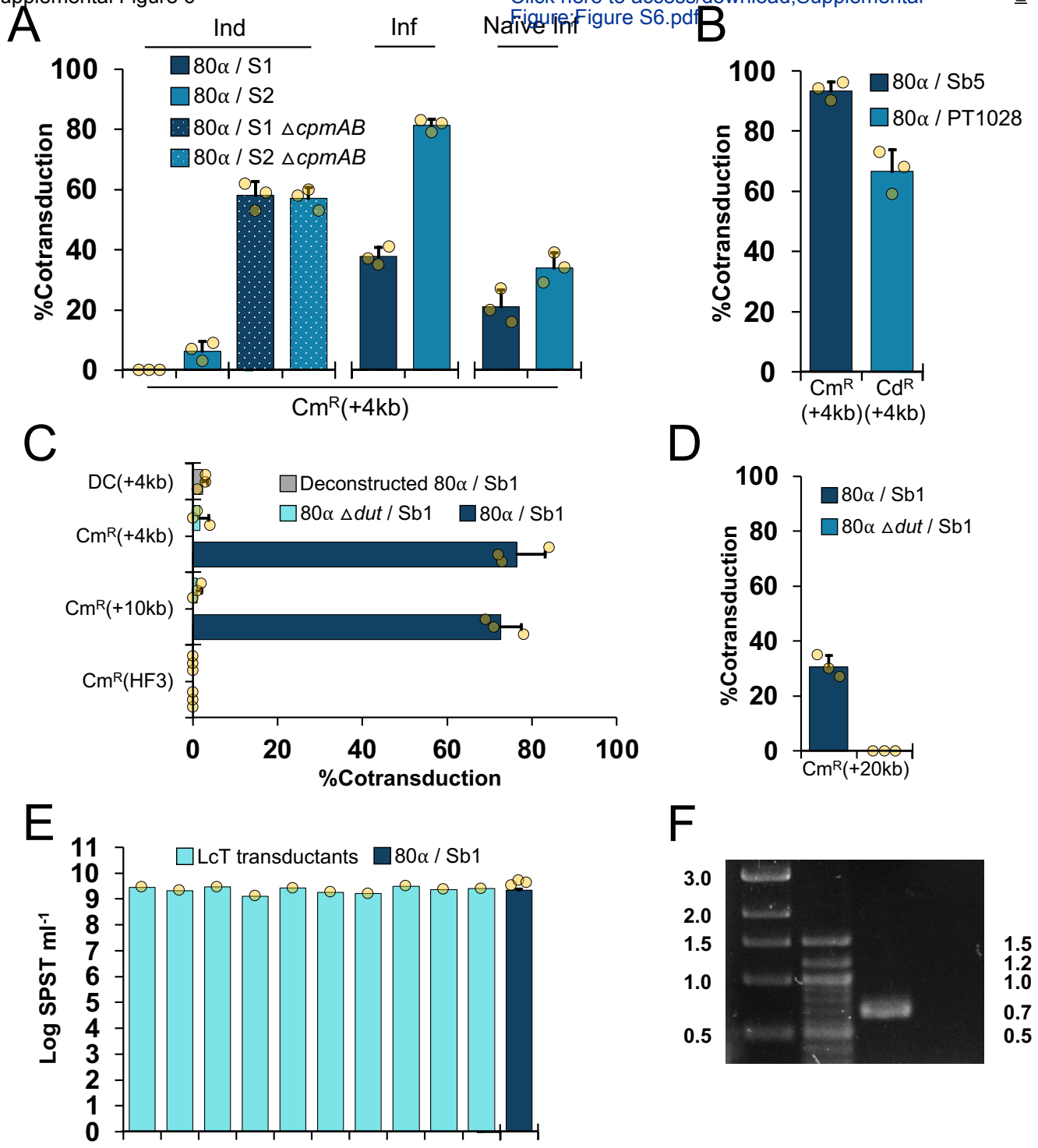

Supplemental Figure 7

Click here to access/download;Supplemental Figure;Figure S7.pdf

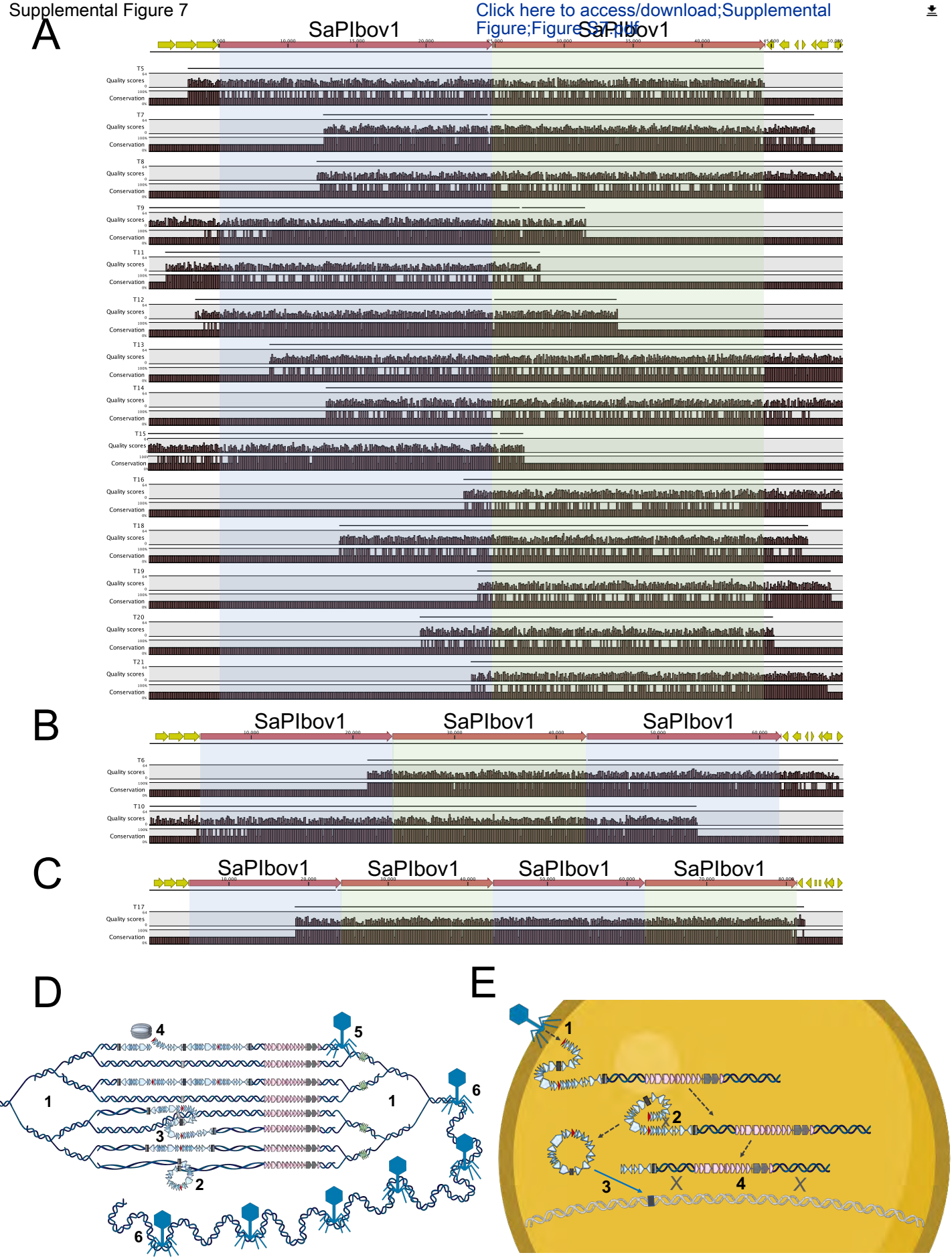

Phage	Phage LT marker	SaPI	SaPI LT marker	Selection	(Cm^R/Cd^R)%	(Cd^R/Cm^R)%	(Cm^R/Tet^R)%	(Cd^R/Tet^R)%
80α	Cd^R (+4 kb)	Sb1::*tetM*	Cm^R (+4 kb)	Cd^R	0.0 ± 0.0	NA	NA	NA
80α	Cd^R (+4 kb)	Sb1::*tetM*	Cm^R (+4 kb)	Cm^R	NA	0.0 ± 0.0	NA	NA
80α	Cd^R (+4 kb)	Sb1::*tetM*	Cm^R (+4 kb)	Tet^R	NA	NA	0.0 ± 0.0	0.0 ± 0.0

Table S1. Cotransduction of lateral transduction markers and SaPI, related to Figure 5.
SaPIbov1 *tsst*::*tetM* strains lysogenic for helper 80α phage with a Cd^R marker 4 kb downstream of the 80α *att*B and Cm^R markers 4 kb downstream of the SaPIbov1 *att*C were induced with mitomycin C. The resulting lysates were tested for cotransduction into *S. aureus* by selecting for one marker (Cd^R, Cm^R, or Tet^R), followed by testing the transductants for the second marker (Cm^R or Cd^R). For each replicate, 100 transductants were tested for Cm^R or Cd^R and the cotransduction frequency was represented as a percentage, calculated as (Cm^R or Cd^R / Cm^R or Cd^R or Tet^R) x 100. Values are means (n = 3 independent samples) ± standard deviation.

Phage	Donor SaPI	Recipient SaPI	Selection	(Em^R/Tet^R)%
80α	Sb1::*tetM*	Sb1::*ermC*	Tet^R	0.33 ± 0.58

Table S2. SaPIs do not form tandems by integration events, related to Figure 6.
A SaPIbov1 *tsst*::*tetM* strain lysogenic for 80α phage was induced with mitomycin C and the resultant lysates were tested for transduction into an *S. aureus* strain with SaPIbov1 Δ*tsst*::*ermC*. The recipient strain was a *recA* deletion (Δ*recA*) to focus only on integrase-mediated integration events. For each replicate, 100 Tet^R transductants were tested for Em^R and the double-positive SaPIbov1 frequency was represented as a percentage, calculated as (Em^R / Tet^R) x 100. Values are means (*n* = 3 independent samples) ± standard deviation.

SaPI Site	Representative SaPIs	# of Genomes	% of Genomes
SaPI-I	SaPI4 PT1028	39	18.3
SaPI-II	SaPIbov1 SaPIbov2	18	8.45
SaPI-III	SaPImw2 SaPIm4	33	15.5
SaPI-IV	SaPI1 SaPI3	36	16.9
SaPI-V	SaPI2 SaPI122	48	22.5

Table S3. SaPI distribution in natural populations of *S. aureus* isolates, related to Figure 7.
SaPIs are normally found at five conserved SaPI integration sites. The number or percentage of genomes indicates the number or percentage of *S. aureus* genomes (from the pangenome synteny network analysis in Figure 7) with a SaPI element present in that site. A total of 213 genomes were interrogated for this analysis.

CELL PRESS DECLARATION OF INTERESTS POLICY

Transparency is essential for a reader's trust in the scientific process and for the credibility of published articles. At Cell Press, we feel that disclosure of competing interests is a critical aspect of transparency. Therefore, we require a "declaration of interests" section in which all authors disclose any financial or other interests related to the submitted work that (1) could affect or have the perception of affecting the author's objectivity or (2) could influence or have the perception of influencing the content of the article.

What types of articles does this apply to?

We require that you disclose competing interests for all submitted content by completing and submitting the form below. We also require that you include a "declaration of interests" section in the text of all articles even if there are no interests to declare.

What should I disclose?

We require that you and all authors disclose any personal financial interests (e.g., stocks or shares in companies with interests related to the submitted work or consulting fees from companies that could have interests related to the work), professional affiliations, advisory positions, board memberships (including membership on a journal's advisory board when publishing in that journal), or patent holdings that are related to the subject matter of the contribution. As a guideline, you need to declare an interest for (1) any affiliation associated with a payment or financial benefit exceeding $10,000 p.a. or 5% ownership of a company or (2) research funding by a company with related interests. You do not need to disclose diversified mutual funds, 401ks, or investment trusts.

Authors should also disclose relevant financial interests of immediate family members. Cell Press uses the Public Health Service definition of "immediate family member," which includes spouse and dependent children.

Where do I declare competing interests?

Competing interests should be disclosed on this form as well as in a "declaration of interests" section in the manuscript. This section should include financial or other competing interests as well as affiliations that are not included in the author list. Examples of "declaration of interests" language include:

> "AUTHOR is an employee and shareholder of COMPANY."
> "AUTHOR is a founder of COMPANY and a member of its scientific advisory board."

NOTE: Primary affiliations should be included with the author list and do not need to be included in the "declaration of interests" section. Funding sources should be included in the "acknowledgments" section and also do not need to be included in the "declaration of interests" section. (A small number of front-matter article types do not include an "acknowledgments" section. For these articles, reporting of funding sources is not required.)

What if there are no competing interests to declare?

If you have no competing interests to declare, please note that in the "declaration of interests" section with the following wording:

> "The authors declare no competing interests."

CELL PRESS DECLARATION OF INTERESTS FORM

If submitting materials via Editorial Manager, please complete this form and upload with your initial submission. Otherwise, please email as an attachment to the editor handling your manuscript.

Please complete each section of the form and insert any necessary "declaration of interests" statement in the text box at the end of the form. A matching statement should be included in a "declaration of interests" section in the manuscript.

Institutional affiliations

We require that you list the current institutional affiliations of all authors, including academic, corporate, and industrial, on the title page of the manuscript. ***Please select one of the following:***

☒ All affiliations are listed on the title page of the manuscript.

☐ I or other authors have additional affiliations that we have noted in the "declaration of interests" section of the manuscript and on this form below.

Funding sources

We require that you disclose all funding sources for the research described in this work. ***Please confirm the following:***

☒ All funding sources for this study are listed in the "acknowledgments" section of the manuscript.*

*A small number of front-matter article types do not include an "acknowledgments" section. For these, reporting funding sources is not required.

Competing financial interests

We require that authors disclose any financial interests and any such interests of immediate family members, including financial holdings, professional affiliations, advisory positions, board memberships, receipt of consulting fees, etc., that:

(1) could affect or have the perception of affecting the author's objectivity, *or*
(2) could influence or have the perception of influencing the content of the article.

Please select one of the following:

☒ We, the authors and our immediate family members, have no financial interests to declare.

☐ We, the authors, have noted any financial interests in the "declaration of interests" section of the manuscript and on this form below, and we have noted interests of our immediate family members.

Advisory/management and consulting positions

We require that authors disclose any position, be it a member of a board or advisory committee or a paid consultant, that they have been involved with that is related to this study. We also require that members of our journal advisory boards disclose their position when publishing in that journal. ***Please select one of the following:***

☒ We, the authors and our immediate family members, have no positions to declare and are not members of the journal's advisory board.

☐ The authors and/or their immediate family members have management/advisory or consulting relationships noted in the "declaration of interests" section of the manuscript and on this form below.

Patents

We require that you disclose any patents related to this work by any of the authors or their institutions. ***Please select one of the following:***

☒ We, the authors and our immediate family members, have no related patents to declare.

☐ We, the authors, have a patent related to this work, which is noted in the "declaration of interests" section of the manuscript and on this form below, and we have noted the patents of immediate family members.

Please insert any "declaration of interests" statements in this space. This exact text should also be included in the "declaration of interests" section of the manuscript. If no authors have a competing interest, please insert the text, "The authors declare no competing interests."

The authors declare no competing interests.

On behalf of all authors, I declare that I have disclosed all competing interests related to this work. If any exist, they have been included in the "declaration of interests" section of the manuscript.

Name: John Chen

Manuscript number (if available): CELL-D-22-02349R1